



VCU

Virginia Commonwealth University
VCU Scholars Compass

Theses and Dissertations


Graduate School

2019

Diuretic and natriuretic activity of FAAH inhibition in the renal medulla: a proposed role of palmitoylethanolamide and its regulation by renal medullary interstitial cells

Sara Dempsey

Follow this and additional works at: <https://scholarscompass.vcu.edu/etd>

 Part of the [Cardiovascular Diseases Commons](#), [Lipids Commons](#), [Other Physiology Commons](#), and the [Pharmacology Commons](#)

© Sara K. Dempsey

Downloaded from

<https://scholarscompass.vcu.edu/etd/5776>

This Dissertation is brought to you for free and open access by the Graduate School at VCU Scholars Compass. It has been accepted for inclusion in Theses and Dissertations by an authorized administrator of VCU Scholars Compass. For more information, please contact libcompass@vcu.edu.

© Sara K. Dempsey 2019
All Rights Reserved

Diuretic and natriuretic activity of FAAH inhibition in the renal medulla: a proposed role of palmitoylethanolamide and its regulation by renal medullary interstitial cells

A dissertation submitted in partial fulfillment of the requirements for the degree of Doctor of Philosophy at Virginia Commonwealth University.

by

Sara Kathleen Dempsey
Master of Science, Virginia Commonwealth University, 2015
Bachelor of Science, University of Mississippi, 2013

Director: Joseph K. Ritter, Ph.D.,
Professor, Department of Pharmacology & Toxicology

Virginia Commonwealth University
Richmond, Virginia
April 2019

Acknowledgments

The path to this dissertation has been an adventure I will never forget, and I would like to express my deepest appreciation to all those who have made this experience possible and contributed to my success. First, I'd like to thank my advisor Dr. Ritter for providing me with the opportunity to work in his laboratory for my dissertation. I have been extremely fortunate to be a member of your lab. Your passion for science is contagious and teaching skills are unmatched. I truly appreciate your insightful feedback and for always supporting my career goals. To the members of the Ritter lab, Dr. Ashfaq Ahmad and Ava Daneva. It was a pleasure working with you both the past few years and thank you for the collaborative experience and for making it an enjoyable place to work.

I'd also like to thank my committee members: Dr. Pin-Lan Li, Dr. Ningjun Li, and Dr. Shanaka Wijesinghe for their guidance and support during the entire process. Special thanks to my other committee member Dr. Carl Wolf. You've been with me from the beginning during my master's program, and I cannot thank you enough for your insightful career and life lessons; it's been an honor to learn from you. Thank you for always pushing me to stay on track. To my honorary committee member, Mr. Justin Poklis, it has been a pleasure to work with you over the past 6 years. Thank you for teaching me instrumentation and analytical experience that cannot be found in any textbook, and for the countless meals and basketball games where we balanced talking science, sports, and life. I am also grateful to Dr. William Dewey and Dr. Hamid Akbarali for giving me the opportunity to be a part of the Department of Pharmacology & Toxicology. Thank you for your support and encouragement during my time as a doctoral student.

I honestly would not have pursued a PhD without the guidance and mentorship of Dr. Alphonse Poklis and Dr. Michelle Peace. Dr. Poklis taught me forensic toxicology, how to have a

successful work-life balance, and how to fish like a champion. I am truly grateful I was able to learn and laugh with him. Dr. Peace, I cannot thank you enough for your mentorship during my time at VCU. Your dedication to science and improvement to the field is truly inspiring. You brought me out of my comfort zone and took me under your wing to help me see my potential as a scientist and a leader. Thank you for the numerous talks about life and for your wise career advice, and I am so thankful to call you a colleague and a friend.

I am also extremely grateful to all of my friends here in Richmond and elsewhere. You have been my biggest support system during all of my ups and downs, and I thank you for your endless encouragement and prayers, continuous life-check-ins, and providing joyful adventures and distractions to rest my mind outside of my research. Finally, biggest thanks to my mom Sue, my dad David, my sister Laura and brother-in-law William for your unwavering and endless support; and to my niece Evelyn for your ability to always make my day better. Laura and William, thank you for your love and positive influence on my life, and continuous prayers. Mom and Dad, thank you for your unconditional belief in me and all the sacrifices you made to help me get where I am today. Even though you may not have understood my day-to-day life, you continued to encourage me and reassure me during this long process. All of your love and support enabled me to reach my goals.

Table of Contents

List of Tables	1
List of Figures	2
List of Abbreviations	5
Abstract	7
Chapter 1: Long- term regulation of blood pressure by the kidney	9
1.1 Hypertension and blood pressure regulation by the kidney	9
1.2 Pressure-natriuresis and renal interstitial hydrostatic pressure	11
1.3 The pro-hypertensive system of the kidney	12
1.4 A proposed antihypertensive system of the kidney	14
1.5 Renal medullary interstitial cells and medullipin.....	16
Chapter 2: Renal lipid ethanolamides	20
2.1 The endocannabinoid system	20
2.2 Endocannabinoids and renal function	23
2.3 The ‘endocannabinoid-related’ lipid palmitoylethanolamide	27
Rationale and hypothesis	31
Chapter 3: Modulation of mean arterial pressure and diuresis by infusion of a selective inhibitor of fatty acid amide hydrolase in anesthetized mice	35
3.1 Introduction	35
3.2 Materials and Methods	37
3.3 Results	42
3.3.1 PF-3845 administration stimulates diuresis-natriuresis and lowers mean arterial pressure in C57BL/6J mice	42
3.3.2 PF-3845 administration stimulates diuresis in FAAH KO mice	48
3.3.3 PF-3845-induced diuresis and blood pressure-reducing effect is CB ₁ mediated	51
3.4 Discussion	52
Chapter 4: Diuretic, natriuretic, and blood pressure-lowering activity of palmitoylethanolamide in normotensive and hypertensive mice	58
4.1 Introduction	58
4.2 Materials and Methods	60
4.3 Results	65
4.3.1 PEA administration stimulates diuresis and natriuresis in normotensive mice	65
4.3.2 PEA-induced diuresis-natriuresis is FAAH and CB ₁ independent.....	69
4.3.3 Intramedullary infusion of PEA decreases mean arterial pressure and stimulates diuresis in L-NAME-induced hypertensive mice	75

4.4 Discussion	79
Chapter 5: Regulation of palmitoylethanolamide and related lipid ethanolamides by mouse medullary interstitial cells.....	87
5.1 Introduction	87
5.2 Materials and Methods	88
5.3 Results	94
5.3.1 Characterization of cultured mouse medullary interstitial cells	94
5.3.2 FAAH inhibition and high osmolarity increases Sudan Black B stained lipid granules in cultured MMICs and lipid ethanolamide concentrations in MMIC culture medium	97
5.3.3 High osmolarity increases NAPE-PLD protein levels in cultured MMICs.....	102
5.4 Discussion	106
Final discussion and conclusions	111
Funding	114
References	115
Vita.....	130

List of Tables

Chapter 3

Table 1. Multiple reaction monitoring (MRM) parameters for 2-AG, AEA, OEA, and PEA analysis by UPLC-MS/MS	41
--	----

List of Figures

Chapter 1

Figure 1. The pro-hypertensive vs antihypertensive systems of the kidney 19

Chapter 2

Figure 2. Synthetic and degradative pathways of major endocannabinoids 23

Figure 3. Metabolic pathways and molecular targets of palmitoylethanolamide (PEA) 30

Chapter 3

Figure 4. The effects of intramedullary and intravenous infusion of PF-3845 on MAP and UV in C57BL/6J mice 44

Figure 5. The effects of intramedullary and intravenous infusions of PF-3845 on UNa and UK and MBF in C57BL/6J mice 46

Figure 6. Anandamide (AEA), palmitoylethanolamide (PEA), oleoylethanolamide (OEA), and 2-arachidonylethanolamide (2-AG) concentrations in kidney tissue and plasma of sham control and intramedullary PF-3845-infused C57BL/6J mice 47

Figure 7. The effects of intramedullary and intravenous infusion of PF-3845 on MAP and UV in FAAH KO mice 49

Figure 8. Anandamide (AEA), palmitoylethanolamide (PEA), oleoylethanolamide (OEA), and 2-arachidonylethanolamide (2-AG) concentrations in kidney tissue and plasma of sham control and intramedullary PF-3845-infused FAAH KO mice 50

Figure 9. The effects of rimonabant pretreatment on the MAP and UV responses to intramedullary infusion of PF-3845 in C57BL/6J mice 52

Chapter 4

Figure 10. The effects of intramedullary and intravenous infusion of PEA on MAP and UV in C57BL/6J mice	67
Figure 11. The effects of intramedullary and intravenous infusions of PEA on UNa and UK and MBF in C57BL/6J mice.....	68
Figure 12. The effects of intramedullary and intravenous infusion of PEA on MAP and UV in FAAH KO mice	70
Figure 13. The effects of intramedullary and intravenous infusions of PEA on UNa and UK and MBF in FAAH KO mice.....	71
Figure 14. The effects of rimonabant pretreatment on the MAP and UV responses to intramedullary infusion of PEA in C57BL/6J mice and the effect of intramedullary infusion of PEA on MAP and UV in CB ₁ KO mice	73
Figure 15. The effects of rimonabant pretreatment on the MAP and UV responses to intravenous infusion of PEA in C57BL/6J mice	74
Figure 16. The effects of intramedullary infusion of palmitoylethanolamide (PEA) on MAP and UV in L-NAME-induced hypertensive mice	76
Figure 17. The effects of intramedullary and intravenous infusions of PEA on UNa and UK and MBF in L-NAME-induced hypertensive mice	77
Figure 18. Medullary blood flow of C57BL/6J sham control mice and L-NAME-induced hypertensive sham control mice.....	78
Figure 19. The effect of L-NAME-induced hypertension on AEA, OEA, and PEA concentrations and NAPE-PLD and FAAH protein levels in kidney tissue of C57BL/6J mice	79

Chapter 5

Figure 20. Immunohistochemical and histochemical analysis of cultured MMICs and kidney tissue sections.....	96
Figure 21. Transmission electron micrographs of vehicle- and PF-3845-treated MMICs	97
Figure 22. The effects of PF-3845 on lipid staining in cultured MMICs	99
Figure 23. The effects of FAAH inhibition, increased osmolarity, and high-pressure treatment on lipid staining in cultured MMICs.....	100
Figure 24. The effects of FAAH inhibition, increased osmolarity, and high pressure treatment on lipid ethanolamide concentrations in MMIC culture medium.....	101
Figure 25. The effects of pharmacologic and physiologic stimuli on the immunohistochemical analysis of cultured MMICs treated.....	103
Figure 26. Immunohistochemical and histochemical analysis of cultured MMICs exposed to high pressure	104
Figure 27. The effects of FAAH inhibition, increased osmolarity, and high-pressure treatment on NAPE-PLD (A) and FAAH (B) protein levels in cultured MMICs	105

List of Abbreviations

2-AG	2-arachidonoyl glycerol
AA	Arachidonic acid
ACE	Angiotensin converting enzyme
AEA	Anandamide, <i>N</i> -arachidonoylethanolamine
ABHD4	Serine α/β -hydrolases 4
Ang I	Angiotensin I
Ang II	Angiotensin II
ANRL	Antihypertensive neutral renomedullary lipid
AT₁	Angiotensin receptor 1
ATP	Adenosine triphosphate
CB₁	Cannabinoid receptor 1
CB₂	Cannabinoid receptor 2
CNS	Central nervous system
DAG	Diacylglycerol
DAGL	Diacylglycerol lipase
EC	Endocannabinoid system
ECFV	Extracellular fluid volume
FAAH	Fatty acid acyl hydrolase
GPR	G-protein coupled receptor
GFR	Glomerular filtration rate
HPLC	High pressure liquid chromatography
HRP	Horseradish peroxidase
IDFP	Isopropyl dodecylfluorophosphonate
IHC	Immunohistochemistry
L-NAME	<i>N</i> ^G -nitro-L-arginine methyl ester
MAGL	Monoacylglycerol lipase
MAP	Mean arterial pressure
MAPK	Mitogen-activated protein kinase
MBF	Medullary blood flow
MMIC	Mouse medullary interstitial cell
NAE	<i>N</i> -acylethanolamine
NAAA	NAE-hydrolyzing acid amidase
NAPE	<i>N</i> -arachidonoyl-phosphatidylethanolamine
NKCC2	Na ⁺ /K ⁺ /Cl ⁻ co-transporter
NO	Nitric oxide
NOS	Nitric oxide synthase
OEA	Oleylethanolamide
PEA	Palmitoylethanolamide
PBS	Phosphate-buffered saline
PPAR	Peroxisome proliferated activated receptor
PF-3845	<i>N</i> -3-Pyridinyl-4-[[3-[[5-(trifluoromethyl)-2-pyridinyl]oxy]phenyl]methyl]-1-piperidinecarboxamide
PKC	Protein kinase C

PLC	Phospholipase C
PLD	Phospholipase D
RAAS	Renin-angiotensin-aldosterone system
RIHP	Renal interstitial hydrostatic pressure
RMIC	Renal medullary interstitial cells
RPP	Renal perfusion pressure
SBB	Sudan Black B
SNS	Sympathetic nervous system
SR141716A	Rimonabant
TRPV1	Transient receptor potential channel
UK	Urinary potassium excretion rate
UNa	Urinary sodium excretion rate
UV	Urine excretion rate
UPLC-MS/MS	Ultra-performance liquid chromatography tandem mass spectrometry
WIN 55,212-2	(<i>R</i>)-(+)-[2,3-Dihydro-5-methyl-3-(4-morpholinylmethyl)pyrrolo[1,2,3- <i>de</i>]-1,4-benzoxazin-6-yl]-1-naphthalenylmethanone mesylate

Abstract

DIURETIC AND NATRIURETIC ACTIVITY OF FAAH INHIBITION IN THE RENAL MEDULLA: A PROPOSED ROLE OF PALMITOYLETHANOLAMIDE AND ITS REGULATION BY RENAL MEDULLARY INTERSTITIAL CELLS

By Sara Kathleen Dempsey, M.S.

A dissertation submitted in partial fulfillment of the requirements for the degree of Doctor of Philosophy at Virginia Commonwealth University.

Virginia Commonwealth University, 2019

Director: Joseph K. Ritter, Ph.D.,
Professor, Department of Pharmacology & Toxicology

Hypertension is a critical public health issue worldwide, and in the United States, it is the leading cause of heart disease, stroke, and kidney failure, contributing to more than 1,100 deaths per day. It is proposed that the renal medulla combats increased blood pressure by releasing a neutral lipid from the lipid droplets of medullary interstitial cells, termed medullipin, which induces diuresis- natriuresis and vasodepression. The renal medulla is enriched with fatty acid lipid ethanolamides including the endocannabinoid anandamide (AEA), palmitoylethanolamide (PEA), and oleoylethanolamide (OEA), along with their primary hydrolyzing enzyme fatty acid amide hydrolase (FAAH). Our lab is investigating the relationship of these lipid ethanolamides and their metabolites to medullipin. We have shown that intramedullary infusion of AEA stimulated diuresis-natriuresis without changing mean arterial pressure (MAP) in an acute surgical model using anesthetized normotensive C57BL/6J mice. The hypothesis that infusion of a FAAH-

selective inhibitor, PF-3845, would produce similar responses as exogenous AEA was tested. Intramedullary infusion of PF-3845 stimulated diuresis-natriuresis, decreased MAP, and increased lipid ethanolamide concentrations in kidney tissue in C57BL/6J mice. Since the decrease in MAP observed with PF-3845 was not consistent with the results of exogenous AEA, this study hypothesized that increased PEA concentrations in the renal medulla observed with PF-3845 produced the decrease in MAP. Therefore, the effects of PEA administration into the renal medulla were investigated. Intramedullary infusion of PEA stimulated diuresis and natriuresis without changing MAP in normotensive C57BL/6J mice. However, intramedullary PEA administration to mice made hypertensive using L-NAME, an inhibitor of nitric oxide synthase, was assessed. Intramedullary infusion of PEA stimulated diuresis, but also decreased MAP in L-NAME-induced hypertensive mice. The mechanism of PEA-induced diuresis was evaluated for the contributions of its FAAH-mediated hydrolysis and the CB₁ receptor. Intramedullary infusion of PEA stimulated diuresis in FAAH knockout mice and CB₁ knockout mice. The possible source of PEA in the renal medulla was investigated using renal medullary interstitial cells cultured from mice. In cultured mouse medullary interstitial cells (MMICs), treatment with PF-3845 increased cytoplasmic lipid droplets detected by Sudan Black B (SBB) staining and increased PEA in the culture medium. Physiologic stimuli that may regulate PEA production and release from MMICs were also evaluated. Increased osmolarity increased NAPE-PLD protein levels, increased SBB stained droplets in MMICs, and increased PEA concentrations in the culture medium. Overall, it is concluded that the PEA-induced diuretic and natriuretic effect is independent of FAAH-mediated hydrolysis and the CB₁ receptor, and that PEA can serve as an antihypertensive regulator in the renal medulla that may be regulated by medullary interstitial cells.

Chapter 1: Long- term regulation of blood pressure by the kidney

1.1 Hypertension and blood pressure regulation by the kidney

Maintenance of normal blood pressure is important to a person's overall health. Normal blood pressure readings are defined as a systolic pressure of less than 120 mmHg and a diastolic pressure of less than 80 mmHg. Hypertension, or high blood pressure, is a critical public health issue worldwide, and in the United States, approximately 1 in 3 U.S. adults 20 years and older have high blood pressure, for a total of 103 million adults. It is also an increasing problem in childhood and adolescence with about 4% of youth aged 12-19 diagnosed with hypertension. Hypertension is defined as having a systolic pressure of greater than or equal to 130 mmHg or a diastolic pressure of greater than or equal to 80 mmHg. Increased blood pressure leads to other health issues, and currently hypertension is the leading cause of heart disease, stroke, and kidney failure, contributing to more than 1,100 deaths per day. (Mozaffarian et al., 2015; Yoon et al., 2015). In addition, approximately only half of those with hypertension have adequate blood pressure control (54%). Hypertension is a burden economically as well, with the total socioeconomic cost of hypertension estimated at \$51 billion each year. This cost includes the cost of health care services, medications to treat hypertension, and missed days of work, with direct medical expenses mounting to \$47.5 billion. (Mozaffarian et al., 2015).

An important factor for maintaining a normal blood pressure is the body's endogenous mechanisms for long-term blood pressure regulation. More specifically, the importance of the kidney in the regulation of blood pressure has been stressed for many years. Due to its vital function to regulate salt and water balance, the kidney has been proposed to be the dominant long-term controller of blood pressure. Blood pressure is defined as the product of cardiac output and total peripheral resistance, with cardiac output the product of heart rate and stroke volume. These

definitions made cardiac and vascular models the dominant areas of hypertension research initially. However, this viewpoint was challenged in 1972 when it was suggested that long-term blood pressure was primarily influenced by the effective circulating volume, the result of extracellular fluid volume (ECFV), determined by sodium balance (Guyton et al., 1972a). According to Guyton, when ECFV is increased, there is an increase in arterial pressure with subsequent increase in renal perfusion pressure (RPP). The kidneys respond to this increase in perfusion pressure by increasing urinary sodium excretion and water excretion until ECFV and therefore blood volume is reduced sufficiently to return arterial pressure to normal levels. This mechanism is called pressure-natriuresis, and in theory, hypertension would develop if the excretory ability of the kidney is impaired.

Another mechanism in which the kidney regulates the salt and water balance in the body is by sympathomodulation of the efferent sympathetic nervous system. The kidney is innervated with efferent sympathetic nerve fibers that contact essential renal structures, including the vasculature, tubules, and juxtaglomerular apparatus. As a result, renal sympathetic activation results in sodium reabsorption, water retention, reduced blood flow and activation of the renin-angiotensin-aldosterone system (RAAS) (DiBona and Kopp, 1997; Johns et al., 2011). The kidney also has an extensive network of afferent nerves that relay information from the chemoreceptors and mechanoreceptors in the kidney to the central nervous system. It has been proposed that under normal conditions, tonic activation of renal afferent nerve fibers serve as a compensatory mechanism to prevent increased sympathetic activation and thus an increase in blood pressure (DiBona and Esler, 2010).

1.2 Pressure-natriuresis and renal interstitial hydrostatic pressure

It is well recognized that changes in arterial blood pressure influence water and salt excretion through pressure-natriuresis, but the mechanism by which this occurs is unknown. Researchers proposed that the response was mediated by changes in renal interstitial hydrostatic pressure (RIHP). Studies in the early 1970s demonstrated increases in RPP produced a significant rise in RIHP (Ott et al., 1971). Later, it was shown that small increases in RIHP enhanced water and urinary salt excretion (Wilcox et al., 1984). Further evidence includes a small increase in RIHP occurring when RPP was increased by 50 mmHg in dogs, and these results have been replicated in rat models (Granger and Scott, 1988; Roman, 1988; Roman et al., 1988).

The relationship between RPP and sodium excretion can be altered by the physiologic status of the animal as well. Renal vasodilation caused by acetylcholine produced enhancement of RPP on sodium excretion, and this was associated with a greater increase in RIHP despite efficient autoregulation of renal blood flow (Granger and Scott, 1988). Another study showed that the volume status also affects the relationship. Greater increases in RIHP and sodium excretion occurring secondary to increases in RPP were observed in volume-expanded rats compared to volume-maintained rats (Garcia-Estan and Roman, 1989). In the same study it was also reported that decapsulation of the kidney significantly attenuated the increased RIHP and sodium excretion in response to an increase in RPP, further indicating the importance of RIHP in the pressure-natriuresis response.

Many studies were performed to illustrate the relationship between RIHP and medullary hemodynamics. The hypothesis was tested that an increase in RPP would result in increased vasa recta flow and vasa recta hydrostatic pressure, thus leading to a reduction in fluid uptake across the vasa recta capillary wall, and ultimately leading to increased medullary fluid and pressure that

would transmit through the kidney. It was demonstrated that renal medullary blood flow (MBF) and vasa recta hydrostatic pressure increased directly with increased RPP in volume-expanded rats, while total and cortical blood flow were efficiently auto-regulated (Roman et al., 1988). Subsequent experiments demonstrated that increased RPP is associated with elevated medullary blood flow and decreased sodium and water reabsorption in the proximal tubule and/or thin descending loop of Henle (Roman, 1988). It was proposed that alterations in the Starling forces in the medulla due to increased RPP leads to inhibition of tubular reabsorption (Schafer, 1990). Sodium reabsorption is further inhibited by increased RPP causing the inhibition of the Na^+/K^+ -ATPase activity and internalization of the transport protein Na^+/H^+ exchanger isoform 3 (NHE3) (Zhang et al., 1998; McDonough, 2010). The mechanism behind this phenomenon is unclear, but it has been proposed that paracrine signaling may contribute. Adenosine triphosphate (ATP), 20-hydroxyeicosatetraenoic acid (20-HETE), reactive oxygen species and endothelin-1 are regarded as important modulators of the pressure-natriuresis response (Williams et al., 2007; O'Connor and Cowley, 2010; Garvin et al., 2011; Burnstock et al., 2014). In addition, nitric oxide (NO) is increased with an increase in MBF, and NO has been shown to enhance the pressure-natriuresis response by inhibiting the $\text{Na}^+/\text{K}^+/\text{Cl}^-$ co-transporter (NKCC2) in the loop of Henle (Ivy and Bailey, 2014). Despite the effort to fully explain pressure-natriuresis, the mechanistic link between changes in medullary perfusion and water and sodium balance and arterial blood pressure has not been clearly established.

1.3 The pro-hypertensive system of the kidney

The first observations that the kidney releases a substance that causes an increase in arterial blood pressure were made in 1898 by the Finnish physiologist Robert Tigerstedt and his student

Per Gunnar Bergman at the Karolinska Institute in Stockholm. They demonstrated that extracts from rabbit kidney caused a prolonged blood pressure elevation when injected into the renal cortex. This pressor substance was termed renin and became the foundation for the renin-angiotensin-aldosterone system (RAAS) which continues to be a major focus of study for researchers today (Peart, 1969; Hall, 2003). Tigerstedt's finding sparked research to develop a model of hypertension by manipulation of renal function, but many attempts were unsuccessful. The first successful experiment was not until the 1930s when Harry Goldblatt and his colleagues at Case Western University in Cleveland, Ohio demonstrated in dogs that constriction of the renal arteries produced chronic hypertension (Goldblatt et al., 1934). This model of hypertension became known as "Goldblatt hypertension" and renewed interest in the pressor substance of the kidney.

The next major discovery came in the late 1930s when Irvine Page's group in Indianapolis and Eduardo Braun-Menendez' group in Buenos Aires independently showed that renin was not the pressor agent itself, but rather an enzyme that formed a pressor polypeptide from a plasma globulin. Page called it 'angiotonin' and Braun- Menendez 'hypertensin,' and in 1958 the two agreed on the name 'angiotensin' for the pressor substance and the substrate from which angiotensin is released was called 'angiotensinogen' (Braun-Menendez et al., 1940; Page and Helmer, 1940; Braun-Menendez and Page, 1958). After the discovery of angiotensin, there were further advances in the 1950s with Leonard Skeggs and his colleagues at the Case Western Reserve University. Angiotensin was purified in 1954, and its two forms were discovered, angiotensin I (Ang I), a decapeptide, and angiotensin II (Ang II), an octapeptide (Skeggs et al., 1954b; Skeggs et al., 1954a). Angiotensin converting enzyme (ACE) was discovered in 1956, and Ang II was synthesized in 1957 by Merlin Bumpus and Page at the Cleveland Clinic and by Schwyzer in Switzerland (Lentz et al., 1956; Bumpus et al., 1957). All of these findings filled in the missing

puzzle pieces of the RAAS system and paved the way for many notable studies to come. Briefly, the RAAS system begins with activation of β 1-adrenergic receptors on the renal juxtaglomerular cells to stimulate the secretion of the enzyme renin. Renin cleaves angiotensinogen to form the decapeptide angiotensin (Ang I). This is transformed by ACE in the lung to the octapeptide, angiotensin II (Ang II), which is considered the most potent pre-capillary smooth muscle constrictor (Fig. 1).

1.4 A proposed antihypertensive system of the kidney

The first suggestion that the kidney may have an incretory depressor mechanism that acts in opposition to the RAAS system began in the 1940s, mainly by Arthur Grollman. With the renin story dominating the scene at the time, it is no surprise that the idea of a renal antihypertensive system was overlooked by many. Grollman and his colleagues compared the effects of several different procedures on blood pressure in dogs. He reported that in bilaterally nephrectomized animals, blood pressure rose to hypertensive levels, and pathological findings of malignant hypertension were found at autopsy. Ligation of both ureters only caused a temporary increase in blood pressure, while no increase in blood pressure occurred if only one ureter was ligated. Similarly, no increase in pressure occurred if one ureter was implanted into the vena cava or small intestine, and the contralateral kidney was removed. All of his results led Grollman et al. to conclude that intact renal tissue was essential for the maintenance of normal blood pressure levels (Grollman et al., 1949).

Grollman's colleague, Eric Muirhead, continued this work on the importance of the kidney in blood pressure regulation. Muirhead induced hypertension in animals by a mixture of intravenous saline and oral protein, and performed different renal manipulations to demonstrate

the incretory function of the kidney. Similar levels of hypertension were attended after bilateral nephrectomy and ureteral ligation, while uretero-caval anastomosis caused a significant fall in blood pressure. He also noted that ureteral ligation caused ischemic necrosis in the papilla of the kidney, and this damage was avoided under the preparation of anastomosed ureters (Muirhead et al., 1972b). This led Muirhead to suggest that the cells in the renal papilla were involved in preventing hypertension.

He next investigated this idea by showing transplants of fragmented 'normal' renal medullary tissue into rats with renoprival hypertension reversed the hypertensive state. He also showed that transplants of renal cortex, liver, and spleen had no effect on the hypertensive state (Muirhead et al., 1960). Muirhead reported similar findings in other models of hypertension, including accelerated renoprival hypertension, malignant hypertension, Goldblatt one-kidney one-clip hypertension, and salt-loaded renoprival hypertension. In all experiments, transplanted renomedullary tissue reversed the hypertensive states, while renal cortical tissue did not. In addition, removal of the renomedullary transplants was followed by a return of blood pressure to hypertensive levels. (Muirhead, 1980).

Further experiments by Muirhead and others supported the hypothesis of a renomedullary vasodepressor substance. Several studies noted the rapid normalization of arterial pressure following unclipping of the renal artery in the Goldblatt one-kidney one-clip model of hypertension. These studies demonstrated that the rapid hypotensive response was not due to changes in vasopressor substances such as angiotensin, prostaglandins, or vasopressin (Russell et al., 1982a; Russell et al., 1982b; Muirhead et al., 1985). The fall in arterial blood pressure was also not due to blood volume loss, but to a fall in peripheral resistance (Thurston et al., 1980; Russell et al., 1983). Furthermore, in rats pretreated with 2-bromoethylamine to chemically

ablate the renal medulla, blood pressure remained significantly elevated after unclipping of the renal artery, confirming again that an intact renal medulla is essential to reverse hypertensive states (Bing et al., 1981; Russell et al., 1986).

The above experiments using the unclipping of the renal artery also gave rise to the idea that increased perfusion pressure causes release of the depressor substance from the kidney. This influenced the design of the early experiments by Gunnar Gothberg. These “cross circulation” experiments involved normotensive rats prepared with carotid artery and jugular vein catheters that were connected to an extracorporeal pump-perfusion circuit with an isolated kidney. The isolated kidney was one from a two-kidney, one-clip hypertensive rat. He showed that the acute unclipping of the isolated kidney produced a decrease in blood pressure in the normotensive rat (Gothberg et al., 1982). In another experiment, one rat served as a “donor” to perfuse the isolated normotensive or hypertensive kidney in another “recipient” rat. Venous effluent from the recipient kidney was returned to the venous circulation of the donor rat. Therefore, the arterial pressure of the donor rat could react to a vasodepressor substance released from the recipient kidney in response to renal manipulations. It was shown that when the recipient kidneys were perfused with increased pressure, the blood pressure of the donor rat significantly decreased (Karlstrom and Gothberg, 1987). These findings were instrumental in demonstrating the circulatory control of the antihypertensive system of the kidney.

1.5 Renal medullary interstitial cells and medullipin

Muirhead’s transplantation experiments led him investigate the renomedullary transplants further to identify the origin of the antihypertensive substance. Microscopic analysis showed that the transplants he was using consisted of almost entirely renomedullary interstitial cells (RMICs)

and a microvasculature. He also noted that the RMICs were in groups or clusters, suggesting they were proliferating, and they were in close proximity to the developing capillaries (Muirhead et al., 1972a). Due to the characteristics of these interstitial cells, Muirhead concluded they were the most eligible cell for secretion of the antihypertensive substance. It was actually Muehrcke and his colleagues that first postulated that RMICs might be the cell type in the renal medulla to secrete the antihypertensive substance, and observations made by Tobian's group supported this hypothesis (Muehrcke et al., 1969; Tobian and Ishii, 1969; Tobian and Azar, 1971).

Muirhead put this hypothesis to the test and first isolated and cultured the interstitial cells from the renal medulla of the rabbit. His cultured cells exhibited similar morphological and biochemical characteristics as the proliferating cells from the tissue transplants. The cultured cells displayed the ability to produce prostaglandins and stained positively with two lipid dyes, Oil Red O and Sudan Black B (Muirhead et al., 1972c; Muirhead et al., 1973). Muirhead went on to test if the cultured cells elicited similar antihypertensive effects as the renomedullary transplants. He found that implanted RMICs exerted a potent antihypertensive function in hypertensive animals. The effect was rapid, reaching a maximum within 12 to 24 hours, where blood pressure returned to normal levels. The blood pressure of the animals with the RMIC transplants remained at normal levels for eight days. Since the morphology of the implanted cultured RMICs was identical to that previously observed with the transplanted medullary fragments, Muirhead confirmed that the interstitial cells of the medulla were crucial for the reduction of blood pressure in hypertensive conditions (Muirhead et al., 1974; Muirhead et al., 1977).

Shortly after RMICs were identified as the source of the kidney's incretory function, Muirhead and his colleagues began extracting renal medulla for the antihypertensive substance, which they named the 'antihypertensive neutral renomedullary lipid' (ANRL). They were able to

extract this lipid from cultured RMICs and in collaboration with Bjorn Folkow's group, they showed that ANRL was present in renal venous effluent. Their studies demonstrated that ANRL possessed several antihypertensive actions, including stimulating diuresis-natriuresis, suppressing sympathetic tone, causing vasodilation, and a suppressive effect on the central nervous system (Muirhead, 1988). When ANRL was administered as a bolus intravenously, there was a 1-2 min delay until blood pressure began to decline, a characteristic different from other known vasodilators. They demonstrated that if ANRL was administered into the portal vein, the delay in blood pressure decline was significantly decreased. This led them to the liver. Several experiments secured the hepatic contribution to the renomedullary antihypertensive system, and ANRL was renamed Medullipin I (Muirhead, 1990a). They proposed medullipin I was secreted by RMICs and carried to the liver by the blood, where it was converted to its active form, medullipin II, by the cytochrome P-450 enzyme system (Muirhead, 1990b) (Fig. 1). Thus the 'Medullipin System' was born and the elucidation of medullipin surged on. However, despite intense investigation by Muirhead and other groups, the chemical nature of medullipin has not yet been determined (Brooks et al., 1994; Thomas et al., 1996; Glodny and Pauli, 2006).

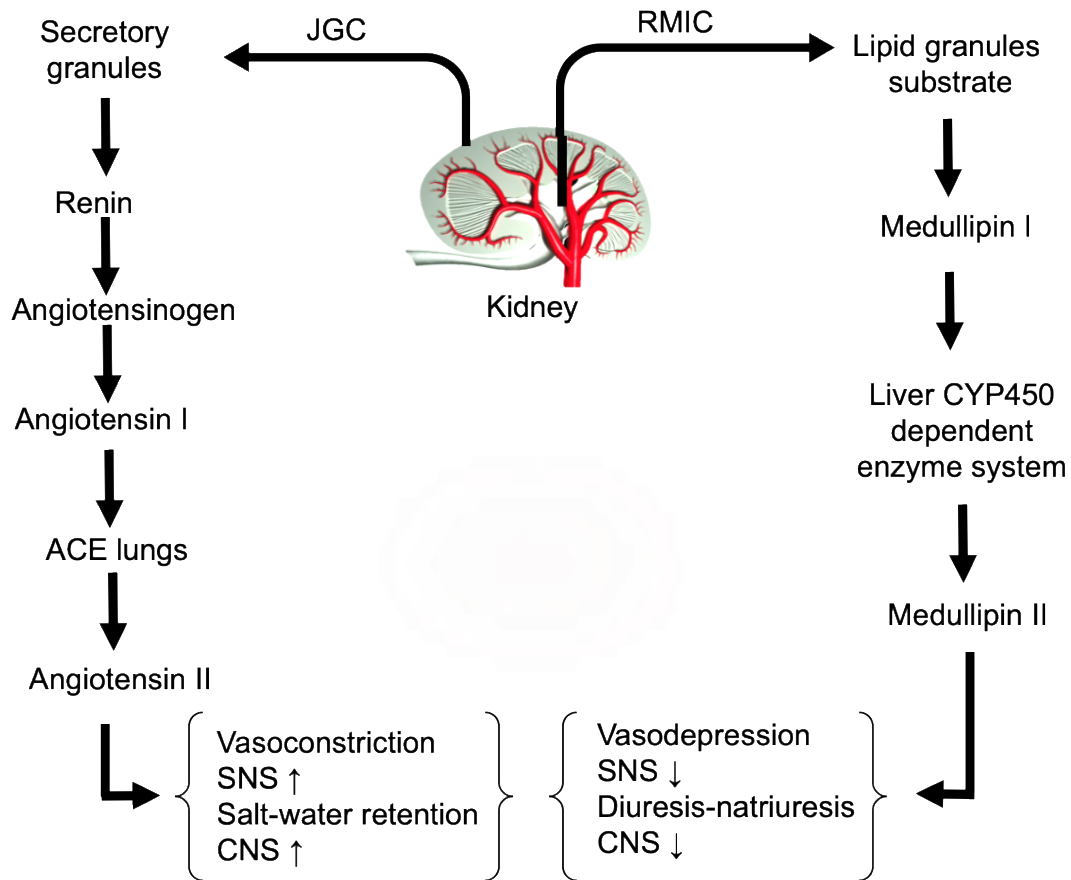


Figure 1. The pro-hypertensive vs antihypertensive systems of the kidney. In the RAAS system (left), juxtaglomerular cells in the kidney release renin which cleaves angiotensinogen to angiotensin I. Angiotensin converting enzyme (ACE) in the lungs converts angiotensin I to angiotensin II which has pro-hypertensive actions. In Muirhead's medullipin system (right), the renal medullary interstitial cells (RMICs) release a neutral lipid from their lipid granules, medullipin I, which is converted into the active medullipin I in the liver. Medullipin II acts in an antihypertensive manner. *Adapted from Folkow 2007*

Chapter 2: Renal lipid ethanolamides

2.1 The endocannabinoid system

The endocannabinoid system is comprised of the two endocannabinoid receptors, CB₁ and CB₂, their endogenous ligands, and their hydrolyzing enzymes. Among these ligands are the nonselective agonists, noladin and arachidonyl dopamine, and the CB₁ antagonist virodhamine (Gomez-Ruiz et al., 2007). The two most studied and well-characterized endocannabinoid ligands are anandamide (AEA) and 2-arachidonylglycerol (2-AG).

AEA, the *N*-acyl ethanolamide derivative of the fatty acid arachidonic acid, was first identified in porcine brain in the early 1990s (Devane et al., 1992). Given the subsequent finding of the ubiquitous distribution of AEA and its metabolizing enzyme, fatty acid amid hydrolase (FAAH), AEA has been linked with many diverse physiological effects such as antinociception, inflammation, analgesia, and regulation of energy consumption and balance (Cravatt et al., 2001; Pacher et al., 2006; Turcotte et al., 2015).

Biosynthesis of AEA, along with other *N*-acylethanolamines (NAEs), occurs through the enzymatic hydrolysis of *N*-arachidonyl phosphatidylethanolamine (NAPE). NAPE is formed by the enzymatic transfer of arachidonic acid at the *sn*-1 position of phosphatidylcholine to the primary amino group of phosphatidylethanolamine. This is the rate-limiting step in its biosynthetic pathway and is catalyzed by a Ca²⁺-dependent *N*-acyltransferase (Wang and Ueda, 2009). The next step is the formation of AEA from NAPE. The four different mechanisms of AEA synthesis from NAPE that have been reported are summarized in Figure 2. The primary mechanism is the cleavage of NAPE at the terminal phosphodiester bond by NAPE-specific phospholipase D (NAPE-PLD) resulting in AEA and phosphatidic acid (Wang and Ueda, 2009). Another pathway involves the conversion of NAPE to *N*-acyl-lyso phosphatidylethanolamine catalyzed by

phospholipase A₂, followed by the metabolism by lyso-PLD to form AEA (Sun et al., 2004). A third pathway is composed of double-deacylation of NAPE by α/β -hydrolase 4 (ABHD4) and hydrolysis of the phosphodiester bond by glycerolphosphoethanolamine diesterase, releasing AEA and glycerol phosphate (Simon and Cravatt, 2006; Simon and Cravatt, 2008). In a fourth pathway, AEA is generated by a two-step process involving the PLC-like hydrolysis of NAPE and subsequent dephosphorylation by PTPN22 (Liu et al., 2006). The hydrolysis of AEA by the enzyme FAAH was first described in 1993 (Deutsch and Chin, 1993). The integral membrane serine hydrolase hydrolyzes AEA to form the biologically active arachidonic acid and ethanolamine. An important property of FAAH is its wide substrate specificity, as it is also responsible for hydrolyzing other lipid amides such as linoleamide and oleamide, as well as other *N*-acylethanolamine derivatives of long-chain fatty acids such as palmitoylethanolamide (PEA) and oleoylethanolamide (OEA) (Ueda et al., 1995; Waluk et al., 2014).

2-AG is synthesized from diacylglycerol (DAG) by DAG lipase (DAGL). DAG can be generated either from phosphoinositides by a specific PLC or from phosphatidic acid by phosphatidic acid phosphohydrolase. The enzyme DAGL exists as two isoforms, α and β , and hydrolyzes DAG at the *sn*-1 position to give 2-AG and free fatty acid (Bisogno et al., 2003). Other pathways of 2-AG synthesis have been described but are less understood (Sugiura et al., 2006). 2-AG is rapidly metabolized by various cell types to yield arachidonic acid and glycerol. The primary enzyme responsible for 2-AG hydrolysis is monoacylglycerol lipase (MAGL) (Konrad et al., 1994). There is also evidence that 2-AG can be metabolized by FAAH under certain circumstances, but this appears to be negligible in brain (Di Marzo et al., 1998; Blankman et al., 2007).

Endocannabinoids elicit their effects primarily by binding to and activating the CB₁ and CB₂ receptors. CB₁ receptors are a member of the superfamily of transmembrane receptors that are

coupled to Gi/o proteins, and also Gs proteins under certain conditions. Activation of the CB₁ receptor results in inhibition of adenylyl cyclase, regulation of Ca²⁺ and K⁺ channels, and activation of the ERK-MAP kinase pathway. CB₂ receptors also couple to Gi/o proteins and inhibit adenylyl cyclase activity. Activation of CB₂ receptors also regulates several other pathways, including p42/p44 MAP kinase and PCL-mediated Ca²⁺ release (Gomez-Ruiz et al., 2007; Howlett and Abood, 2017). Another well-characterized site of action for AEA is the transient receptor potential channel (TRPV1), which is a nonselective cation channel that mediates a variety of effects such as vasodilation, smooth muscle tone modulation, and bronchoconstriction (Di Marzo et al., 2002).

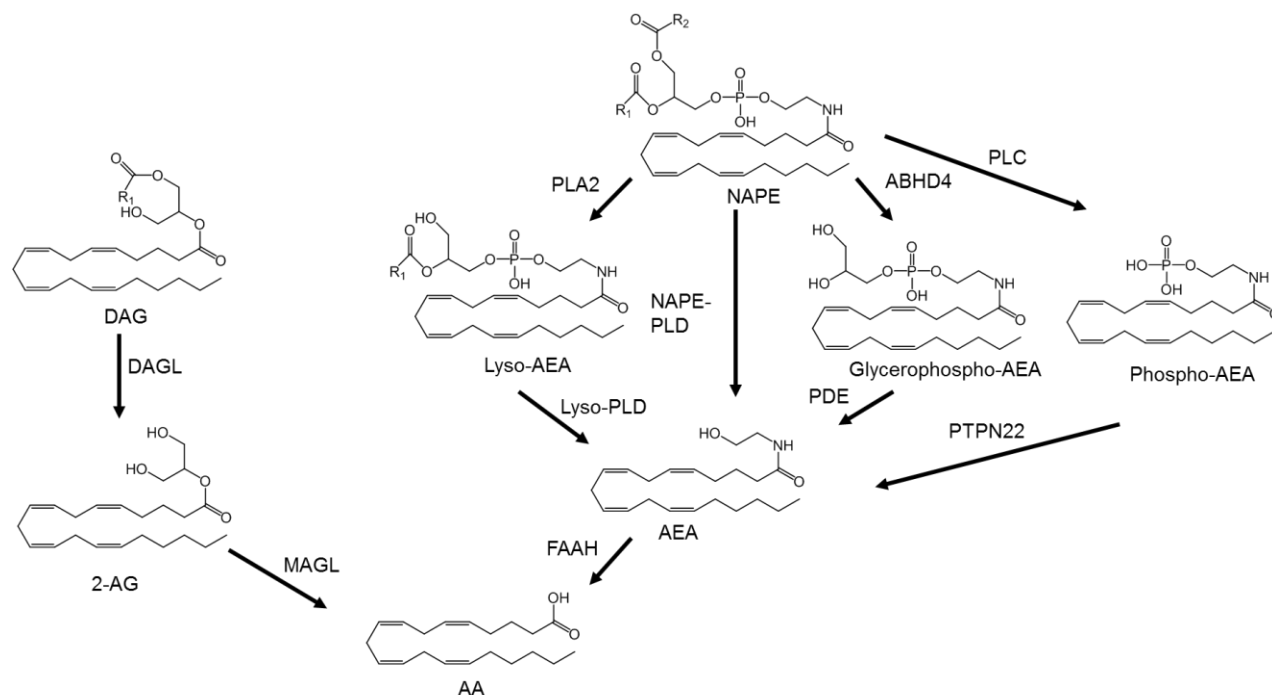


Figure 2. Synthetic and degradative pathways of major endocannabinoids. *N*-arachidonylethanolamide (AEA) can be generated from *N*-arachidonylphosphatidylethanolamine (NAPE) by 1) hydrolysis by NAPE-PLD, 2) a PLC-like hydrolysis of NAPE with subsequent dephosphorylation of phospho-AEA by PTPN22, 3) the double-deacylation of NAPE by α/β -hydrolase 4 (ABHD4) with subsequent hydrolysis of the phosphodiester bond of the resultant glycerophospho-AEA by phosphodiesterase (PDE), or 4) release of Lyso-AEA by phospholipase A2 (PLA2) followed by cleavage by Lyso-phospholipase D (Lyso-PLD). The major pathway for the biosynthesis of 2-arachidonylglycerol (2-AG) involves sequential hydrolysis of diacylglycerol (DAG) by diacylglycerol lipase (DAGL). The degradation of the AEA and 2-AG is catalyzed by fatty acid amide hydrolase (FAAH) and monoacylglycerol lipase (MAGL), respectively, and results in arachidonic acid (AA).

2.2 Endocannabinoids and renal function

The presence and biological significance of the endocannabinoid system in the kidney was first studied soon after the identification of AEA. Deutsch and Chin demonstrated the amidase activity that degrades AEA in the kidney, and later others discovered the transcripts for the CB₁

receptor in the kidney (Deutsch and Chin, 1993; Shire et al., 1995). Further studies have shown the expression of the CB₁ receptor in various areas of the kidney including collecting ducts, glomeruli, loop of Henle, podocytes, mesangial cells and proximal and distal tubular cells (Tam, 2016). The expression and localization of the CB₂ receptor in the kidney is less understood and remains controversial. Some reports were unable to detect its expression in human and rat renal tissues, while others reported expression in human and rat renal cortical tissue, specifically in podocytes, mesangial cells, and proximal tubule cells (Deutsch et al., 1997; Jenkin et al., 2010; Larrinaga et al., 2010; Barutta et al., 2011; Silva et al., 2013). The discrepancy in findings may be attributed to the two splice variants of the CB₂ receptor differing in their distribution in the kidney (Hryciw and McAinch, 2016).

The kidney is unique in its higher basal concentrations of endocannabinoids and their biosynthetic and degrading enzymes. More specifically, the kidney is among a small number of tissues that are enriched with AEA (Long et al., 2011). While the cortex of the kidney contains similar concentrations of AEA and 2-AG, the medulla is reported to have more than two-fold higher concentrations of AEA than 2-AG. In agreement with this finding, the medulla contained lower expression levels of FAAH than the cortex (Ritter et al., 2012). The cellular localization that accounts for the higher concentrations of AEA is still being investigated. Cultured renal mesangial and endothelial cells were shown to synthesize and hydrolyze AEA, and in another study the presence of the biosynthetic and degradative enzymes for AEA was confirmed in renal proximal tubule cells (Deutsch et al., 1997; Sampaio et al., 2015). Altogether, these findings suggest AEA serves a unique functional role in the kidney and in particular the renal medulla.

As mentioned earlier, the most important role of the kidney is the regulation of salt and water homeostasis, and this is essential in the long-term control of arterial blood pressure. Many

years of research of the kidney and the endocannabinoid system provide evidence that AEA has the capacity to regulate the mechanisms of salt and water balance. AEA is a known vasodilator of arteries and arterioles, a mechanism mediated by the CB₁ receptor (Randall et al., 2004). *In vitro* studies reported that exogenously administered AEA had the ability to vasodilate juxtamedullary afferent arterioles and stimulate the release of nitric oxide (NO) by renal endothelial cells (Deutsch et al., 1997). These effects were blocked by both a NO synthase inhibitor and a CB₁ receptor antagonist. Another study showed that in rats receiving AEA intraarterially, total renal blood flow increased and glomerular filtration rate (GFR) decreased, and these effects were completely blocked by the CB₁ receptor antagonists AM281 and AM251 (Koura et al., 2004). Intramedullary infusion of a stable analog of AEA, methanandamide, in anesthetized rats increased the urine excretion rate and decreased mean arterial blood pressure without changing the sodium excretion rate (Li and Wang, 2006). Reports from our laboratory have shown intramedullary infusion of AEA in anesthetized mice stimulated urine and sodium excretion rate (Ritter et al., 2012). The effect of AEA on renal circulation has also been evaluated since medullary circulation is considered to have an important influence on the control of sodium excretion and blood pressure. Li and Wang also showed that intramedullary methanandamide administration had no effect on either renal cortical or medullary blood flow. This is in agreement with data showing that intramedullary infusion of AEA had no effect on renal medullary blood flow (Ritter, J.K., unpublished data).

The reabsorption of sodium and water is an important renal tubular excretory function in maintaining homeostasis, and it has been shown that this can be altered by the endocannabinoid system. In 1977, the well-known CB₁ receptor agonist Δ^9 tetrahydrocannabinol, the main psychoactive ingredient of marijuana, increased urine output which was accompanied by increased

sodium and potassium excretion after oral administration in rats (Sofia et al., 1977). Furthermore, the CB₁ receptor agonist AM2389 elicited a stronger diuretic effect over the non-selective agonists THC and AM4054 (Paronis et al., 2013). In regard to AEA's effect on tubular function, it was demonstrated that AEA can regulate sodium transport at the medullary thick ascending limb by stimulating NO production, resulting in blocking of the Na⁺/H⁺ transporter and NKCC2 cotransporter activity (Silva et al., 2013). Another study reported the Na⁺/K⁺-ATPase in proximal tubule cells activity was modulated by the CB₁/CB₂ agonist WIN55,2112-2 (Sampaio et al., 2015).

The endocannabinoid system has also been implicated to play a sympathoinhibitory role in the modulation of sympathetic neurotransmission. Shortly after the discovery of AEA, Varga et al. studied the effects on blood pressure and discovered a prolonged depressor response to an intravenous bolus of AEA in anesthetized rats (Varga et al., 1996). This response was dose-dependently inhibited by a CB₁ receptor antagonist and by a blockade of α -adrenergic receptors by phentolamine, suggesting the depressor response was due to inhibition of sympathetic tone mediated by CB₁ receptors (Varga et al., 1995). In addition, the effect was shown to be dependent on basal sympathetic tone, as it did not occur in conscious normotensive rats, which lack significant basal tone (Lake et al., 1997). Another study showed that when spontaneously hypertensive rats were treated with the FAAH inhibitor, AM3506, which increases AEA and other lipid ethanolamides, blood pressure and cardiac contractility decreased to normal levels (Godlewski et al., 2010). Overall, these findings highlight the importance of the endocannabinoid system in mediating renal hemodynamics and neuroregulation of cardiovascular functions.

2.3 The ‘endocannabinoid-related’ lipid palmitoylethanolamide

In addition to AEA, there are other endogenous fatty acid derivatives that are present at high concentrations in the kidney, most notably palmitoylethanolamide (PEA) (Long et al., 2011). This lipid ethanolamide is actually present in much higher concentrations than AEA (~10-fold), and similar to AEA, is more concentrated in the medulla compared to the cortex (4.6-fold) (Ritter et al., 2012). It has also been reported that PEA concentrations are significantly increased in kidney tissue of homozygous FAAH knockout mice and of C57BL/6J mice treated with the FAAH inhibitor PF-3845 (Ozalp and Barroso, 2009; Long et al., 2011). These data support the hypothesis of an important role of PEA in the kidney, which is not fully understood.

Like the endocannabinoids, the production of PEA is proposed to occur through on-demand synthesis within the lipid bilayer, though the physiological stimuli that regulate PEA concentrations are largely unknown (Schmid et al., 1990; Cadas et al., 1997). However, this is a topic of debate since PEA concentrations are considerably higher than those of AEA, suggesting a tonic production. In addition, many pro-inflammatory stimuli dampen the production of PEA while triggering AEA formation in the same cell (Solorzano et al., 2009; Zhu et al., 2011a). Nevertheless, biosynthesis of PEA occurs through similar pathways as AEA, with the formation of *N*-palmitoylphosphatidylethanolamine and the subsequent hydrolysis by NAPE-PLD. PEA is hydrolyzed by FAAH and NAE-hydrolyzing acid amidase (NAAA) to form palmitic acid and ethanolamine (Fig. 3) (Piomelli and Sasso, 2014).

PEA was first isolated in 1957 from soy lecithin, peanut meal, and egg yolk and was shown to possess anti-inflammatory properties (Kuehl et al., 1957). In the 1970s PEA was temporarily formulated as tablets under the brand name Impulsin[®] in former Czechoslovakia for its immunosupportive effects in respiratory disorders and influenza (Masek et al., 1974). Further

studies supported the anti-inflammatory actions of PEA in several animal models. However, the mechanism of action was unknown (Benvenuti et al., 1968; Perlik et al., 1973; Lackovic et al., 1977; Lackovic et al., 1978). Furthermore, one study discovered the presence of PEA in various tissues, but its role remained a mystery (Bachur et al., 1965). However, these findings remained largely unnoticed until the work by Rita Levi-Montalcini in the early 1990s. In her 1993 paper, Levi-Montalcini presented evidence that PEA is capable of modulating mast cell activation *in vivo*. She referred to PEA as ‘ALIAmide’ based on the findings that the compound reduced mast cell granulation, a part of local autacoid regulatory effect (‘ALIA’ for ‘autacoid local inflammation antagonist’) (Aloe et al., 1993). This was the first insight into PEA’s pharmacologic activities.

This revival of interest in PEA coincided with the discovery of the endocannabinoid system, and many researchers were determined to find a connection between the system and the “endocannabinoid-related” compound. In his 1992 paper reporting the isolation of AEA, Devane did not classify PEA as an endocannabinoid since his work showed PEA had no affinity for the CB₁ receptor (Devane et al., 1992). However, in 1995, one group suggested AEA and PEA shared activity at the CB₂ receptor based on the finding that PEA could replace the binding of the CB agonist WIN55, 2112-2 on white blood cells and mast cells. They concluded that some of the properties of PEA were due to interactions with CB₂ receptors on mast cells (Facci et al., 1995). Subsequent studies could not replicate these findings, as many tried but failed to show affinity of PEA for the CB₂ receptor (Showalter et al., 1996; Lambert et al., 1999; Sugiura et al., 2000). A putative non-cannabinoid receptor was proposed to explain the lack of PEA binding in CB₁-CB₂-transfected cells, but no receptor for PEA could be identified (Lambert and Di Marzo, 1999).

After it became clear that PEA did not bind to the cannabinoid receptors, a new hypothesis emerged for its effects. This was called the “entourage effect,” and stated that PEA exerts its

actions by potentiation of endocannabinoid actions by reducing the enzymatic degradation of AEA by competition for FAAH, resulting in higher AEA concentrations, which in turn can result in various effects (Ben-Shabat et al., 1998; Lambert and Di Marzo, 1999; Di Marzo et al., 2001; Smart et al., 2002; Ho et al., 2008). This hypothesis was supported by the finding that many actions, mostly its analgesic actions, of PEA were inhibited by the CB₂ receptor antagonist SR144528 (Calignano et al., 1998; Jaggar et al., 1998; Conti et al., 2002). In addition, *in vitro* and *in vivo* studies have shown the enhancement of endocannabinoid actions by PEA (Ho et al., 2008; García et al., 2009).

Though the basis of these observations still remain a mystery, further studies have shown PEA to interact with different receptors and non-receptor targets, so it remains a possibility that its ultimate biological actions are a result of combined-target actions. PEA has been referred to as a “promiscuous” molecule, as it has been demonstrated to possess a broad spectrum of activities, including interactions with peroxisome proliferator activated receptors $\alpha/\gamma/\delta$ (PPAR), TRPV1, G-coupled protein receptors GPR55 and 119, ATP-sensitive K⁺ channels, and Ca²⁺-activated K⁺ channels (Overton et al., 2006; Alexander and Kendall, 2007; Ryberg et al., 2007; Costa et al., 2008; de Novellis et al., 2012; Romero and Duarte, 2012; Syed et al., 2012; Ambrosino et al., 2013) (Fig. 3).

The anti-inflammatory and analgesic effects of PEA has been expounded on as well as the extension of PEA to be effective in treating chronic pain and exerting neuroprotective effects in the brain and spinal cord after trauma or stroke (LoVerme et al., 2005; Esposito et al., 2011; Paterniti et al., 2013). Recent studies have also shown PEA’s capacity to modulate processes in peripheral tissues as well. PEA treatment reduced blood pressure in spontaneously hypertensive rats while increasing urine output and limited kidney damage secondary to high perfusion pressure

(Mattace Raso et al., 2013; Mattace Raso et al., 2015). Clearly, PEA shows a complex pharmacological and biological profile that has the potential to be an important signaling molecule in a variety of disease states.

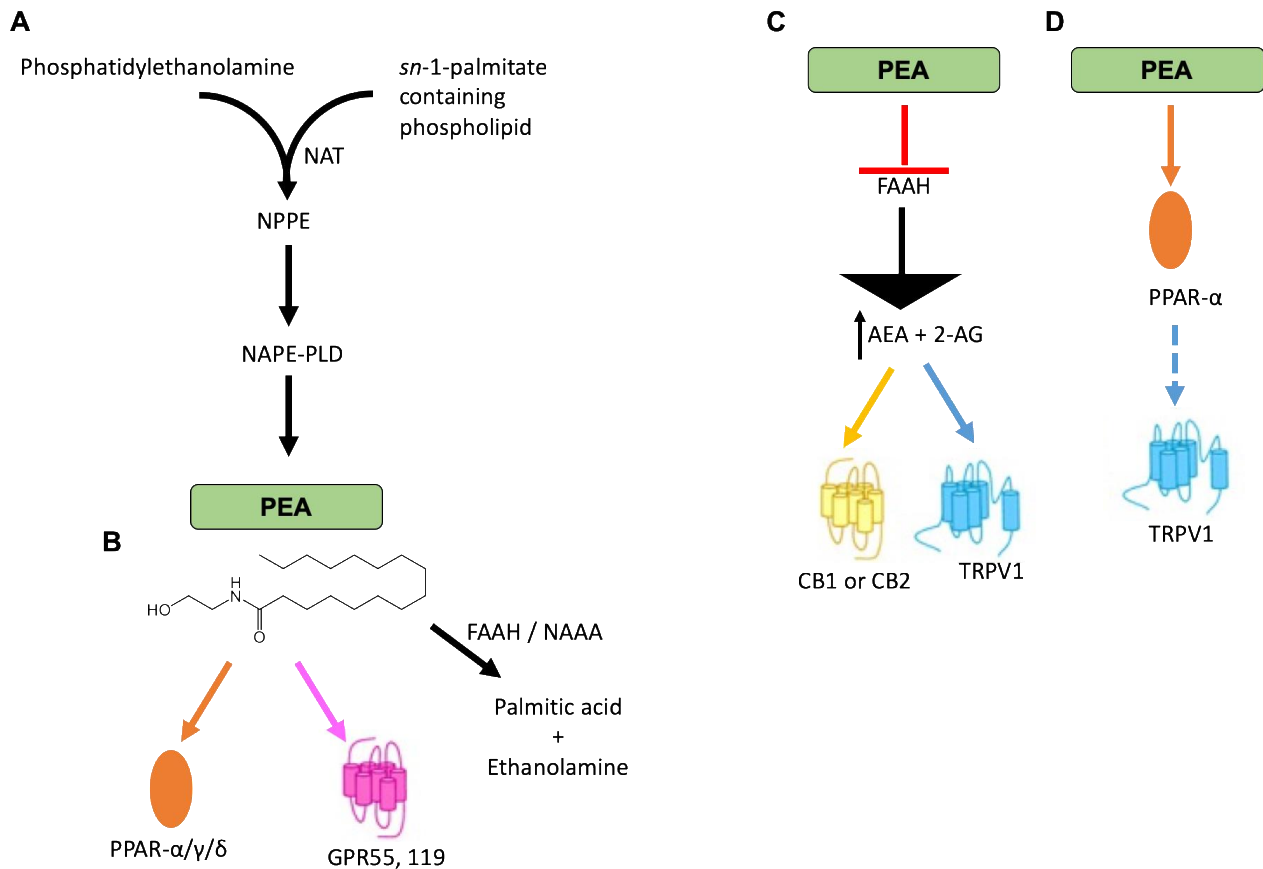


Figure 3. Metabolic pathways and molecular targets of palmitoylethanolamide (PEA). (A) PEA is biosynthesized from a membrane phospholipid, N-palmitoylphosphatidylethanolamine (NPPE) through the direct hydrolysis by NAPE-PLD. PEA can be then degraded to palmitic acid and ethanolamine by either FAAH or NAAA. (B) PEA can directly activate PPAR- $\alpha/\gamma/\delta$, GPR55, or GPR119. (C) PEA can indirectly activate CB₁ or CB₂ receptors and TRPV1 channels by increasing the endogenous levels of AEA and 2-AG through competition for FAAH (entourage effect). (D) PEA may also activate TRPV1 channels via PPAR- α . FAAH, fatty acid amide hydrolase; NAAA, NAE-hydrolyzing acid amidase; NAT, N-acyl-transferase. Adapted from Petrosino et al. 2017

Rationale and hypothesis

The significance of the current research was to investigate the mechanisms underlying the antihypertensive action of the renal medulla in response to elevated arterial blood pressure. Hypertension is a critical public health issue worldwide, and in the United States, it is the leading cause of heart disease, stroke, and kidney failure, contributing to more than 1,100 deaths per day. (Mozaffarian et al., 2015; Yoon et al., 2015). According to the Centers for Disease Control and Prevention, about 1 in 3 adults in the U.S. have high blood pressure and only about half have their high blood pressure under control with medication and life-style changes. Nearly 1 of 3 adults in the U.S. are pre-hypertensive, with the prevalence increasing with age (Merai et al., 2016). The total socioeconomic cost of hypertension is estimated at \$51 billion each year, which includes the cost of health care services, medications to treat hypertension, and missed days of work (Mozaffarian et al., 2015).

The renal medulla is proposed to be critical for the long-term control of body fluid and sodium balance and the regulation of arterial blood pressure. Though the pro-hypertensive system of the kidney, the renin-angiotensin system, is well established, the antihypertensive system of the kidney proposed by Muirhead is less understood. Muirhead described a feedback pressure control system operating from the renal medulla to down-regulate arterial blood pressure. He showed that a rise in blood pressure stimulated the secretion of a neutral lipid from the renal medulla that reduced blood pressure by inducing diuresis and natriuresis, and vasodepression (Muirhead et al., 1976; Muirhead, 1991; Folkow, 2007). He was able to determine this neutral antihypertensive lipid originated from the interstitial cells of the renal medulla and termed this lipid “medullipin.” Although much research has been published on medullipin, its identity still remains unknown. Consequently, the pursuit for neutral lipids that originate from the renal medulla and serve as

antihypertensive regulators continues.

This project was focused on determining whether the lipid ethanolamide palmitoylethanolamide (PEA) produced by renal medullary interstitial cells correspond to or have similar characteristics to the neutral antihypertensive lipid proposed by Muirhead (Muirhead, 1991). PEA is an endogenous neutral lipid ethanolamide that is hydrolyzed by fatty acid amide hydrolase (FAAH). The renal medulla is unique in its high concentration of PEA, along with unique expression pattern of FAAH, suggesting an important role of PEA in the kidney (Long et al., 2011). Recently, FAAH inhibitors have been of interest to a wide variety of research areas. Inhibition of FAAH has been found to be a therapeutic target in the DOCA-salt chronic model (Biernacki et al., 2016; Biernacki et al., 2017). Recently we reported that exogenous intramedullary administration of a dual inhibitor of FAAH and MAGL, isopropyl dodecylfluorophosphonate (IDFP), resulted in augmented diuretic and natriuretic effects without changing mean arterial pressure (MAP) in C57BL/6 mice (Ahmad et al., 2017). Most recently we demonstrated that intramedullary administration of a selective FAAH inhibitor, PF-3845, produced a decrease in MAP and an increase in urine excretion (UV) in C57BL/6 mice (Ahmad et al., 2018). These data suggest that inhibition of FAAH in the renal medulla leads to both a diuretic/natriuretic and blood pressure-lowering response mediated by increased lipid ethanolamides. However, our lab has shown that intramedullary infusion of AEA resulted in diuretic and natriuretic effects, but no effect on mean arterial pressure in C57BL/6 mice (Ritter et al., 2012). Therefore, it is possible that the blood pressure-lowering effect and increase in UV seen with administration of PF-3845 is not due to increased AEA concentrations, but rather increased PEA concentrations in the kidney.

Currently, there is little literature on the possible role of PEA in the kidney in the regulation of blood pressure. Investigating the role of PEA as a possible medullary antihypertensive lipid and understanding its mechanisms will contribute to knowledge needed for the development of improved approaches for treatment or prevention of hypertension by enhancing the endogenous antihypertensive mechanism of the kidney. Therefore, this project investigated the production and regulation of PEA from renal medullary interstitial cells and its possible role in blood pressure regulation.

Chemical inhibition of FAAH in the renal medulla

The first subset of studies tested whether increasing endogenous lipid ethanolamide concentrations can result in antihypertensive actions such as diuresis-natriuresis, decrease in mean arterial pressure (MAP), and an increase in medullary blood flow. Our laboratory has demonstrated FAAH knockout mice are less sensitive to hypertension induced by chronic angiotensin administration (Ritter, J.K., unpublished data). These observations suggest FAAH inhibitors have potential as antihypertensive agents and to elucidate endogenous antihypertensive compounds. The FAAH specific inhibitor, PF-3845, was administered to mice and its effect on renal function and blood pressure was determined.

Effects of PEA administration on renal function and mean arterial pressure

The second set of studies investigated the potential of PEA to serve as neutral lipid antihypertensive compound in the kidney. Since it is reported that intramedullary administration of AEA does not affect MAP, the decrease in MAP observed with administration of the selective FAAH inhibitor PF-3845 is hypothesized to be due to an increase in PEA in the renal medulla and

not AEA. The effects of administration of exogenous PEA on MAP and renal function was determined in normotensive animals. The ability of PEA to counteract increased blood pressure in a chronic hypertension model by exerting antihypertensive actions of inducing diuresis-natriuresis, increasing medullary blood flow and decreasing MAP were also evaluated.

PEA regulation by renal medullary interstitial cells

The last set of experiments studied the cellular mechanism of the antihypertensive system of the kidney in renal medullary interstitial cells cultured from mice. Muirhead and others have postulated that renal medullary interstitial cells (RMICs) are the source of the neutral antihypertensive lipid he termed medullipin. The cells' association with the thin loops of Henle and the vasa recta in the medulla indicate they may be able to regulate tubular functions in response to altered medullary blood flow. Experiments showing that transplantation of renal medullary interstitial cells decreased pressure in hypertensive animal models further support the hypothesis that RMICs contain an antihypertensive compound. RMICs are also characterized by numerous lipid droplets in the cytoplasm (Muirhead et al., 1976). It has been reported that AEA is stored in lipid droplets, and it is hypothesized that PEA is also stored in the lipid droplets of RMICs (Oddi et al., 2008). RMICs were cultured from mice and the production of PEA by the mouse medullary interstitial cells (MMICs) were evaluated using pharmacological and physiological stimuli.

Chapter 3: Modulation of mean arterial pressure and diuresis by infusion of a selective inhibitor of fatty acid amide hydrolase in anesthetized mice

3.1 Introduction

The kidneys play a vital role in the long-term regulation of blood pressure by control of body fluid volume and electrolytes. Thus, it is not surprising that disorders affecting the kidney or renal vasculature commonly lead to secondary form of hypertension (Wadei and Textor, 2012). Kidneys modulate pressure and diuresis through multiple systems including the renin-angiotensin system (Wakui et al., 2015), the sympathetic nervous system (Buckley and Johns, 2011), the endocannabinoid (EC) system (Ahmad et al., 2017), and a possible antihypertensive system (Gothberg, 1994). The roles of the EC system have been well studied in gastrointestinal tract disorders (Wasilewski et al., 2017), peripheral neuropathic pain management (O'Hearn et al., 2017), immunoregulatory role in infectious diseases (Hernández-Cervantes et al., 2017) and brain (Stopponi et al., 2018). However, little is known about specific mechanisms of EC and endocannabinoid-related regulation of renal functions and its role in hypertension.

The EC system consists of the two main cannabinoid receptor agonists, anandamide (AEA) and 2-arachidonylglycerol (2-AG), their hydrolyzing enzymes, fatty acid amide hydrolase (FAAH) and monoacylglycerol lipase (MAGL), and the cannabinoid receptors, CB₁ and CB₂. AEA is synthesized mostly by release from *N*-arachidonoyl phosphatidylethanolamine, mediated by *N*-arachidonoyl phosphatidylethanolamine-specific phospholipase D, and its agonist effect on CB receptors is controlled by FAAH-mediated metabolism to arachidonic acid and ethanolamine (Munro et al., 1993). FAAH is also responsible for hydrolysis of other abundant lipid ethanolamides including palmitoylethanolamide (PEA) and oleoylethanolamide (OEA). In contrast, 2-AG is synthesized from membrane phospholipids by phospholipase C, β , and diacylglycerol lipase (DAGL), and it undergoes hydrolysis by MAGL to form arachidonic acid

and glycerol (Fowler, 2013). Both EC agonists, AEA and 2-AG, have been a subject of great interest due to their capacities to activate cannabinoid receptors (De Petrocellis and Di Marzo, 2009).

In the cardiovascular system, AEA is reported to have a vasodepressor activity and to cause bradycardia by inhibition of the baroreceptor reflex and sympathetic tone (Varga et al., 1995). In the kidney, intramedullary infusion of AEA was reported by our laboratory to stimulate diuretic and natriuretic effects with little or no effect on mean arterial pressure (MAP) in C57BL/6J mice (Ritter et al., 2012). It has been observed that increasing the tissue concentrations of AEA by pharmacological inhibition or genetic ablation of FAAH resulted in augmented hypotensive action of exogenous AEA (Pacher et al., 2005). It can be assumed that inhibiting the EC-hydrolyzing enzymes may produce similar effects as exogenous administration of ECs. There has been much interest in FAAH as a therapeutic target in the treatment of pain and central nervous system disorders (Ahn et al., 2009a), inflammation and pain (Ahn et al., 2009b), and hypertension (Baranowska-Kuczko et al., 2016; Biernacki et al., 2017). More recently, we reported that administration of isopropyl dodecylfluorophosphate (IDFP), a potent inhibitor of both FAAH and MAGL, into the renal medulla of C57BL/6J mice, stimulated diuresis and natriuresis accompanied by increased MBF but did not affect MAP (Ahmad et al., 2017).

These observations led us to test the effect of a FAAH-selective inhibitor infused into the renal medulla. For this purpose, we used PF-3845 (N-3-pyridinyl-4-[[3-[[5-(trifluoromethyl)-2-pyridinyl]oxy]phenyl]methyl]-1-piperidine carboxamide), a highly selective FAAH inhibitor (Ahn et al., 2009b), and evaluated its effects on MAP, medullary blood flow (MBF) and urine excretion rate (UV) after intramedullary or intravenous infusion. To determine the role of FAAH in the mechanism of PF-3845 effects, the responses were also evaluated in mice carrying homozygous

knockout (KO) mutations in the FAAH gene (FAAH KO mice). We also tested the hypotheses that the responses produced by PF-3845 were mediated through cannabinoid receptors. For this purpose, the effects of PF-3845 were also assessed after pretreatment with rimonabant (SR141716), a CB₁ receptor antagonist. To correlate any observed functional changes elicited by PF-3845, the concentrations of 2-AG, AEA, and related lipid ethanolamides PEA and OEA, were measured in kidney tissue and plasma after intramedullary infusion of PF-3845.

3.2 Materials and Methods

Reagents

Phenylmethanesulfonyl fluoride (PMSF), rimonabant, 2-AG, AEA, PEA, and OEA and their deuterated internal standards (2-AG-d₅, AEA-d₈, PEA-d₄, and OEA-d₄) were purchased from Cayman Chemical (Ann Arbor, MI). PF-3845 was purchased from Apex BioTech (San Jose, CA). Ammonium acetate, formic acid, sodium chloride, chloroform, HPLC grade methanol, HPLC grade acetonitrile and HPLC grade water were purchased from Fisher Scientific (Hanover Park, IL). Medical grade nitrogen was purchased from Airgas (Richmond, VA). All other reagents for *in vivo* use were of the highest grade available.

Animals

Two- to four -month old male and female C57BL/6 mice were obtained from Jackson Laboratory (Bar Harbor, ME) while male and female FAAH KO (homozygous gene knockout) mice were from colonies maintained at Virginia Commonwealth University by Dr. Aron Lichtman. The FAAH KO mice were maintained by backcrossing onto a C57BL/6 background for 20 generations (Wise et al., 2008). All mice used in experiments weighed 25-35 g and were housed

4-5 per cage in a temperature- (20-22°C) and humidity-controlled (50-55%) facility with a 12/12 h light/dark cycle and *ad libitum* food and water. All animal protocols were approved by the Institutional Animal Care and Use Committee of Virginia Commonwealth University and were in concordance with the National Institutes of Health Guide for the Care and Use of Laboratory Animals.

Acute surgical preparation

Mice were prepared for acute renal function studies as described (Ahmad et al., 2017). Briefly, anesthesia was induced by intraperitoneal administration of ketamine (Ketathesia™, 100 mg/kg, Harry Schein Animal Health, Dublin, OH) and thiobutabarbital (Inactin™, 75 mg/kg, Sigma Chemical Co., St. Louis, MO). The body temperature of the mice was maintained by placing them on a surgical table that was thermally stable at 37°C. A tracheotomy was performed to facilitate breathing which was followed by cannulation of the left carotid artery with a blood pressure probe for continuous monitoring of blood pressure and of the right jugular vein for constant rate infusion of vehicle and vehicle containing drugs into the systemic circulation. The blood pressure probe was attached to a pressure transducer connected to a data acquisition system (Windaq, DATAQ Instruments, Akron, OH).

The infusion of drugs into the renal medulla was through a catheter with a tapered tip (2.5 mm in length) inserted into the outer medulla from the dorsal side of the right kidney and anchored on the surface of the kidney using VetBond tissue adhesive (3M Co., Minneapolis, MN) as described (Li et al., 2005; Zhu et al., 2011b; Ritter et al., 2012). The infusion solution contained phosphate-buffered saline (205 mM NaCl, 40.5 mM Na₂HPO₄, and 9.5 mM NaH₂PO₄ (pH 7.4, 610 mOsM) and 10% ethanol at a rate of 2 µL/min. The left kidney ureter was ligated and cut

proximal to the kidney. The bladder was cannulated to enable the collection of urine into pre-weighed tubes for gravimetric determination of UV. Urine sodium and potassium concentrations were measured by flame photometry to permit determination of the urinary sodium (UNa) and potassium (UK) excretion rates. All urinary parameters were calculated on a per gram kidney weight (g kwt) basis. Mice were infused through the jugular vein with a vehicle containing 0.9% NaCl solution and 2% bovine serum albumin at the rate of 5 μ L/min/25 g body weight to maintain fluid homeostasis in the body. MBF was measured using a laser Doppler flow probe (OxyFlo Probe, MNP 100XP, Oxford, UK) placed on the lower lateral surface of the kidney. After a 1 hr equilibration period and establishment of a stable baseline, urine was collected every 10 min during the experimental period. The two 10 minute samples collected immediately prior to the start of drug treatments, representing the pre-treatment control periods, were designated C1 and C2. PF-3845 was administered into the renal medulla in the infusion solution at rates of 3.75, 7.5, 15 and 30 nmol/min/kg for 30 min at each dose. The first 10 min average of the values between 10 and 30 min equilibration period was used to calculate. The effects of rimonabant (3mg/kg, i.p. bolus) and celecoxib (15mg/kg, i.v.) on the responses to PF-3845 were determined using the same strategy. Sham control mice were treated identically to drug-treated mice except that they received intravenous and intramedullary vehicle solutions only for the entire experimental duration. At the termination of the experiment, blood was drawn from the carotid artery into a heparinized tube and centrifuged. The plasma and the right and left kidneys were collected, weighed, and stored at -80C for later analyses. The position of the medullary catheter was confirmed after sagittal sectioning of the right kidney.

Kidney tissue and plasma analysis of 2-AG, AEA, OEA, and PEA by ultra-high performance liquid chromatography-tandem mass spectrometry (UPLC-MS/MS)

Internal standard solution (10 μ L) containing 10 ng each of AEA-d₈, PEA-d₄, and OEA-d₄ and 100 ng 2-AG-d₅ was added to each plasma (100 μ L), kidney tissue (90-100 mg) or calibrator samples. 1 mM PMSF was added to all samples. Chloroform: methanol (3 mL of 2:1 (v/v)) and aqueous sodium chloride (200 μ L) of 0.73% were added to all samples and calibrators. The tissue samples were then homogenized for 30 sec using a Brinkmann Polytron[®] PT 3000 homogenizer and centrifuged at 3500 rpm for 5 min. Plasma samples and calibrators were mixed for 5 min then centrifuged at 3500 rpm for 5 min. The organic phases were collected and the aqueous phases were extracted twice more with chloroform (1 mL). The organic phases were combined and evaporated to dryness under nitrogen, reconstituted in 100 μ L 60:40 water: acetonitrile and placed in autosampler vials for UPLC-MS/MS analysis.

The UPLC-MS/MS analysis was performed on a Sciex 6500+ QTRAP system with an IonDrive Turbo V source for TurbolonSpray[®] (Ontario, Canada) attached to a Shimadzu Nexera X2 UPLC system (Kyoto, Japan) controlled by Analyst 1.6.3 software (Ontario, Canada). Chromatographic separation was performed on a Discovery[®] HS C18 Column 15cm x 2.1mm, 3 μ m (Supelco: Bellefonte, PA) kept at 40°C and 2 μ L of sample was injected. The mobile phase consisted of A: water with 1 g/L ammonium acetate and 0.1% formic acid and B: acetonitrile. The following gradient was used: 0.0 to 2.4 minutes at 40% B, 2.5 to 6.0 minutes at 60% B, hold for 2.1 minutes at 60% B, then 8.1 to 9 min 100% B, hold at 100% B for 3.1 min and return to 40% B at 12.1 min. The flow rate was 1.0 mL/min and total run time was 14 minutes. The acquisition mode used was Multiple Reaction Monitoring (MRM). The transition ions (m/z), deprotonation potentials (V), and corresponding collision energies (V) for all of the compounds can be found in

Table 1. A calibration curve was constructed for the assay by linear regression using the peak area ratios of the calibrators and internal standards. The standard curve ranged from 1-100 ng for AEA, PEA, and OEA, and 10-1,000 ng for 2-AG. Calibration curves had a correlation (r^2) of 0.9988 or better.

Table 1. Multiple reaction monitoring (MRM) parameters for 2-AG, AEA, OEA, and PEA analysis by UPLC-MS/MS

Compound	Transition ions (<i>m/z</i>)	DP (V)	CE (V)
2-AG	379 > 287	45	26
	379 > 269	45	28
2-AG-d ₅	384 > 62	45	26
AEA	348 > 62	26	13
	348 > 91	26	60
AEA-d ₈	356 > 62	26	13
OEA	326 > 62	40	30
	326 > 309	40	20
OEA-d ₄	330 > 66	40	30
PEA	300 > 62	31	28
	300 > 283	31	19
PEA-d ₄	304 > 62	31	28
Deprotonation Potential = DP		Collision Energy = CE	

Statistical Analyses

Data are presented as the mean \pm S.E.M. For multiple group comparisons, one- or two-way analysis of variance (ANOVA) was performed using a Tukey post-hoc test when significant differences were found, using the first pre-infusion control phase, C1, as the control. For cross group comparisons of intramedullary PF-3845 treatment alone to intramedullary PF-3845 treatment after rimonabant pretreatment, one way ANOVA was performed using a Fisher's LSD post-hoc test. Data were considered statistically significant when $p \leq 0.05$.

3.3 Results

3.3.1 PF-3845 administration stimulates diuresis-natriuresis and lowers mean arterial pressure in C57BL/6J mice

Effects of intramedullary and intravenous infusions of PF-3845 on MAP and UV in C57BL/6J mice

The effect of PF-3845 infusion into the right renal medulla of C57BL6/J mice on MAP and UV are presented in Figs. 4A and 4B. The baseline MAP of C57BL/6J mice during the pre-treatment control phases, C1 and C2, was 112 and 116 mmHg, respectively. Although intramedullary (i.med.) infusion of PF-3845 at increasing sequential doses of 3.75, 7.5, 15 and 30 nmol/min/kg did not significantly decrease MAP, a downward trend in MAP that was dose-dependent was evident. MAP further declined during the post-treatment control phases, P1 and P2, to 82 and 79 mmHg, respectively, which were significantly lower compared to the C1 pre-treatment control phase ($p < 0.05$). The baseline rate of urine formation in C57BL/6J mice was 11 and 12 $\mu\text{l}/\text{min}/\text{g}$ kwt for the C1 and C2 control phases, respectively. Intramedullary infusion of

PF-3845 increased UV ($p < 0.05$) to 22 and 28 $\mu\text{l}/\text{min}/\text{g kwt}$ at the two highest dose rates, 15 and 30 $\text{nmol}/\text{min}/\text{kg}$, respectively, compared to the C1 phase. During the post-treatment phases, UV remained significantly elevated at P1 ($p < 0.05$) but not P2. There were no significant changes in either MAP or UV of sham-treated control C57BL/6J mice, which received only vehicle infusion during the entire experimental period.

For comparison, the effects of intravenous (i.v.) PF-3845 on MAP and UV at the same dose rates were determined (Fig. 4C and 4D). The baseline MAP of C57BL/6J mice during the C1 and C2 control phases was 116 and 113 mm Hg, respectively, while intravenous administration of PF-3845 dropped MAP significantly ($p < 0.05$) by 20, 22 and 25 mmHg at 7.5, 15, and 30 $\text{nmol}/\text{kg}/\text{min}$ doses, respectively, relative to C1. MAP declined further during the post-treatment phases, 35 and 38 mm Hg for P1 and P2. In contrast, intravenous PF-3845 significantly increased UV from 11 and 12 $\mu\text{l}/\text{min}/\text{g kwt}$ for C1 and C2 to 21 and 28 $\mu\text{l}/\text{min}/\text{g kwt}$ at the two highest doses ($p < 0.05$). The peak increase in UV (35 $\mu\text{l}/\text{min}/\text{g kwt}$) was reached during the P1 post-treatment phase, declining during P2.

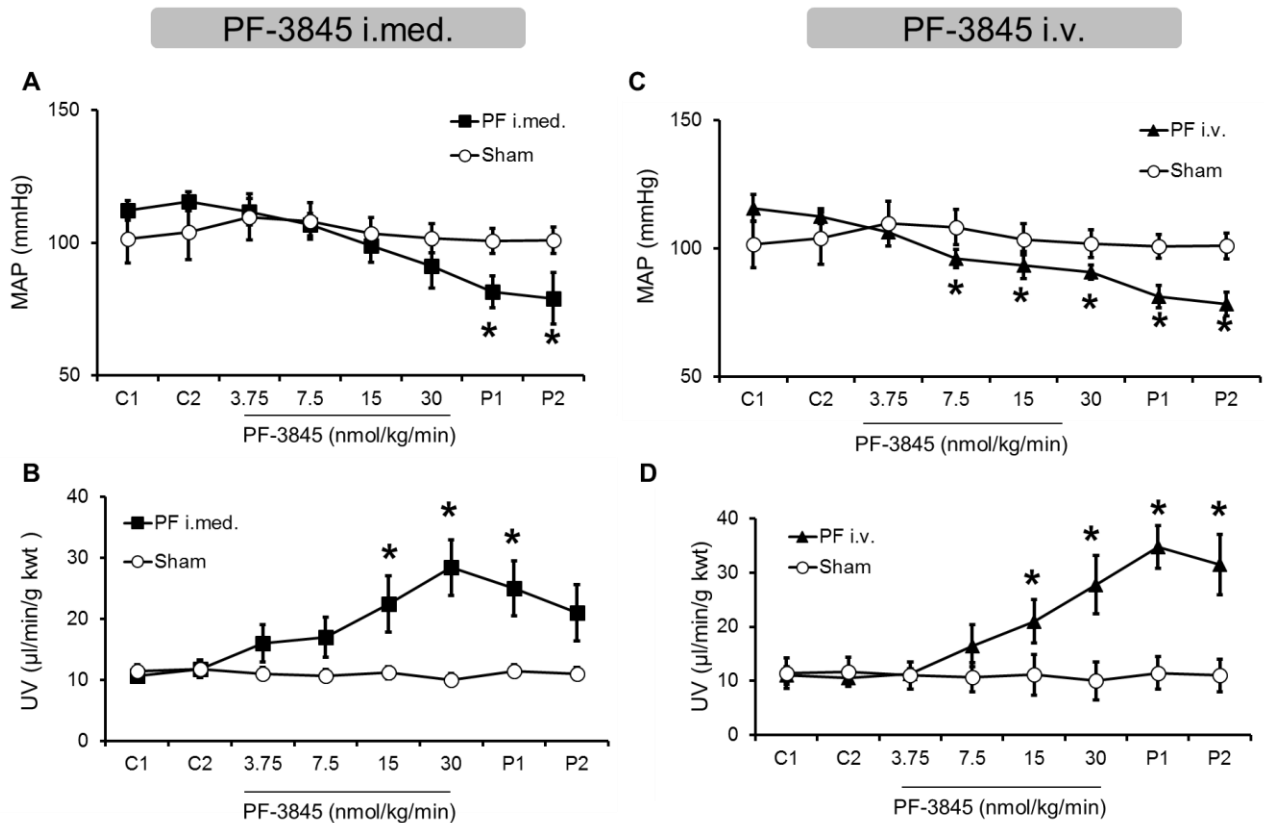


Figure 4. The effects of intramedullary and intravenous infusion of PF-3845 on MAP and UV in C57BL/6J mice. Control infusion periods with vehicle alone (C); 3.75, 7.5, 15, and 30 indicate dose rates for PF-3845 infusion (in $\text{nmol}\cdot\text{kg}^{-1}\cdot\text{min}^{-1}$) and post-treatment control infusion periods (P). Data represent the mean \pm the standard error of each group. *Significant difference vs. the C1 control group ($p < 0.05$; $n = 5-7$ per group). kwt, kidney weight; MAP, mean arterial pressure; PF, PF-3845; N-3-pyridinyl-4-[[3-[[5-(trifluoromethyl)-2-pyridinyl]oxy]phenyl]methyl]-1-piperidine carboxamide; UV, urine formation rate; n, sample size.

Effects of intramedullary and intravenous infusion of PF-3845 on urinary sodium and potassium excretion rates and medullary blood flow in C57BL/6J mice.

Intramedullary infusion of PF-3845 into the medulla of the right kidney produced significant elevations in both urinary sodium and potassium excretion rate (1.2 and 2.2 $\mu\text{mol}/\text{min}/\text{g}$ kwt at 30 $\text{nmol}/\text{min}/\text{kg}$, $p < 0.05$), in comparison with C1 (Figs. 5A and 5B). MBF was also

increased ($p < 0.05$), but the effect was significant after administration of 7.5, 15 and 30 nmol/min/kg. MBF increased from 0.9 and 0.9 volts in C1 and C2 to 1.4, 1.5 and 1.8 volts at the three highest doses (Fig. 5C). Intravenous infusion of PF-3845 at increasing doses elevated urinary sodium excretion from 0.16 to 1.28 $\mu\text{mol}/\text{min}/\text{g}$ kwt and potassium excretion from 0.32 to 1.45 $\mu\text{mol}/\text{min}/\text{g}$ kwt respectively at 30 nmol/min/kg vs. the C1 control phase (Fig. 5D and 5E). MBF increased significantly ($p < 0.05$) at the 7.5, 15 and 30 nmol/min/kg doses, respectively (Fig. 5F).

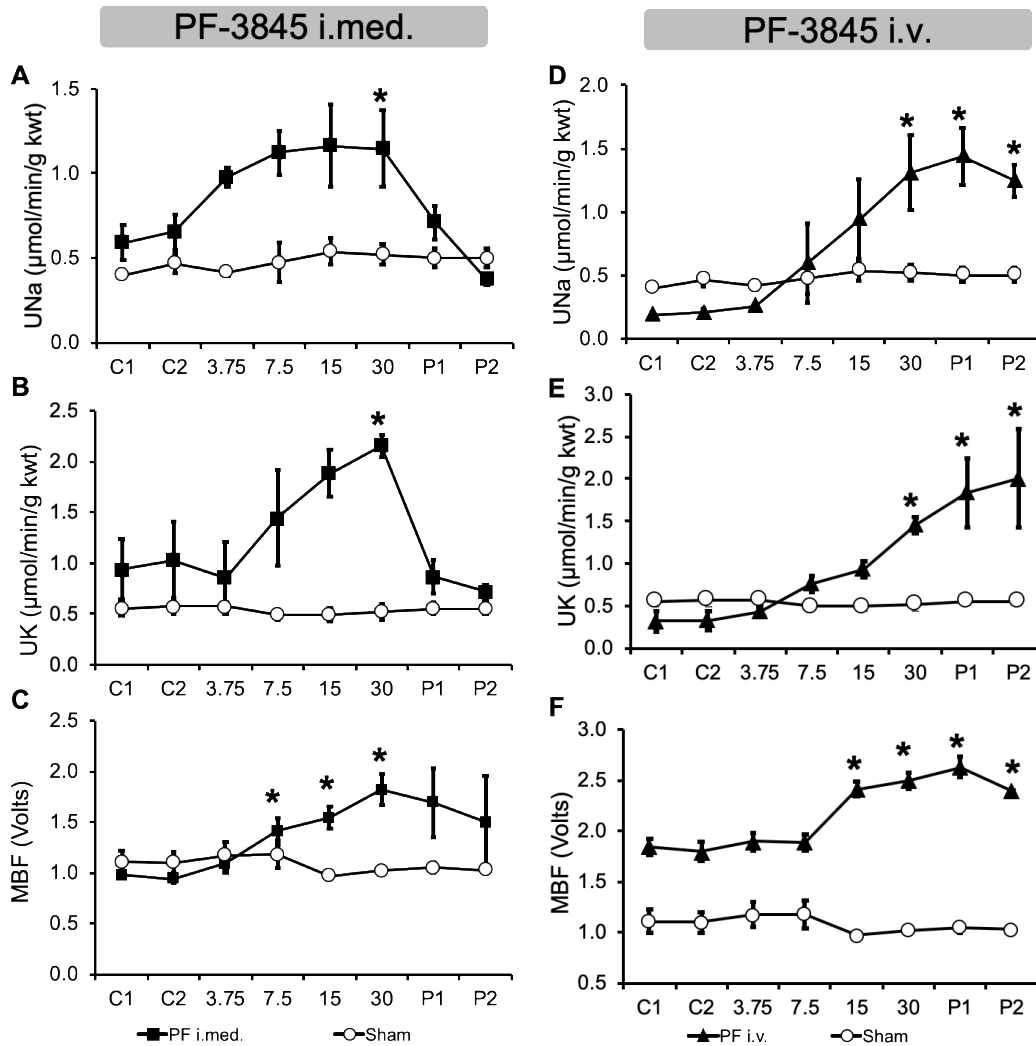


Figure 5. The effects of intramedullary and intravenous infusions of PF-3845 on UNa and UK and MBF in C57BL/6J mice. Control infusion periods with vehicle alone (C); 3.75, 7.5, 15, and 30 indicate dose rates for PF-3845 infusion (in units of $\text{nmol}\cdot\text{kg}^{-1}\cdot\text{min}^{-1}$), and post-treatment control infusion periods (P). Data represent the mean \pm the standard error of each group. *Significant difference vs. the respective C1 control group ($p < 0.05$; $n = 5-7$ for PF-3845 and $n = 3$ for Sham control). kwt, kidney weight; MBF, medullary blood flow; PF, PF-3845; N-3-pyridinyl-4-[[3-[[5-(trifluoromethyl)-2-pyridinyl]oxy]phenyl]methyl]-1-piperidine carboxamide; UK, urine potassium excretion rate; UNa, urine sodium excretion rate; n, sample size.

Effects of intramedullary infusion of PF-3845 on 2-AG, AEA, OEA, and PEA concentrations in plasma and kidney tissue of C57BL/6J mice

The concentrations of AEA, OEA, PEA, and 2-AG in kidney tissue and plasma of control and PF-3845-treated mice were determined by UPLC-MS/MS (Fig. 6). In C57BL/6J mice, AEA, PEA, and OEA were all significantly increased with intramedullary PF-3845 in kidney tissue ($p < 0.05$) (Fig. 6A). In contrast, AEA, PEA, and OEA were decreased in the plasma of intramedullary-PEA treated mice, but this decrease was not significant (Fig. 6B). 2-AG was significantly increased in the plasma by intramedullary PF-3845 ($p < 0.05$) (Fig. 6B).

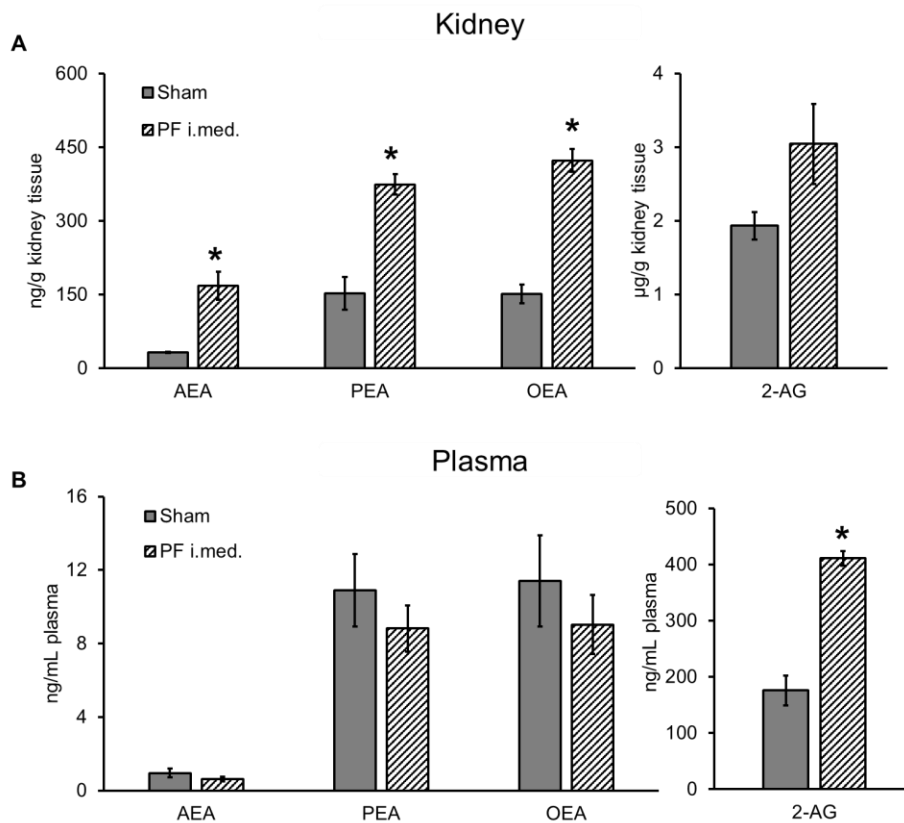


Figure 6. Anandamide (AEA), palmitoylethanolamide (PEA), oleoylethanolamide (OEA), and 2-arachidonylglycerol (2-AG) concentrations in kidney tissue and plasma of sham control and intramedullary PF-3845-infused C57BL/6J mice. Data represent the mean \pm the standard error of each group. * Significant difference vs the sham control group ($p < 0.05$; $n = 5-6$ per group) in an unpaired, two-tailed t-test. PF; N-3-pyridinyl-4-[[3-[[5-(trifluoromethyl)-2-pyridinyl]oxy]phenyl]methyl]-1-piperidine carboxamide.

3.3.2 PF-3845 administration stimulates diuresis in FAAH KO mice

Effects of intramedullary and intravenous infusions of PF-3845 on MAP and UV in FAAH KO mice

Corresponding experiments were conducted to characterize the effect of intramedullary and intravenous PF-3845 in FAAH KO mice (Figs. 7A-7D). The baseline MAP of FAAH KO mice following the 1 hr equilibration period was 95 and 96 mmHg during C1 and C2, respectively. Intramedullary infusion of PF-3845 did not significantly change MAP at any of the four doses tested or during the post-treatment phases (Fig. 7A). The baseline UV in FAAH KO mice prior to intramedullary PF-3845 infusion was 4 and 3 $\mu\text{l}/\text{min}/\text{g}$ kwt for C1 and C2, respectively. Intramedullary administration of the lowest PF-3845 dose tested (3.75 nmol/min/kg) did not change UV. However, UV was significantly increased ($p < 0.05$) after the three highest doses (18, 20 and 24 $\mu\text{l}/\text{min}/\text{g}$ kwt after 7.5, 15 and 30 nmol/min/kg, respectively when compared to the C1 phase (Fig. 7B). UV remained elevated during both post-treatment phases. There were no significant changes in either MAP or UV of sham-treated control FAAH KO mice, which received only vehicle infusion during the entire experimental period.

In the experiment to assess intravenously administered PF-3845 on MAP in FAAH KO mice (Fig. 7C and 7D), the average MAP during the C1 and C2 control phases was 98 and 96 mmHg, respectively. MAP was not significantly different from the C1 control group at any of the four intravenous PF-3845 doses tested (3.75, 7.5, 15 and 30 nmol/min/kg). Interestingly, a significant drop in MAP occurred in both post-treatment groups, P1 and P2: 80 and 77 mmHg, respectively (Fig. 7C). The baseline UV of FAAH KO mice measured prior to intravenous PF-3845 was 4 and 2 $\mu\text{l}/\text{min}/\text{g}$ kwt during C1 and C2, respectively. Whereas intravenous administration of PF-3845 at the lowest dose did not significantly increase UV, the 7.5, 15 and 30

nmol/min/kg groups were increased to 23, 23 and 26 respectively and this increase in UV was significant (all $p < 0.05$) compared to the C1 group. After shifting back to the vehicle, UV remained elevated during the P1 period but not P2.

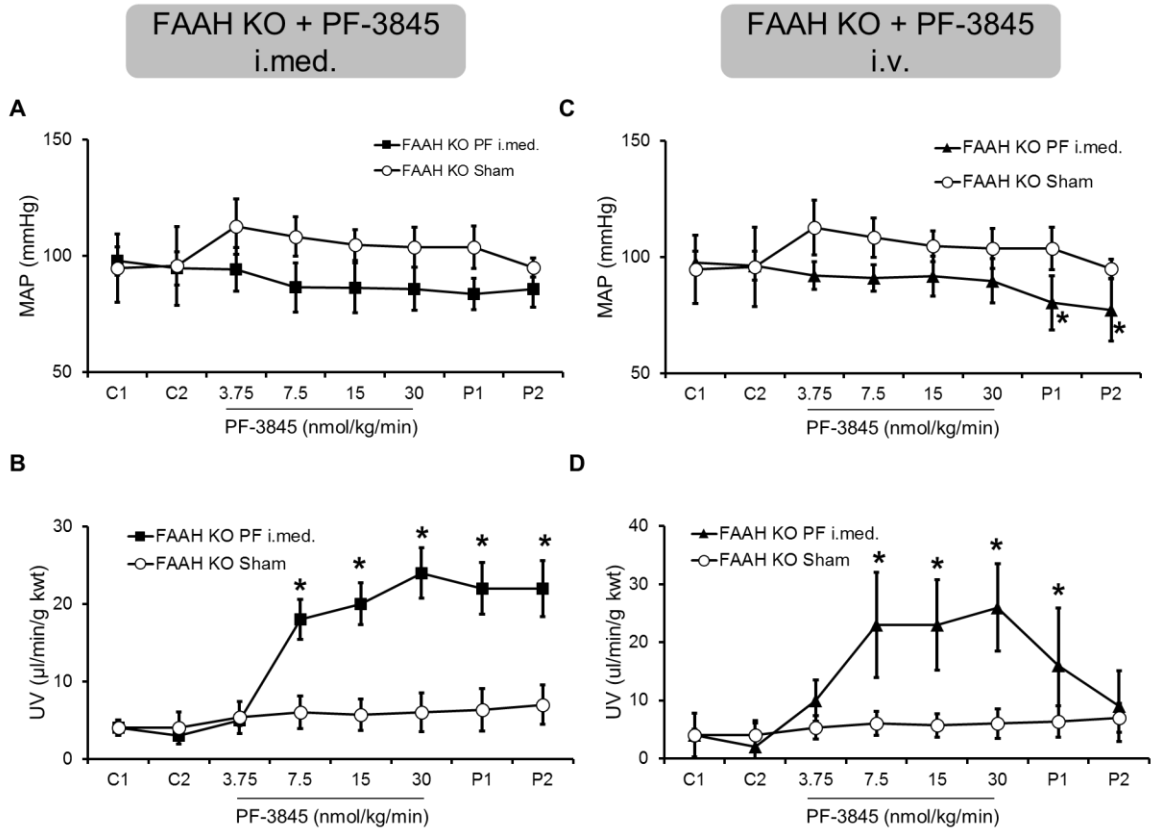


Figure 7. The effects of intramedullary and intravenous infusion of PF-3845 on MAP and UV in FAAH KO mice. Control infusion periods with vehicle alone (C); 3.75, 7.5, 15, and 30 indicate dose rates for PF-3845 infusion (in $\text{nmol}\cdot\text{kg}^{-1}\cdot\text{min}^{-1}$) and post-treatment control infusion periods (P). Data represent the mean \pm the standard error of each group. *Significant difference vs. the C1 control group ($p < 0.05$; $n = 5-7$ per group). kwt, kidney weight; MAP, mean arterial pressure; PF, PF-3845; N-3-pyridinyl-4-[[3-[[5-(trifluoromethyl)-2-pyridinyl]oxy]phenyl]methyl]-1-piperidine carboxamide; UV, urine formation rate; n, sample size.

Effects of intramedullary infusion of PF-3845 on 2-AG, AEA, OEA, and PEA concentrations in plasma and kidney tissue of FAAH KO mice

The concentrations of 2-AG, AEA, OEA, and PEA in kidney tissue and plasma of control and PF-3845-treated FAAH KO mice were determined by UPLC-MS/MS (Fig. 8). In FAAH KO

mice, AEA, PEA, and OEA were all significantly decreased with intramedullary PF-3845 in kidney tissue ($p < 0.05$) (Fig. 8A). AEA, PEA, and OEA were decreased in the plasma of intramedullary treated mice, but this decrease was not significant (Fig. 8B). 2-AG concentrations in kidney and plasma were not significantly affected by PF-3845 administration.

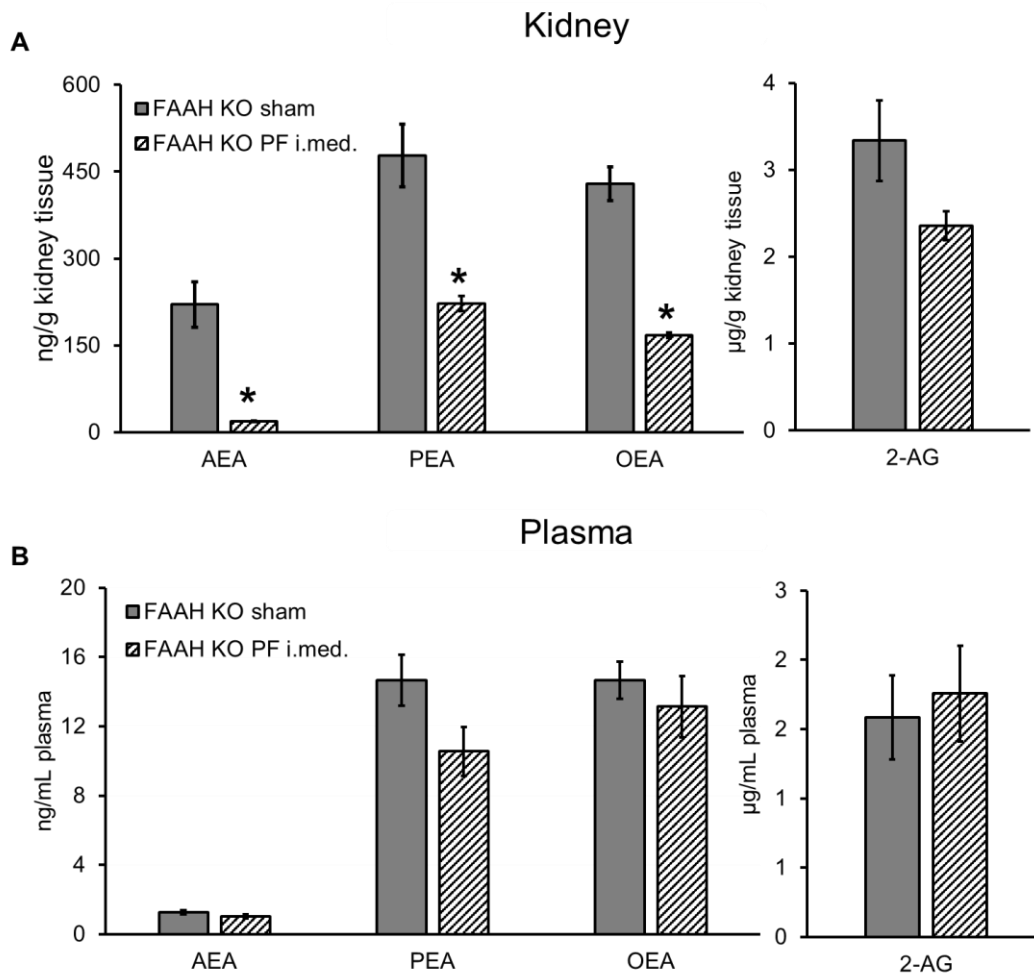


Figure 8. Anandamide (AEA), palmitoylethanolamide (PEA), oleoylethanolamide (OEA), and 2-arachidonylglycerol (2-AG) concentrations in kidney tissue and plasma of sham control and intramedullary PF-3845-infused FAAH KO mice. Data represent the mean \pm the standard error of each group. * Significant difference vs the sham control group ($p < 0.05$; $n = 5-6$ per group) in an unpaired, two-tailed t-test. PF; N-3-pyridinyl-4-[[3-[[5-(trifluoromethyl)-2-pyridinyl]oxy]phenyl]methyl]-1-piperidine carboxamide.

3.3.3 PF-3845-induced diuresis and blood pressure-reducing effect is CB₁ mediated

Effects of a CB₁ receptor antagonist on the blood pressure-lowering and diuresis stimulating responses to intramedullary PF-3845

The baseline MAP of C57BL/6J mice prior to rimonabant treatment was 112 and 109 mmHg during the C1 and C2 phases, respectively (Fig. 9A). Administration of rimonabant (3 mg/kg, i.p.) decreased MAP significantly ($p < 0.05$) to 91 mmHg, compared to C1. MAP was not changed with subsequent intramedullary administration of PF-3845, compared to the rimonabant pretreatment group. MAP remained at 79, 81, 80 and 80mmHg at the 3.75, 7.5, 15 and 30 nmol/min/kg dose rates. The baseline UV of the C57BL/6J mice was 15 and 16 $\mu\text{l}/\text{min}/\text{g}$ kwt during C1 and C2, which was not significantly changed by the rimonabant pretreatment (Fig. 9B). PF-3845 subsequently administered into the medulla of the right kidney did not significantly stimulate diuresis at any dose rate.

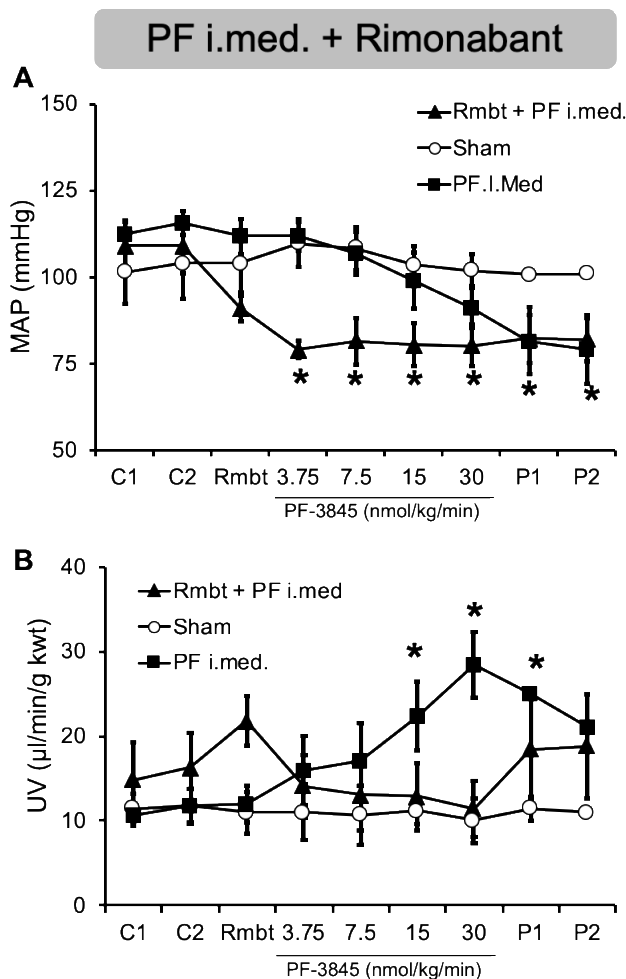


Figure 9. The effects of rimonabant pretreatment on the MAP and UV responses to intramedullary infusion of PF-3845 in C57BL/6J mice. Control infusion periods with vehicle alone (C); 3.75, 7.5, 15, and 30 indicate dose rates for intramedullary PF-3845 infusion ($\text{nmol}\cdot\text{kg}^{-1}\cdot\text{min}^{-1}$). Period of rimonabant (SR141716A) pretreatment (Rmbt; 3 mg/kg, i.p.) and post-treatment control infusion periods (P). Data represent the mean \pm the standard error of each group. *Significant difference vs. the respective C1 control group ($p < 0.05$; $n = 5-7$ per group). kwt, kidney weight; MAP, mean arterial pressure; PF, PF-3845, N-3-pyridinyl-4-[[3-[[5-(trifluoromethyl)-2-pyridinyl]oxy]phenyl]methyl]-1-piperidine carboxamide; Rmbt, rimonabant; UV, urine formation rate; n, sample size.

3.4 Discussion

The present study was designed to investigate the hypothesis that exogenous administration of a selective FAAH inhibitor into the right renal medulla would produce similar responses in UV and modulation of MAP as that of AEA. It also explored the hypothesis that EC receptors would

be required for PF-3845 to modulate UV and MAP. Lastly, the design also enabled us to examine possible interactions between the EC AEA and other lipid ethanolamides, by evaluating the effect of pharmacological inhibition of FAAH on AEA, PEA, and OEA concentrations in plasma and kidney tissue. The study resulted in several novel observations. Intramedullary and systemic infusions of PF-3845 increased urinary and salt excretion while decreasing MAP. The data also showed that the mechanism by which PF-3845 increased UV and decreased MAP was dependent on CB₁, effects that were accompanied by elevated kidney and decreased plasma concentrations of AEA, PEA, and OEA. Lastly, the MAP-reducing effect of PF-3845 was not observed in FAAH KO mice, but diuresis was still stimulated.

Intramedullary infusion of PF-3845 in C57BL/6J mice resulted in increased urinary excretion (Fig. 4B), and the analytical data showed that this effect was accompanied by elevated kidney concentrations of AEA, PEA, and OEA. (Fig. 7A). These data are consistent with earlier data from our laboratory (Ritter et al., 2012) and others (Li and Wang, 2006) showing that infusion of exogenous AEA into the renal medulla elicits a diuretic effect (Li and Wang, 2006; Ritter et al., 2012). The current study extends this by showing that elevation of endogenous AEA in the kidney, along with PEA and OEA, in response to FAAH inhibition can produce the diuretic effect as well. Interestingly, intramedullary PF-3845 decreased plasma concentrations of AEA, PEA and OEA. This may be due to the time of plasma collection. The post-treatment time period might have allowed for lipid ethanolamide reuptake by tissues, since it has been reported that PEA and AEA uptake can occur rapidly (Bisogno et al., 1997; Glaser et al., 2005). FAAH is highly expressed in kidney relative to most tissues (Long et al., 2011), and in the kidney, it is most highly expressed in renal tubular cells (Ritter et al., 2012). Our recent observation that an inhibitor of both FAAH and MAGL, isopropyl dodecylfluorophosphonate (IDFP), was an effective stimulator of diuresis

(Ahmad et al., 2017) led us to evaluate a highly selective FAAH inhibitor. The present study found that the diuretic action of PF-3845 is CB₁-dependent (Fig. 6B) in C57BL/6J mice. The finding of CB₁-dependence agrees with other studies reporting diuretic effects of CB₁ receptor agonists (Chopda et al., 2013; Paronis et al., 2013), but it appears contrary to the data of Li and Wang (2006), who found that the diuretic effect of intramedullary methanandamide, a longer-lasting derivative of AEA, was insensitive to CB₁ blockade (Li and Wang, 2006).

Treatment of C57BL/6J mice with PF-3845 resulted in increased urinary excretion of both sodium and potassium. These effects were observed after either intramedullary or intravenous administration of the drug and they were accompanied by increased MBF (Fig. 5C and 5D). These data support a role of increased MBF in the diuretic mechanism of PF-3845. A washing out of the hyperosmotic environment of the renal medulla is consistent with decreased capacity to reabsorb sodium and fluid from the urinary filtrate. These data have similarity to those described for intramedullary infusion of the FAAH and MAGL inhibitor, IDFP, including stimulated diuresis, salt excretion and MBF (Ahmad et al., 2017). The data in the current study support that inhibition of FAAH may account for the reported effects of IDFP. The mechanism of increased MBF by intramedullary PF-3845 in C57BL/6J may be attributed to an action of AEA or PEA to produce medullary nitric oxide which increases MBF (Rajapakse and Mattson, 2011).

Another interesting finding of this study was the drop in MAP after intramedullary or intravenous infusion of PF-3845 in C57BL/6J mice (Figs. 4A and 4C). Similar to the diuretic effect, this MAP-reducing effect in C57BL/6J mice appears to be mediated by CB₁ receptors, based on its blockade by pretreatment with rimonabant. The mechanism of the reduced MAP after PF-3845 treatment remains to be determined, but there are several possibilities. The first is that it may be related to the ongoing loss of effective blood volume secondary to increased diuresis and

salt excretion. However, the observation that acute intramedullary AEA (Ritter et al., 2012) has apparent similar diuresis-inducing capacity in the absence of any changes in MAP argues against this possibility. The MAP-lowering effect could be mediated by a substance entering the circulation from the kidney after PF-3845 treatment to lower systemic resistance by an action on the peripheral vasculature. AEA has well known vasodepressor properties mediated by CB₁ receptors (Varga et al., 1995). However, its plasma level was not found to be altered by intramedullary PF-3845 in this study. The possibility that it is a substance indirectly stimulated by AEA in the kidney and released into the circulation, such as nitric oxide (NO) (Deutsch et al., 1997; Mombouli et al., 1999) may be considered. NO is considered to have a critical role in the renal medulla for the control of MBF and blood pressure (Mattson et al., 1994; Mattson, 2003). Two additional possibilities are that it is mediated by 2-AG, which is increased in plasma of PF-3845 treated mice (Fig. 6B) or that it is due to escape of PF-3845 into the systemic circulation to inhibit FAAH and elevate AEA in the peripheral vasculature. Another possibility for the drop in MAP by PF-3845 is the reduced production of vasoconstrictors. Inhibition of FAAH by PF-3845 decreases the pool of arachidonic acid to be metabolized into vasoconstrictors such as 20-HETE and thromboxane A₂ (Cediel et al., 2002; Pandey et al., 2017).

Surprisingly, infusion of PF-3845 either intravenously or intramedullary into FAAH KO mice was still able to produce a diuretic response (Figs. 7B and 7D). This observation suggests that a second mechanism independent of FAAH can be activated by PF-3845 treatment in the renal medulla of FAAH KO mice. It is noteworthy that the lipid ethanolamides AEA, PEA, and OEA were elevated in kidney of control FAAH KO mice, but were decreased upon intramedullary PF-3845 (Fig 8A). The mechanism by which lipid ethanolamides are lowered in kidneys by intramedullary PF-3845 in FAAH KO mice is not known. It is possible that PF-3845 has inhibitory

effects on the biosynthesis of lipid ethanolamides in FAAH KO mice, potentially synthesis of NAPE or the hydrolysis by NAPE-PLD.

The data in the present study also suggest that the renomedullary lipid ethanolamide system has a profound effect on the pressure-natriuresis relationship. According to the pressure-natriuresis model (Guyton et al., 1972b), steady state blood pressure is controlled primarily by the effective intravascular volume. As blood pressure rises, the renal perfusion pressure rises in parallel, and the kidneys respond by increasing sodium and fluid excretion, restoring blood pressure to its starting level. The data in the present study suggest that activation of the renomedullary lipid ethanolamide system by treatment with the FAAH inhibitor can fundamentally alter the relationship between blood pressure and diuresis/natriuresis. Even as MAP fell from the intramedullary treatment with PF-3845 to levels below the starting pressure, the kidneys continued to excrete fluid and sodium. These data support an effect of an activated system in the renal medulla on the slope of the pressure natriuresis curve. Other substances including nitric oxide (Cowley et al., 2003), renal prostaglandins (Carmines et al., 1985), renal kinins (Tornel et al., 2000), reactive oxygen species (O'Connor and Cowley, 2010) and renal 20-HETE (Williams et al., 2007; Pandey et al., 2017), have been proposed to contribute to the mechanism of increased diuresis and natriuresis in response to increased renal perfusion pressure (Granger et al., 2002). It is interesting that MBF, which is increased by these agents and may be a downstream mediator of the pressure-natriuresis mechanism, is also increased by PF-3845 treatment (Figs. 5C and 5F).

In summary, the current study supports a role for inhibition of FAAH and elevation of AEA, PEA, or OEA in the renal medulla to stimulate MBF and diuresis and natriuresis and lower MAP through a mechanism involving CB₁ receptors. Studies are ongoing to identify the physiologic response of the renomedullary lipid ethanolamide system to increased renal perfusion

pressure including hypertensive states and to elucidate the mechanisms by which inhibition of FAAH leads to stimulation of MBF and diuresis and lowering of blood pressure.

Chapter 4: Diuretic, natriuretic, and blood pressure-lowering activity of palmitoylethanolamide in normotensive and hypertensive mice

4.1 Introduction

Palmitoylethanolamide (*N*-palmitoylethanolamine, PEA) is a fully saturated endogenous fatty acid amide belonging to the *N*-acylethanolamine (NAE) class of signaling molecules formed by the hydrolysis of palmitate-containing phospholipid by *N*-arachidonyl phosphatidylethanolamine-specific phospholipase D (NAPE-PLD). PEA was first described in 1957 as a potent anti-inflammatory compound in egg yolk (Kuehl et al., 1957). More recently, the anti-inflammatory effect of PEA have been expounded on as well as the extension of PEA to be effective in treating chronic pain and exerting neuroprotective effects in the brain and spinal cord after trauma or stroke (Esposito et al., 2011; Esposito and Cuzzocrea, 2013). Despite being a structural analog to the endocannabinoid anandamide (*N*-arachidonylethanolamine, AEA) and other NAE ligands of the cannabinoid receptors CB₁ and CB₂, PEA has no agonist activity at these receptors. It has been proposed PEA can indirectly activate the cannabinoid receptors via the “entourage effect”, that is, it enhances the effects of endogenous AEA through an increase in receptor affinity and/or competitive inhibition of AEA hydrolysis by FAAH (Jonsson et al., 2001; Smart et al., 2002; Ho et al., 2008). Additional targets of PEA include interactions with the G protein-coupled receptors, GPR 55 and 119, the peroxisome proliferator activated receptors (PPAR) $\alpha/\gamma/\delta$, and other signaling pathways (LoVerme et al., 2005; Pertwee, 2007; Syed et al., 2012; Paterniti et al., 2013).

The kidneys have a high concentration of PEA and one of its main hydrolyzing enzymes, fatty acid amide hydrolase (FAAH), which hydrolyzes PEA to palmitic acid and ethanolamine, as well as other NAEs including AEA and oleoylethanolamide (OEA) to their free fatty acids and

ethanolamine (Cravatt and Lichtman, 2003; Long et al., 2011). However, the role and mechanisms of PEA in the kidney are not fully understood. Recently we reported the intramedullary infusion of a selective FAAH inhibitor, PF-3845, stimulated diuresis and caused a decrease in mean arterial pressure in C57BL/6J mice (Ahmad et al., 2018). These data suggest that inhibition of FAAH in the renal medulla leads to both a diuretic/natriuretic and blood pressure-lowering response mediated by increased lipid ethanolamides, possibly AEA, PEA, and/or OEA. AEA is reported to have vasodepressor effects along with bradycardia by inhibition of baroreceptor reflex and sympathetic tone (Varga et al., 1995). Although the intramedullary infusions of AEA and the structurally related methanandamide were able to stimulate diuretic and natriuretic effects, mean arterial pressure was unaffected (Li and Wang, 2006; Ritter et al., 2012). Similar to AEA, PEA is produced on demand, but in concentrations substantially higher compared to AEA. Therefore, it is possible that the effects observed from PF-3845 administration are caused either fully or in part by increased concentrations of PEA.

This part of the study was designed to evaluate PEA's ability to stimulate diuresis and natriuresis and lower blood pressure by measuring its effect on mean arterial pressure (MAP), medullary blood flow (MBF), urine excretion rate (UV), and urinary sodium and potassium excretion (UNa and UK) after intramedullary and intravenous infusion. To determine the role of FAAH in the mechanism of PEA's effects, the responses were also evaluated in mice with homozygous knockout mutations in the FAAH gene (FAAH KO mice). The hypothesis that the effects of PEA were mediated through the CB₁ receptor was assessed by pre-treatment with the CB₁ antagonist, rimonabant, and PEA administration in CB₁ knockout mice (CB₁ KO). PEA was also evaluated in a chronic hypertensive model induced by inhibition of nitric oxide synthase by *N*-nitro-*L*-arginine methyl ester (L-NAME). PEA concentrations and the relative levels of NAPE-

PLD and FAAH protein in kidney tissue of normotensive control and L-NAME-induced hypertensive mice were also determined.

4.2 Materials and Methods

Reagents

Rimonabant, L-NAME, PMSF, AEA, PEA, OEA and their deuterated internal standards (AEA-d₈, PEA-d₄, and OEA-d₄) were purchased from Cayman Chemical (Ann Arbor, MI). Ammonium acetate, formic acid, sodium chloride, chloroform, HPLC grade methanol, HPLC grade acetonitrile and HPLC grade water were purchased from Fisher Scientific (Hanover Park, IL). Polyclonal IgG antibodies to FAAH (C841F) from Cell Signaling (Danvers, MA) and NAPE-PLD from Cayman Chemical (Ann Arbor, MI). Medical grade nitrogen was purchased from Airgas (Richmond, VA). All other reagents for *in vivo* use were of the highest grade available.

Animals

Two- to four -month old male and female C57BL/6 mice were obtained from Jackson Laboratory (Bar Harbor, ME) while male and female FAAH KO (homozygous gene knockout) mice and CB₁ knockout mice were from colonies maintained at Virginia Commonwealth University by Dr. Aron Lichtman. The FAAH KO mice and CB₁ KO mice were maintained by backcrossing onto a C57BL/6 background for 20 generations (Wise et al., 2008). All mice used in experiments weighed 25±5 g and were housed 4-5 per cage in a temperature- (20-22°C) and humidity-controlled (50-55%) facility with a 12/12 h light/dark cycle and *ad libitum* food and water. All animal protocols were approved by the Institutional Animal Care and Use Committee

of Virginia Commonwealth University and were in concordance with the National Institutes of Health Guide for the Care and Use of Laboratory Animals.

Acute surgical preparation

Mice were prepared for acute renal function studies by a procedure previously reported (Ahmad et al., 2017). Anesthesia was induced by intraperitoneal administration of thiobutabarbital (Inactin™, 75 mg/kg, Sigma Chemical Co., St. Louis, MO) and ketamine (Ketathesia™, 100 mg/kg, Harry Schein Animal Health, Dublin, OH). Animals were placed on surgical table that was thermally control at 37°C to avoid hypothermia due to anesthesia during course of experiment. After confirmation of the anesthesia level by observing negative response to mechanical toe pressing, a tracheotomy was performed to facilitate breathing by inserting a cut length of polyethylene tubing (PE-60) into the trachea. The left carotid artery was cannulated with PE-10 tubing filled with heparin sodium dissolved in saline (Fisher BioReagents, 0.005 mg/mL, 50 IU/mL) attached to a pressure transducer connected to a data acquisition system (Windaq, DATAQ Instruments, Akron, OH) for continuous mean arterial pressure measurement. The right jugular vein was catheterized similarly for the infusion of 0.9% saline. The rate of intravenous infusion was 1 mL/h/100 g body wt to maintain fluid volume and hematocrit concentration throughout the experiment.

For the acute renal function experiments, an incision was performed along the midline of the abdominal area. The left ureter was ligated with a surgical suture and cut on the kidney side of the ligation to allow urine produced from the left kidney to exit freely into the abdominal cavity. The right kidney was cannulated with a pulled PE-10 catheter implanted into the outer medulla to a depth of 2.5 mm vertically from the dorsal surface and anchored to the kidney capsule using

VetBond tissue adhesive (3M Animal Care Products, St. Paul, MN) as described (Li and Wang, 2006; Zhu et al., 2011b; Ritter et al., 2012; Ahmad et al., 2017; Ahmad et al., 2018). The infusion solution contained phosphate-buffered saline (205 mM NaCl, 40.5 mM Na₂HPO₄, and 9.5 mM NaH₂PO₄ (pH 7.4, 610 mOsm) and 10% ethanol at a rate of 2 µL/min. The bladder was cannulated with a 2.5 cm cut length of PE-50 tubing. The urine formation rate (UV) was measured by timed collections of urine into pre-weighed tubes for gravimetric determination of urine volume. Sodium and potassium concentrations in urine were measured by flame photometry. All urinary parameters were calculated on a per gram kidney weight (g kwt) basis. For the measurement of MBF, a laser Doppler flow probe (OxyFlo Pro; MNP 100XP; Oxford Optronix, Oxford, United Kingdom) was stabilized on the ventromedial surface of the right kidney to continuously measure MBF. The recording of the blood flow was measured by using a dual-channel laser-Doppler flowmeter (Transonic Systems Inc., Ithaca, NY).

After a 1 hr equilibration period and establishment of a stable baseline, urine was collected every 10 min during the experimental period. The two 10-minute collections immediately prior to the start of drug treatments representing the pre-treatment control periods were designated C1 and C2. PEA was administered into the renal medulla in the infusion solution at rates of 3.75, 7.5, and 15 nmol/min/kg for 30 min at each dose. The mean value between 10 and 30 min was designated used to calculate the average at each dose level. Sham mice treated identically to PEA-treated mice, except that they received vehicle solution for the entire experimental duration, were included as controls. At the termination of the experiment, blood was drawn from the carotid artery into a heparinized tube and centrifuged. The right and left kidneys were collected, weighed, and stored at -80°C for later analyses. The position of the medullary catheter was confirmed after sectioning of the right kidney.

Chronic hypertension model

Chronic hypertension was induced by inhibiting nitric oxide synthase (NOS) with L-NAME by mixing 1 mg/mL L-NAME in the drinking water of C57BL/6J mice for 4 weeks (Koka et al., 2008; Nagano et al., 2013). Mice were then prepared for acute renal function studies as described above.

Western blot analysis of kidney tissue

Kidney tissue was homogenized in 20 mM TrisCl buffer pH 7.5 buffer containing 1mM EDTA and 20% glycerol (microsome resuspension buffer), and then briefly sonicated. The homogenate was transferred to a microcentrifuge tube and centrifuged at 5,000 rpm for 2 min to remove nuclei and unbroken cells. The supernatant was collected and centrifuged at 16,000 g for 1 min. The supernatant was transferred to an ultracentrifuge tube and centrifuged at 68,000 g for 1 hr. The pellet was suspended in the microsome resuspension buffer and the protein concentration was measured by BCA protein assay (Pierce Chemical Co.). Protein (30ug) was electrophoresed through a 12% SDS- polyacrylamide gel together with a protein size standard, followed by electroblotting onto a polyvinylidene difluoride membrane. The membranes were blocked in 5% nonfat milk in Tris-buffered saline-0.1% Tween 20 (TBS-T). Membranes were probed for FAAH and NAPE-PLD proteins using antibodies from Cell Signaling Technology (FAAH, 38295) and Cayman Chemical (NAPE-PLD, 10305) at 1:1000 dilutions in TBS-T incubated overnight at 4°C. After washing, the membranes were incubated with 1:3000 horseradish peroxidase- conjugated anti-rabbit secondary antibody. Images were developed by using enhanced chemiluminescence detection solution and developed with Odyssey FC Imaging (LI-COR, Lincoln, NE). Anti- β -actin antibody (1:5,000), Santa Cruz Biotechnology) was used as a housekeeping probe to normalize for

difference in protein loading. Image Studio 5.2 (LI-COR, Lincoln, NE) was used to quantify the intensities of the protein bands.

Kidney tissue analysis of AEA, OEA, and PEA by ultra-high performance liquid chromatography-tandem mass spectrometry (UPLC-MS/MS)

Internal standard solution (10 μ L) containing 10 ng each of AEA-d₈, PEA-d₄, and OEA-d₄ was added to each plasma (100 μ L), kidney tissue (90-100 mg) or calibrator samples. 1 mM PMSF was added to all samples. Chloroform: methanol (3 mL of 2:1 (v/v)) and aqueous sodium chloride (200 μ L) of 0.73% were added to all samples and calibrators. The tissue samples were then homogenized for 30 sec using a Brinkmann Polytron[®] PT 3000 homogenizer and centrifuged at 3500 rpm for 5 min. Plasma samples and calibrators were mixed for 5 min then centrifuged at 3500 rpm for 5 min. The organic phases were collected, and the aqueous phases were extracted twice more with chloroform (1 mL). The organic phases were combined and evaporated to dryness under nitrogen, reconstituted in 100 μ L 60:40 water: acetonitrile and placed in autosampler vials for UPLC-MS/MS analysis.

The UPLC-MS/MS analysis was performed on a Sciex 6500+ QTRAP system with an IonDrive Turbo V source for TurbolonSpray[®] (Ontario, Canada) attached to a Shimadzu Nexera X2 UPLC system (Kyoto, Japan) controlled by Analyst 1.6.3 software (Ontario, Canada). Chromatographic separation was performed on a Discovery[®] HS C18 Column 15cm x 2.1mm, 3 μ m (Supelco: Bellefonte, PA) kept at 40°C and 2 μ L of sample was injected. The mobile phase consisted of A: water with 1 g/L ammonium acetate and 0.1% formic acid and B: acetonitrile. The following gradient was used: 0.0 to 2.4 minutes at 40% B, 2.5 to 6.0 minutes at 60% B, hold for 2.1 minutes at 60% B, then 8.1 to 9 min 100% B, hold at 100% B for 3.1 min and return to 40% B

at 12.1 min. The flow rate was 1.0 mL/min and total run time was 14 minutes. The acquisition mode used was Multiple Reaction Monitoring (MRM). The transition ions (m/z), deprotonation potentials (V), and corresponding collision energies (V) for all of the compounds can be found in Table 1. A calibration curve was constructed for the assay by linear regression using the peak area ratios of the calibrators and internal standards. The standard curve ranged from 1-100 ng for AEA, PEA, and OEA. Calibration curves had a correlation (r^2) of 0.9990 or better.

Statistical Analysis

Data are presented as the mean \pm S.E.M. For multiple group comparisons, one- or two-way analysis of variance (ANOVA) was performed using a Tukey post-hoc test when significant differences were found, using the first pre-infusion control phase, C1, as the control. For cross group comparisons of MBF of C57BL/6J sham and L-NAME sham, one way ANOVA was performed using a Sidak's post-hoc test. Data were considered statistically significant when $p \leq 0.05$.

4.3 Results

4.3.1 PEA administration stimulates diuresis and natriuresis in normotensive mice

Effects of intramedullary and intravenous infusion of PEA on MAP and UV in C57BL/6J mice

The effects of intramedullary (i.med.) and intravenous (i.v.) infusion of PEA on MAP and UV in C57BL/6J mice are shown in Figure. 10. The baseline MAP of C57BL/6J mice during the pre-treatment control phases, C1 and C2, was 107 and 106 mmHg, respectively. Intramedullary infusion of PEA at increasing sequential doses of 3.75, 7.5, and 15 nmol/min/kg did not show any

significant changes in MAP (Fig. 10A). The baseline rate of urine formation in C57BL/6J mice was 12 and 11 $\mu\text{l}/\text{min}/\text{g}$ kwt for the C1 and C2 control phases, respectively. Intramedullary infusion of PEA significantly increased UV ($p < 0.05$) to 39 $\mu\text{l}/\text{min}/\text{g}$ kwt at 7.5 nmol/min/kg respectively when compared to the C1 phase (Fig. 10B). During the post-treatment phases (P1 and P2), UV returned to rates similar to C1 and C2. There were no significant changes in either MAP or UV of sham-treated control C57BL/6J mice, which received only vehicle infusion during the entire experimental period (Figs. 10A and 10B, respectively).

Similar effects were seen with intravenous PEA administration (Figs. 10C and 10D). The baseline MAP during the pre-treatment control phases, C1 and C2, was 112 and 112 mmHg, respectively. Intravenous infusion of PEA at increasing sequential doses of 3.75, 7.5, and 15 nmol/min/kg did not show any significant changes in MAP. The baseline rate of urine formation was 12 and 12 $\mu\text{l}/\text{min}/\text{g}$ kwt for the C1 and C2 control phases, respectively. Intravenous infusion of PEA increased UV with 3.75 nmol/min/kg, and further increased UV significantly ($p < 0.05$) to 21 and 20 $\mu\text{l}/\text{min}/\text{g}$ kwt at the 7.5, and 15 nmol/min/kg respectively when compared to the C1 phase (Fig. 10D). There were no significant changes in either MAP or UV of sham-treated control mice (Figs. 10C and 10D, respectively).

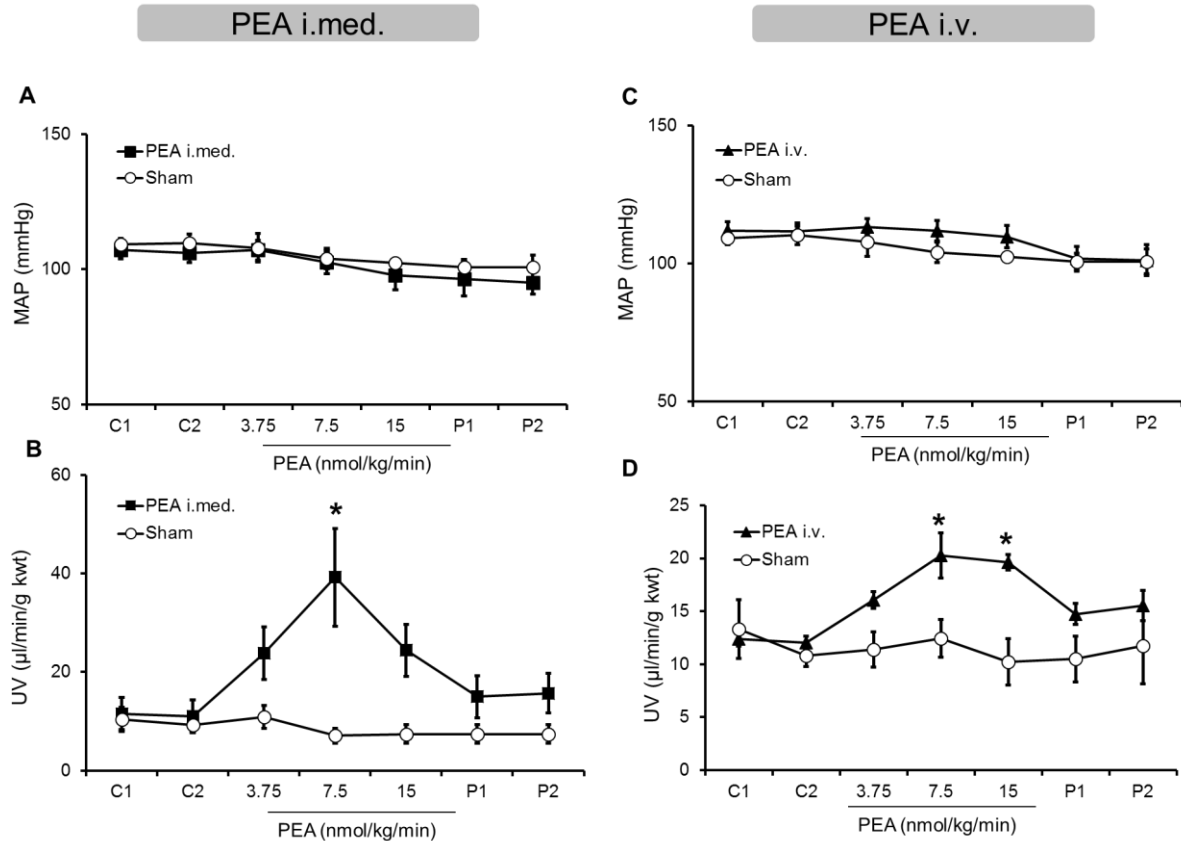


Figure 10. The effects of intramedullary and intravenous infusion of PEA on MAP and UV in C57BL/6J mice. Control infusion periods with vehicle alone (C); 3.75, 7.5, and 15 indicate dose rates for PEA infusion (in $\text{nmol}\cdot\text{kg}^{-1}\cdot\text{min}^{-1}$) and post-treatment control infusion periods (P). Data represent the mean \pm the standard error of each group. The data shown represent the mean \pm the standard error of the mean of each period. *Significant difference vs. the C1 control group ($p < 0.05$; $n = 4-8$ per group). kwt, kidney weight; MAP, mean arterial pressure; PEA, palmitoylethanolamide; UV, urine formation rate; n, sample size.

Effects of intramedullary and intravenous infusion of PEA on urinary sodium and potassium excretion rates and medullary blood flow in C57BL/6J mice

In C57BL/6J mice the intramedullary infusion of PEA into the medulla of the right kidney produced significant elevations in both urinary sodium and potassium excretion rates (2.7 and 2.8 $\mu\text{mol}/\text{min}/\text{g}$ kwt at 7.5 and 15 $\text{nmol}/\text{min}/\text{kg}$, 1.1 and 1.1 $\mu\text{mol}/\text{min}/\text{g}$ kwt at 7.5 and 15 $\text{nmol}/\text{min}/\text{kg}$ $p < 0.05$), in comparison with C1 (Figs. 11A and 11B). Intravenous infusion of PEA also produced significant elevations in both urinary sodium and potassium excretion rates (4.2 and 4.1 $\mu\text{mol}/\text{min}/\text{g}$ kwt at 7.5 and 15 $\text{nmol}/\text{min}/\text{kg}$, 1.0 at 15 $\text{nmol}/\text{min}/\text{kg}$, $p < 0.05$), in comparison with

C1 (Figs. 11D and 11E). Sodium and potassium excretion rates returned to baseline levels during the post-phases in both routes of administration. There were no significant changes in either sodium or potassium excretion rates in sham-treated control mice. Intramedullary infusion of PEA at 3.75, 7.5, and 15 nmol/min/kg did not affect medullary blood flow in C57BL/6J mice (Fig. 11C). There were no changes in MBF of sham-treated control mice.

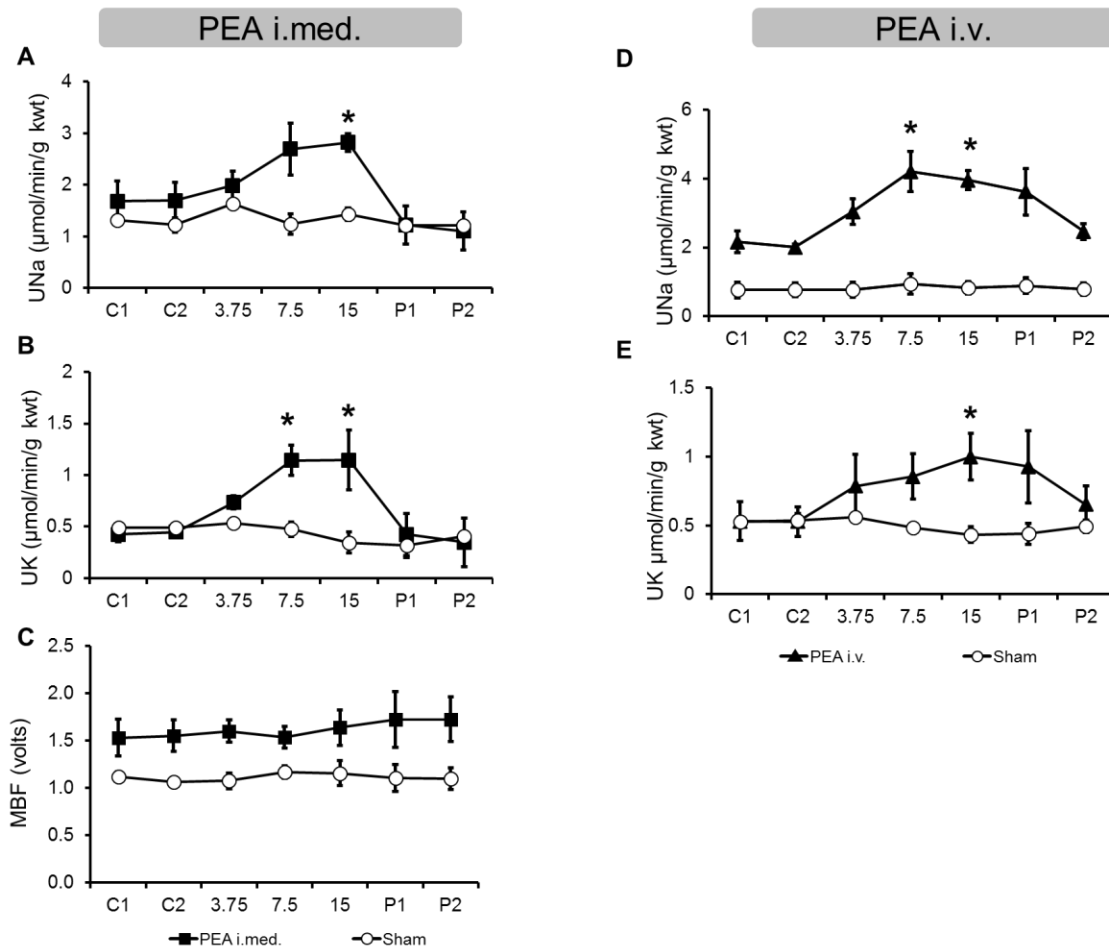


Figure 11. The effects of intramedullary and intravenous infusions of PEA on UNa and UK and MBF in C57BL/6J mice. Control infusion periods with vehicle alone (C); 3.75, 7.5, and 15, indicate dose rates for PEA infusion (in units of $\text{nmol}\cdot\text{kg}^{-1}\cdot\text{min}^{-1}$), and post-treatment control infusion periods (P). Data represent the mean \pm the standard error of each group. *Significant difference vs. the respective C1 control group ($p < 0.05$; $n = 3-5$ per group). kwt, kidney weight; MBF, medullary blood flow; PEA, palmitoylethanolamide; UK, urine potassium excretion rate; UNa, urine sodium excretion rate; n, sample size.

4.3.2 PEA-induced diuresis-natriuresis is FAAH and CB₁ independent

Effects of intramedullary and intravenous infusion of PEA on MAP and UV in FAAH KO mice

The effects of intramedullary infusion of PEA on MAP and UV in FAAH KO mice are shown in Figs. 12A and 12B. The baseline MAP of FAAH KO mice during the pre-treatment control phases, C1 and C2, was 102 and 104 mmHg, respectively. Intramedullary infusion of PEA at increasing sequential doses of 3.75, 7.5, and 15 nmol/min/kg did not show any significant changes in MAP (Fig. 12A). The baseline rate of urine formation was 9 and 9 $\mu\text{l}/\text{min}/\text{g}$ kwt for the C1 and C2 control phases, respectively. Intramedullary infusion of PEA significantly increased UV ($p < 0.05$) to 15 and 16 $\mu\text{l}/\text{min}/\text{g}$ kwt at the 7.5 and 15 nmol/min/kg respectively when compared to the C1 phase (Fig. 12B). During the post-treatment phases in the PEA-infused FAAH knockout mice, UV remained elevated ($p < 0.05$). There were no significant changes in either MAP or UV of sham-treated control FAAH KO mice (Figs. 12A and 12D, respectively).

The effects of intravenous infusion of PEA on MAP and UV in FAAH KO mice are shown in Figs. 12C and 12D. The baseline MAP of FAAH KO mice during the pre-treatment control phases, C1 and C2, was 100 and 101 mmHg, respectively. Intravenous infusion of PEA at increasing sequential doses of 3.75, 7.5, and 15 nmol/min/kg did not show any significant changes in MAP as shown (Fig. 12C). The baseline rate of urine formation was 7 and 6 $\mu\text{l}/\text{min}/\text{g}$ kwt for the C1 and C2 control phases, respectively. Intravenous infusion of PEA significantly increased UV ($p < 0.05$) to 17 $\mu\text{l}/\text{min}/\text{g}$ kwt at the 15 nmol/min/kg respectively when compared to the C1 phase (Fig. 12D). During the post-treatment phases in the PEA-infused FAAH knockout mice, UV remained elevated ($p < 0.05$). There were no significant changes in either MAP or UV of sham-treated control FAAH KO mice (Figs. 12C and 12D, respectively).

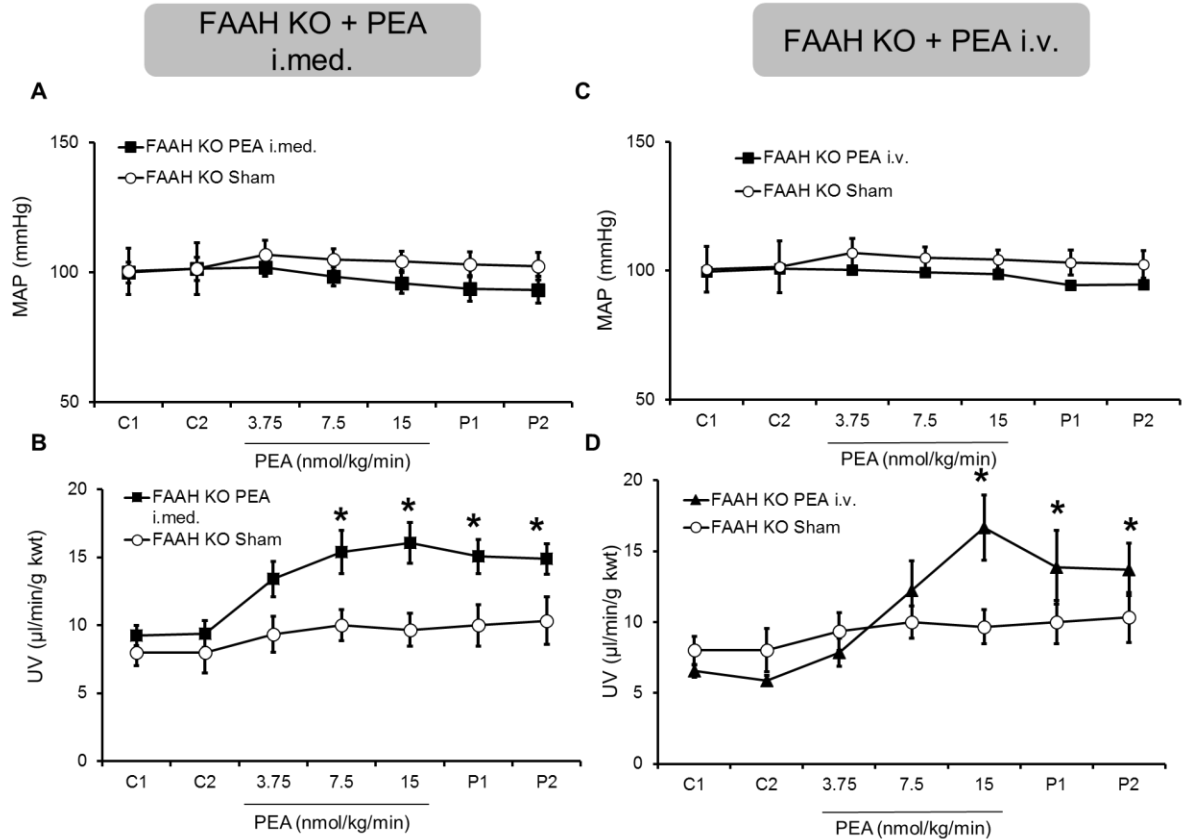


Figure 12. The effects of intramedullary and intravenous infusion of PEA on MAP and UV in FAAH KO mice. Control infusion periods with vehicle alone (C); 3.75, 7.5, and 15 indicate dose rates for PEA infusion (in units of $\text{nmol}\cdot\text{kg}^{-1}\cdot\text{min}^{-1}$), and post-treatment control infusion periods (P). Data represent the mean \pm the standard error of each group. *Significant difference vs. the C1 control group ($p < 0.05$; $n = 4-6$ per group). FAAH, fatty acid amide hydrolase; FAAH KO, FAAH homozygous knockout; kwt, kidney weight; MAP, mean arterial pressure; PEA, palmitoylethanolamide; UV, urine formation rate; n, sample size.

Effects of intramedullary and intravenous infusion of PEA on urinary sodium and potassium excretion rates and medullary blood flow in FAAH KO mice

In FAAH KO mice intramedullary infusion of PEA into the medulla of the right kidney did not produce significant elevations in urinary sodium and potassium excretion rates, but there was a trend in an increase during the treatment periods (Figs. 13A and 13B). Intravenous PEA increased sodium excretion rate and this became significant at the 15 $\text{nmol}/\text{min}/\text{kg}$ dose with an increase from 0.3 to 0.9 $\mu\text{mol}/\text{min}/\text{g}$ kwt ($p < 0.05$) (Fig. 13D). There was a trend in an increase in potassium excretion rate, but it was not significant (Fig. 13E). Neither intramedullary nor intravenous

infusion of PEA at 3.75, 7.5, and 15 nmol/min/kg altered medullary blood flow from C1 and C2 phases (Figs. 13C and 13F). There were no significant changes in urinary sodium and potassium excretion rates or MBF of sham-treated control FAAH KO mice.

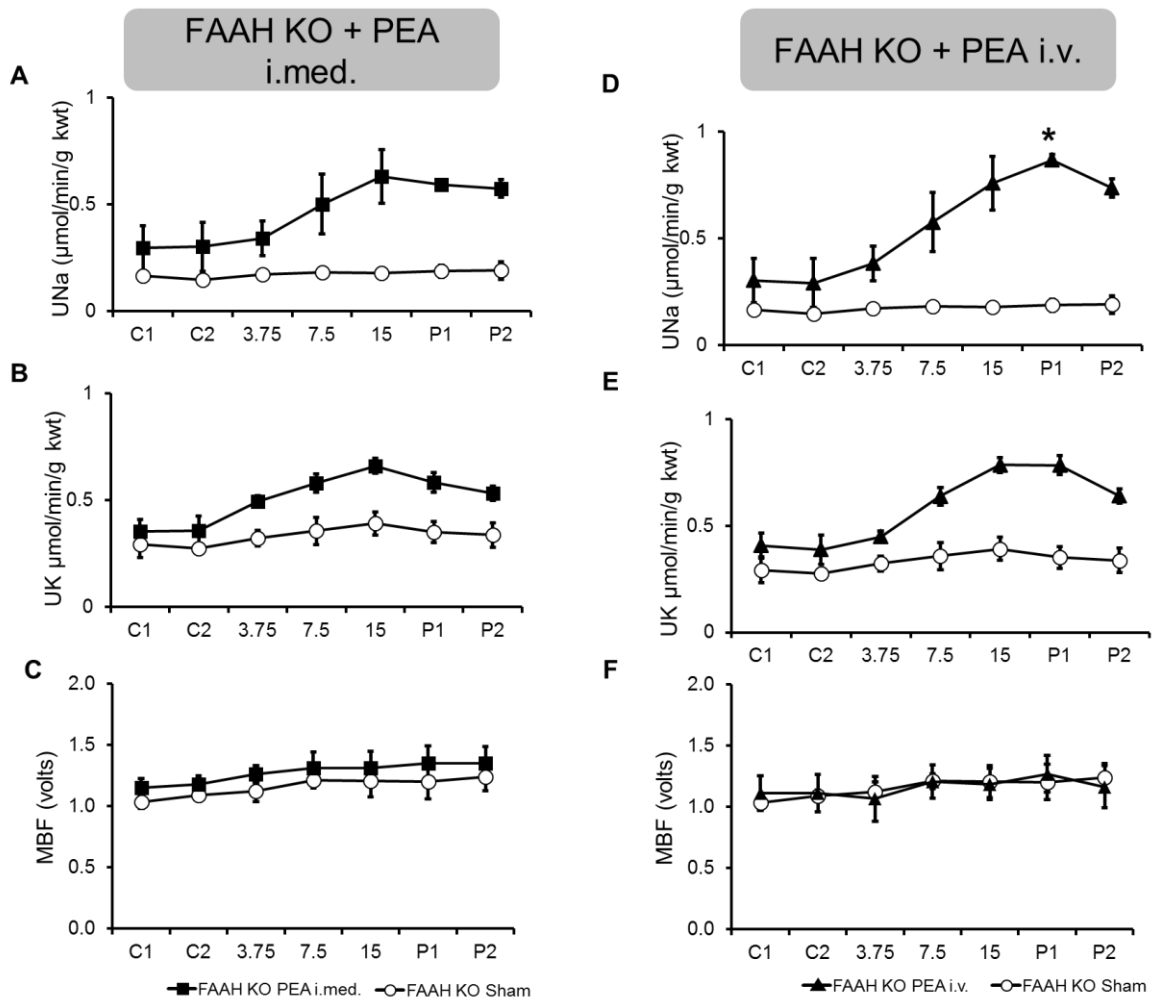


Figure 13. The effects of intramedullary and intravenous infusions of PEA on UNa and UK and MBF in FAAH KO mice. Control infusion periods with vehicle alone (C); 3.75, 7.5, and 15, indicate dose rates for PEA infusion (in units of $\text{nmol}\cdot\text{kg}^{-1}\cdot\text{min}^{-1}$), and post-treatment control infusion periods (P). Data represent the mean \pm the standard error of each group. *Significant difference vs. the respective C1 control group ($p < 0.05$; $n = 3-7$ per group). kwt, kidney weight; MBF, medullary blood flow; PEA, palmitoylethanolamide; UK, urine potassium excretion rate; UNa, urine sodium excretion rate; n, sample size.

Effects of a CB₁ antagonist on the diuresis-stimulating responses to intramedullary PEA and the effects of intramedullary PEA on MAP in UV in CB₁ KO mice

The baseline MAP of C57BL/6J mice prior to rimonabant treatment was 105 and 107 mmHg during the C1 and C2 phases, respectively (Fig. 14A). Administration of rimonabant (3 mg/kg, i.p.) decreased MAP to 98 mmHg, but this was not significant. MAP was not changed with subsequent intramedullary administration of PEA compared to the rimonabant pre-treatment group. The baseline UV of the C57BL/6J mice was 10 and 10 $\mu\text{l}/\text{min}/\text{g}$ kwt during C1 and C2, which was not significantly changed by the rimonabant pretreatment. PEA subsequently administered into the medulla of the right kidney dose-dependently increased UV and this became significant at the 15 nmol/min/kg dose ($p < 0.05$). In the post-treatment phases, UV remained elevated but not significantly different from C1 (Fig. 14B).

The effect of intramedullary infusion of PEA on MAP and UV in CB₁ KO mice are shown in Figs. 14A and 14B. The baseline MAP during the pre-treatment control phases, C1 and C2, was 115 and 115 mmHg, respectively. Intramedullary infusion of PEA at increasing sequential doses of 3.75, 7.5, and 15 nmol/min/kg did not show any significant changes in MAP (Fig. 14A). The baseline rate of urine formation was 5 and 5 $\mu\text{l}/\text{min}/\text{g}$ kwt for the C1 and C2 control phases, respectively. Intramedullary infusion of PEA increased UV to 15 and 21 $\mu\text{l}/\text{min}/\text{g}$ kwt at the 7.5 and 15 nmol/min/kg, but this increase was not statistically significant due to small sample size ($n=2$) (Fig. 14B). UV remained elevated during the post-treatment phases.

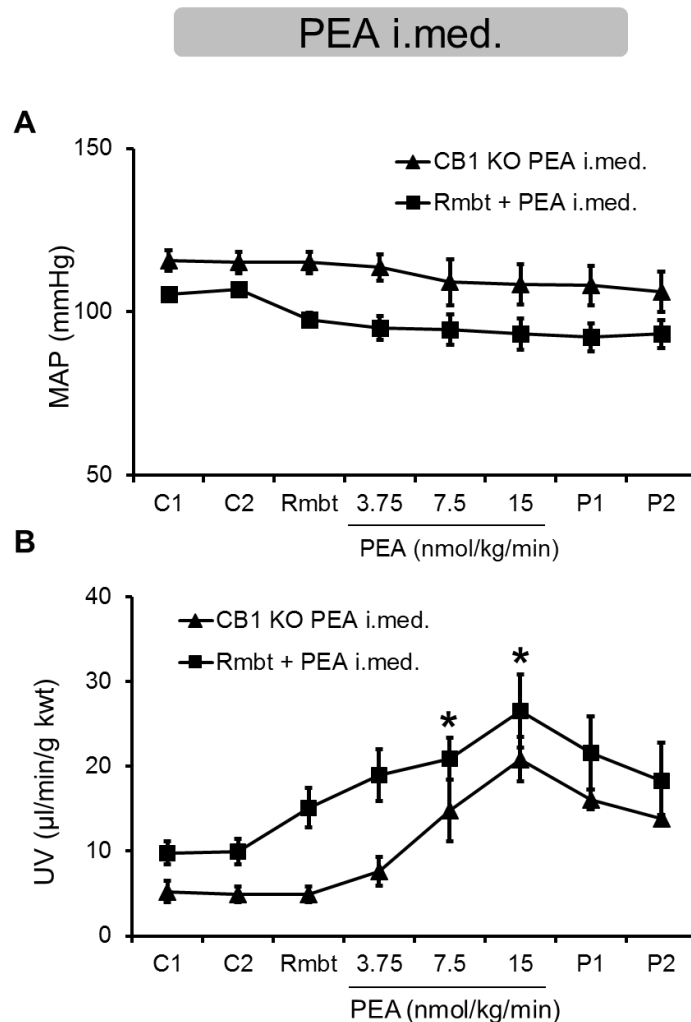


Figure 14. The effects of rimonabant pretreatment on the MAP and UV responses to intramedullary infusion of PEA in C57BL/6J mice and the effect of intramedullary infusion of PEA on MAP and UV in CB₁ KO mice. Control infusion periods with vehicle alone (C); 3.75, 7.5, and 15 indicate dose rates for intramedullary PEA infusion (nmol·kg⁻¹·min⁻¹). Period of rimonabant pretreatment (Rmbt; 3 mg/kg, i.p.) and post-treatment control infusion periods (P). Data represent the mean ± the standard error of each group. *Significant difference vs. the respective C1 control group (p < 0.05; n = 2-7 per group). kwt, kidney weight; MAP, mean arterial pressure; PEA, palmitoylethanolamide; Rmbt, rimonabant; UV, urine formation rate; n, sample size.

Effects of a CB₁ antagonist on the diuresis stimulating response to intravenous PEA

For mice pre-treated with rimonabant and subsequently administered PEA intravenously, baseline MAP was 109 and 108 mmHg during the C1 and C2 phases, respectively (Fig. 15A). Administration of rimonabant (3 mg/kg, i.p.) decreased MAP to 90 mmHg, but this was not

significant. MAP was not changed with subsequent intramedullary administration of PEA compared to the rimonabant pre-treatment phase. However, the decrease in MAP to 81 mmHg with 3.75 nmol/min/kg PEA was significant from the C1 and C2 phases ($p < 0.05$) (Fig. 15A). The baseline UV was 10 and 10 $\mu\text{l}/\text{min}/\text{g}$ kwt during C1 and C2. Rimonabant slightly increased UV, but this was not significant. Intravenous PEA at increasing doses did not change UV from C1 and C2, and there was actually a slight decrease in UV to 7 $\mu\text{l}/\text{min}/\text{g}$ kwt with the 15 nmol/min/kg dose (Fig. 15B).

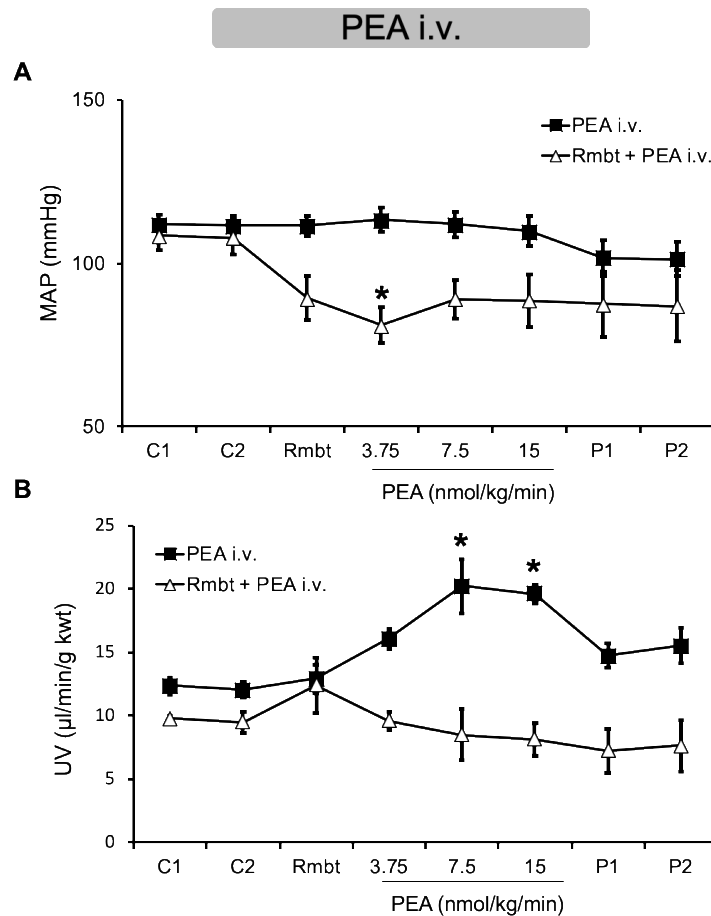


Figure 15. The effects of rimonabant pretreatment on the MAP and UV responses to intravenous infusion of PEA in C57BL/6J mice. Control infusion periods with vehicle alone (C); 3.75, 7.5, and 15 indicate dose rates for intravenous PEA infusion ($\text{nmol}\cdot\text{kg}^{-1}\cdot\text{min}^{-1}$). Period of rimonabant (SR141716A) pretreatment (Rmbt; 3 mg/kg, i.p.) and post-treatment control infusion periods (P). Data represent the mean \pm the standard error of each group. *Significant difference vs. the respective C1 control group ($p < 0.05$; $n = 3-5$ per group). kwt, kidney weight; MAP, mean arterial pressure; PEA, palmitoylethanolamide; Rmbt, rimonabant; UV, urine formation rate; n, sample size.

4.3.3 Intramedullary infusion of PEA decreases mean arterial pressure and stimulates diuresis in L-NAME-induced hypertensive mice

Effects of intramedullary and intravenous infusions of PEA on MAP and UV in L-NAME-induced hypertensive mice

The effect of intramedullary infusion of PEA on MAP and UV in L-NAME-induced hypertensive mice are shown in Figure 16. The baseline MAP during the pre-treatment control phases, C1 and C2, was 154 and 154 mmHg, respectively. Intramedullary infusion of PEA dose-dependently decreased mean arterial pressure, with the decrease becoming significant at the highest dose of 15 nmol/min/kg and remaining decreased during the post phases ($p < 0.05$) (Fig. 16A). The baseline rate of urine formation was 12 and 13 $\mu\text{l}/\text{min}/\text{g}$ kwt for the C1 and C2 control phases, respectively. Intramedullary infusion of PEA significantly increased UV ($p < 0.05$) to 27, and 28 $\mu\text{l}/\text{min}/\text{g}$ kwt at the 7.5 and 15 nmol/min/kg, respectively, when compared to the C1 phase (Fig. 16B). UV remained elevated during the post-treatment phases ($p < 0.05$).

The effect of intravenous infusion of PEA on MAP and UV in L-NAME-induced hypertensive mice are shown in Figs. 16C and 16D. The baseline MAP during the pre-treatment control phases, C1 and C2, was 145 and 144 mmHg, respectively. Intravenous infusion of PEA did not change MAP (Fig. 16C). The baseline rate of urine formation was 9 and 9 $\mu\text{l}/\text{min}/\text{g}$ kwt for the C1 and C2 control phases, respectively. Intravenous infusion of PEA dose-dependently increased UV, with the increase becoming significant during the post phases with an increase to 24 and 23 $\mu\text{l}/\text{min}/\text{g}$ kwt for P1 and P2 respectively ($p < 0.05$) (Fig. 16D). There were no significant changes in either MAP or UV of sham-treated control L-NAME-induced hypertensive mice.

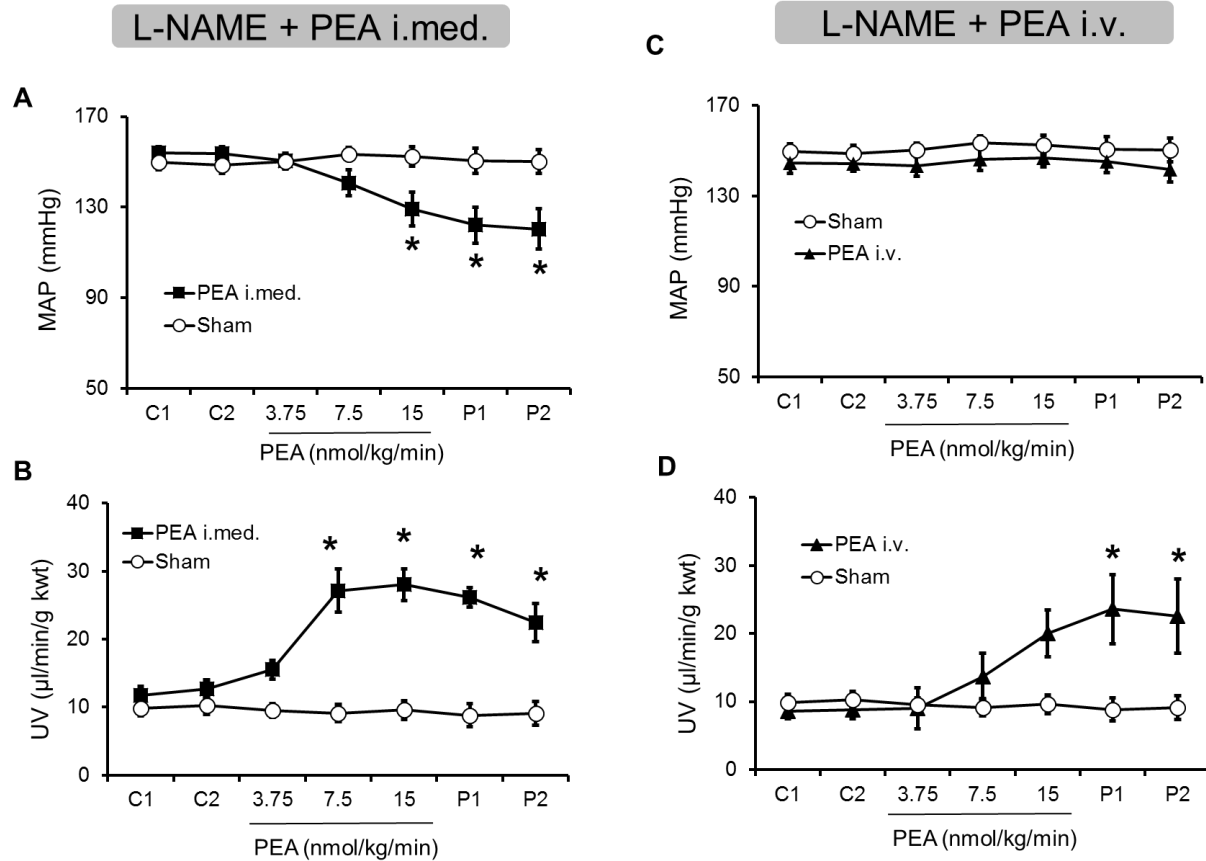


Figure 16. The effects of intramedullary infusion of palmitoylethanolamide (PEA) on MAP and UV in L-NAME-induced hypertensive mice. Control infusion periods with vehicle alone (C); 3.75, 7.5, and 15 indicate dose rates for intravenous PEA infusion ($\text{nmol}\cdot\text{kg}^{-1}\cdot\text{min}^{-1}$) and post-treatment control infusion periods (P). Data represent the mean \pm the standard error of each group. *Significant difference vs. the respective C1 control group ($p < 0.05$; $n = 4$ per group). kwt, kidney weight; MAP, mean arterial pressure; PEA, palmitoylethanolamide; UV, urine formation rate; n, sample size.

Effects of intramedullary and intravenous infusions of PEA on sodium and potassium excretion rates and medullary blood flow in L-NAME-induced hypertensive mice

Intramedullary and intravenous infusion of PEA did not produce significant elevations in urinary sodium and potassium excretion rates, but there was a trend toward an increase during the treatment periods for both routes of administration (Figs. 17A-17D). Intramedullary infusion of PEA at 3.75, 7.5, and 15 $\text{nmol}/\text{min}/\text{kg}$ did not affect medullary blood flow. There were no changes

in urinary sodium and potassium excretion rates or MBF of sham-treated control L-NAME-induced hypertensive mice.

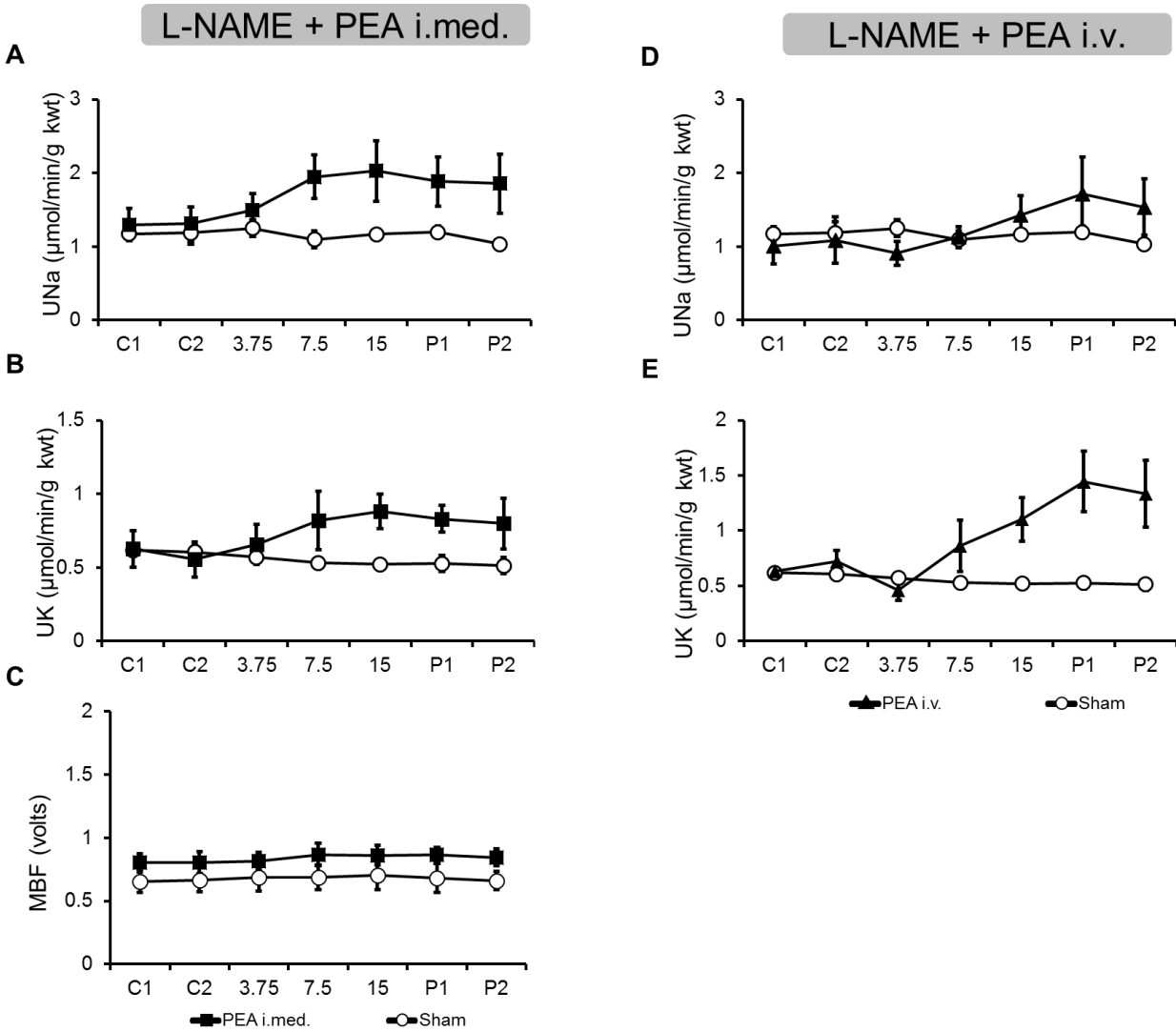


Figure 17. The effects of intramedullary and intravenous infusions of PEA on UNa and UK and MBF in L-NAME-induced hypertensive mice. Control infusion periods with vehicle alone (C); 3.75, 7.5, and 15, indicate dose rates for PEA infusion (in units of $\text{nmol}\cdot\text{kg}^{-1}\cdot\text{min}^{-1}$), and post-treatment control infusion periods (P). Data represent the mean \pm the standard error of each group. ($n=3-5$ per group). kwt, kidney weight; MBF, medullary blood flow; PEA, palmitoylethanolamide; UK, urine potassium excretion rate; UNa, urine sodium excretion rate; n, sample size.

Effect of L-NAME-induced hypertension on medullary blood flow in anesthetized mice

Figure 18 shows the effect of L-NAME-induced hypertension on medullary blood flow. L-NAME-induced hypertensive mice had significantly decreased MBF compared to normotensive mice during the entire experimental time period ($p < 0.05$).

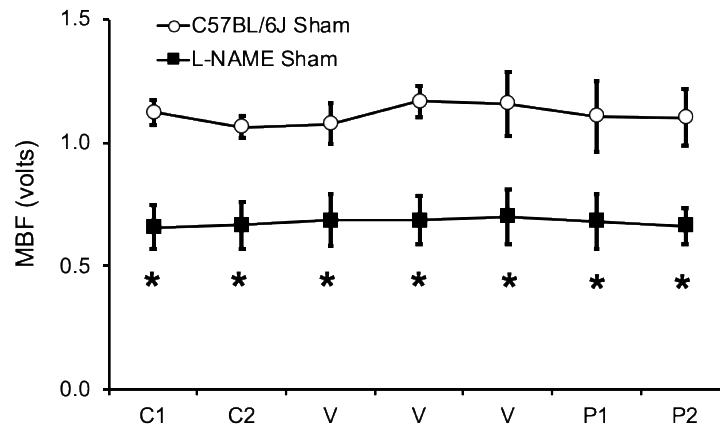


Figure 18. Medullary blood flow of C57BL/6J sham control mice and L-NAME-induced hypertensive sham control mice. Control infusion periods with vehicle alone (C); Vehicle control infusion periods (V), and post-treatment control infusion periods (P). Data represent the mean \pm the standard error of each group. *Significant difference vs. the respective period of C57BL/6J sham ($p < 0.05$; $n=3-4$ per group). MBF, medullary blood flow; n, sample size; v, vehicle.

Effect of L-NAME-induced hypertension on AEA, OEA, and PEA concentrations and NAPE-PLD and FAAH protein levels in kidney tissue of C57BL/6J mice

The concentrations of AEA, OEA, and PEA in kidney tissue of normotensive control and L-NAME-induced hypertensive mice were determined by UPLC-MS/MS (Fig. 19A). L-NAME-induced hypertensive mice had increased kidney concentrations of PEA and OEA, and decreased AEA concentrations compared to normotensive mice ($p < 0.05$). To evaluate if the difference in the concentrations of the lipid ethanolamides were due to changes in NAPE-PLD and/or FAAH, the relative level of these proteins were determined in kidney tissue. There was an apparent

decrease in both NAPE-PLD and FAAH levels in L-NAME-induced hypertensive mice though the decrease was not significant from normotensive controls in either case (Fig. 19B).

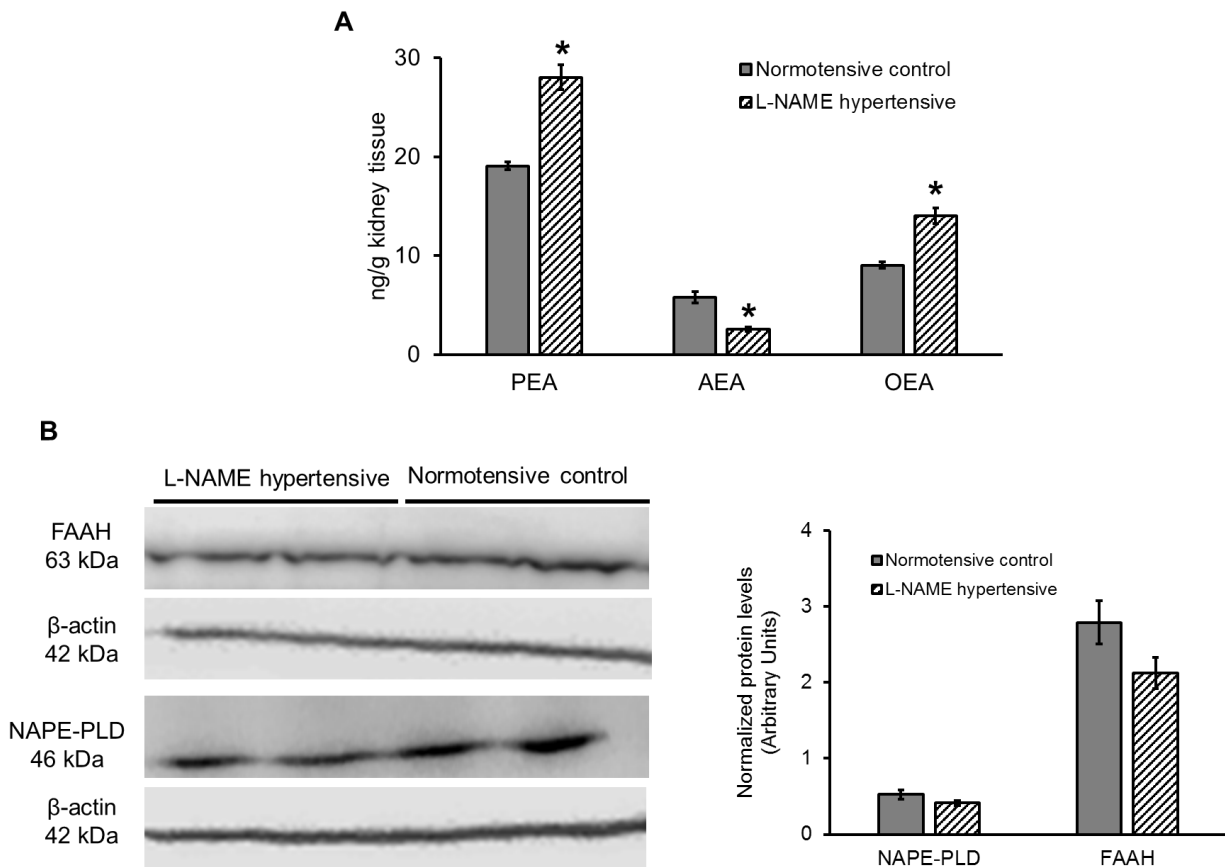


Figure 19. The effect of L-NAME-induced hypertension on AEA, OEA, and PEA concentrations and NAPE-PLD and FAAH protein levels in kidney tissue of C57BL/6J mice. (A) Anandamide (AEA), palmitoylethanolamide (PEA) and oleoylethanolamide (OEA) concentrations in kidney tissue of normotensive control and L-NAME-induced hypertensive mice. (B) Relative NAPE-PLD and FAAH protein levels in normotensive control and L-NAME-induced hypertensive mice. Data represent the mean \pm the standard error of each group. *Significant difference vs. the normotensive control group ($p < 0.05$; $n = 3$ per group) in an unpaired, two-tailed t-test.

4.4 Discussion

This study investigated the effects of palmitoylethanolamide administration in order to test the hypothesis that the effects observed from infusion of the selective FAAH inhibitor PF-3845

are either fully or in part due to increased concentrations of PEA. It also explored the hypothesis that exogenous administration of PEA would produce antihypertensive responses in a model of chronic hypertension. This study revealed several novel observations. Intramedullary and intravenous infusion of PEA increased urinary and salt excretion without changing MAP or MBF in C57BL/6J mice. The effects of intramedullary PEA administration were shown to be FAAH- and CB₁-independent as the same results were observed in FAAH KO and CB₁ KO mice. However, the diuresis-stimulating response due to intravenous PEA was attenuated by pre-treatment with the CB₁ antagonist rimonabant. In addition, intramedullary infusion of PEA produced both a decrease in MAP and an increase in urinary and salt excretion in L-NAME-induced hypertensive mice.

Previously we reported that intramedullary infusion of a selective FAAH inhibitor, PF-3845, stimulated diuresis and decreased mean arterial pressure in C56BL/6J mice (Ahmad et al., 2018). We also showed that these effects were accompanied by an increase in the endocannabinoid anandamide as well as another lipid ethanolamide, PEA. The data were consistent with earlier data from our laboratory (Li and Wang, 2006; Ritter et al., 2012) and others (Li and Wang, 2006) showing that infusion of exogenous anandamide into the renal medulla elicits a diuretic effect. However, in that study, administration of exogenous anandamide did not elicit a change in MAP. Therefore, the stimulation of diuresis and decrease in MAP produced by infusion of PF-3845 may not be due to increased concentrations of AEA in the kidney. The current study aimed to determine if the effects observed from infusion of PF-3845 could be due to increased concentrations of PEA from the chemical inhibition of FAAH.

Intramedullary and intravenous infusions of PEA stimulated diuresis and significantly increased urinary sodium and potassium excretion rates in C567BL/6J mice. To the authors'

knowledge, there is only one other report of PEA administration increasing urine output. In that study, PEA was chronically administered to spontaneously hypertensive rats. A significant increase in urine volume was observed without a change in sodium or potassium excretion, which was thought to be attributed to inhibition of water reabsorption or an increase in glomerular filtration rate (Mattace Raso et al., 2013). Our study demonstrates diuresis accompanied by increased salt excretion. This suggests a different mechanism of diuresis in C57BL/6J mice, possibly the ability of PEA to have direct actions on the tubular epithelium leading to the inhibition of water and salt reabsorption. PEA administration did not affect MAP in C57BL/6J mice. This indicates that the effects observed from administration of PF-3845 in our previous study are not solely due to the increase of PEA in the renal medulla. However, it is possible that increased PEA contributes to the diuretic-natriuretic responses from PF-3845 administration. The mechanisms by which FAAH inhibition leads to a lowering of blood pressure are still being investigated.

Administration of PEA in FAAH KO mice was still able to produce a significant diuretic response and an elevation in urinary sodium and potassium excretion. This indicates that the diuretic action of PEA is not dependent on its hydrolysis to palmitic acid. It is interesting to note the different shapes of the UV dose-response curves for C57BL/6J mice and FAAH KO mice. In contrast to conventional dose-response curves, the diuresis curve for C57BL/6J mice exhibited an inverted-U shape. We also observed U-shaped diuresis dose response curves when the FAAH/MAGL dual inhibitor, isopropyl dodecylfluorophosphonate, was infused into the renal medulla, and also the FAAH specific inhibitor PF-3845 was infused (Ahmad et al., 2017; Ahmad et al., 2018). An inverted-U shaped dose-response curve was not observed for FAAH KO mice. It is possible that since FAAH KO mice already have higher concentrations of PEA in the kidney

compared to wild type mice, the same doses of PEA used in both strains of mice are not able to produce the same dose-response curves.

It has been demonstrated that renal medullary blood flow plays an important role in the regulation of sodium and water excretion, notably that increases in MBF increase salt and water excretion (Haas et al., 1988; Roman et al., 1988). However, the diuretic and natriuretic effects of PEA in both C57BL/6J and FAAH KO mice were not accompanied by an increase in MBF, indicating PEA's effects were independent of renal hemodynamics. This finding has been observed in our laboratory previously when AEA infusion into the mouse renal medulla increased salt and urine formation without effecting renal or medullary blood flow (Ritter et al., 2012).

This study also found the diuretic action of intramedullary PEA to be CB₁-independent by utilization of pre-treatment with the CB₁ antagonist rimonabant and CB₁ KO mice. This finding of CB₁-independence agrees with well-documented reports that PEA has no agonist activity at the CB₁ receptor. It also demonstrates that PEA-induced diuresis is not due to indirect activation of the CB₁ receptor by PEA through the aforementioned mechanisms of the entourage effect. Interestingly, it was found that the diuretic action of intravenous PEA was blunted by pre-treatment with rimonabant. It is possible that the significant decrease in MAP caused by intraperitoneal administration of rimonabant caused a reduction in UV to conserve water and salt. The pressure-natriuresis model states that long term, steady-state blood pressure is primarily controlled by the effective intravascular volume, which is influenced by vascular tone and extracellular fluid volume (ECFV). When blood pressure increases, so does the renal perfusion pressure. The kidneys respond to this rise in pressure by increasing sodium and fluid excretion, thereby decreasing the ECFV, and ultimately lowering blood pressure back to a normal level (Ivy and Bailey, 2014). The converse is also true, in that when there is a decrease in blood pressure, the kidneys will respond

by decreasing fluid and salt excretion. Another possibility is that intravenous PEA-induced diuresis is mediated by the mechanisms of the entourage effect. Systemic PEA may compete with AEA for hydrolysis by FAAH, thereby decreasing AEA inactivation and allowing AEA to act and produce diuresis as previously documented in our lab and others.

Given the diuretic-natriuretic effects of intramedullary PEA in normotensive mice, it was also of interest to evaluate the effects of intramedullary PEA in a chronic hypertension model. Hypertension was induced using the NOS inhibitor L-NAME in the drinking water of C57BL/6J mice. Another novel finding of this study was the effect of PEA administration in L-NAME-induced hypertensive mice. Intramedullary PEA produced a decrease in MAP and increase in UV (Figs. 16A and 16B). MBF was significantly decreased compared to normotensive mice (Fig. 18) but remained unaffected by PEA administration (Fig. 17C). The decreased MBF in L-NAME-induced hypertension is consistent with reports that infusion of L-NAME into the renal medulla produced a reduction in MBF (Mattson et al., 1992; Zou et al., 2001a). Intravenous infusion of PEA also stimulated diuresis but had no effect on MAP. There was a trend toward an increase in sodium and potassium excretion rate with both routes of administration but the increases were not statistically significant.

These data suggest that PEA administration in the renal medulla has a remarkable effect on the pressure- natriuresis relationship and PEA may fundamentally alter the relationship between blood pressure and diuresis/natriuresis. Even as MAP dose-dependently decreased from the intramedullary treatment with PEA in L-NAME treated mice, the kidney continued to excrete fluid and salt. These data support an effect of PEA in the renal medulla in L-NAME-induced hypertension on the slope of the pressure-natriuresis curve. We also observed this apparent effect on the pressure-natriuresis curve with intramedullary infusion of PF-3845 in C57BL/6J mice

(Ahmad et al., 2018). Other substances including NO have been proposed to contribute to the mechanism of increased diuresis-natriuresis in response to increased renal perfusion pressure (Cowley et al., 2003). It has also been shown that increased NO production has prevented the development of hypertension and the improvement of hypertension (Chen and Sanders, 1991; Podjarny et al., 2004; Zanfolin et al., 2006). NO is formed from L-arginine by three distinct isoforms of NOS and the anions nitrate and nitrite were previously thought to be inert end products of NO production. However, it has been shown that these anions can serve as an alternative source for NO synthesis (Lundberg et al., 2008; Milsom et al., 2012). It has also been shown that dietary doses of nitrite restore circulating nitric oxide levels and decrease blood pressure in L-NAME-induced hypertensive rats (Okamoto et al., 2005; Kanematsu et al., 2008). PPAR α activation has also been shown to increase nitrate/nitrite in tissue, increase NO production, and ameliorate hypertension (Newaz et al., 2005; Banks and Oyekan, 2008; Yousefipour and Newaz, 2014). PEA is a PPAR α ligand, therefore it is possible that an increase in nitrate/nitrite production in the kidney by activation of PPAR α by PEA may contribute to the decrease in MAP in L-NAME-induced hypertensive mice.

The blood pressure-lowering activity may also be due to modulation of the RAAS system by PPAR α activation of PEA. It has been reported that hypertension resulting from chronic inhibition of NO synthesis can lead to activation of the RAAS system (Qiu et al., 1994). It has also been demonstrated that NO inhibits ACE activity and down-regulates AT₁ receptors (Cahill et al., 1995; Kumar and Das, 1997; Ackermann et al., 1998; Ichiki et al., 1998). Furthermore, L-NAME-induced microvascular structural changes were prevented by ACE inhibitors and AT₁ receptor antagonists, indicating the involvement of the RAAS system in the L-NAME-induced hypertension model (Arnal et al., 1993; Pollock et al., 1993; Takemoto et al., 1997). PPAR α is

highly expressed in the liver, heart, and kidney, and has been shown to be involved in blood pressure regulation (Shin et al., 2009; Gelosa et al., 2010). The protective role for PPAR α activators has been attributed to anti-inflammatory and anti-oxidant properties by downregulation of inflammatory cytokines and reduction of oxidative stress (Vera et al., 2005; Hou et al., 2010). In addition, PPAR α has been shown to affect the gene expression of RAAS components (Jonkers et al., 2001). One group reported that chronic PEA treatment to spontaneously hypertensive rats alleviated hypertension and reduced AT₁ expression and ACE activity in the kidney, effects that were attributed to PPAR α activation (Mattace Raso et al., 2013).

Interestingly, intravenous infusion of PEA also stimulated diuresis but had no effect on MAP in L-NAME-induced hypertensive mice. It is possible that systemically administered PEA is rapidly hydrolyzed, and that not enough PEA reaches the site of action in the renal medulla necessary for lowering blood pressure. This could also account for the different shape in UV curves as well. Although intravenous PEA still stimulated UV, the increase did not occur with each dose of PEA in the same manner as intramedullary PEA. A trend toward an increase in UV was apparent with the first dose of intramedullary PEA, but this dose did not produce any effect when administered intravenously. In addition, the increase in UV was not significant until the post phases, while intramedullary PEA produced a significant increase with the second dose.

Another interesting finding of this study was the effect of the L-NAME hypertension model on concentrations of lipid ethanolamides determined by UPLC-MS/MS. L-NAME-induced hypertensive mice had significantly increased concentrations of PEA and OEA and decreased AEA in the kidney tissue compared to normotensive control mice. These results agreed with western blot analysis showing a trend toward lower relative FAAH protein levels compared to normotensive mice in kidney tissue. Less FAAH activity would lead to decreased PEA degradation

and increased tissue concentrations. These data suggest that a hypertensive state might result in a decrease in degradation of PEA in order to combat the increase in blood pressure. L-NAME-induced hypertensive mice also had lower levels of NAPE-PLD. This could explain the decreased AEA concentrations and would suggest that the NAPE-PLD pathway is the primary biosynthetic pathway for AEA in the kidney. The decreased AEA kidney concentrations might also be due to AEA release into the systemic circulation. Clearly, the synthesis and hydrolysis of PEA and other lipid ethanolamides are in a delicate balance that requires further experiments to determine their relationship to the levels of NAPE-PLD and FAAH.

In summary, PEA administration stimulated urine formation and salt excretion rates in C57BL/6J without affecting MAP or MBF. These effects were independent of FAAH and CB₁ when PEA was infused intramedullary. This indicates that the effects observed from administration of PF-3845 in the previous study are not solely due to the increase of PEA in the renal medulla but does not exclude PEA as a contributor in PF-3845's effects. In L-NAME-induced hypertensive mice, intramedullary infusion of PEA decreased MAP and increased urine excretion and urinary sodium and potassium excretion rates. These effects were accompanied by an increase in PEA concentrations in kidney tissue. Further studies are needed to elucidate the mechanisms by which intramedullary PEA stimulates diuresis and natriuresis and decreases MAP in the model of L-NAME-induced hypertension.

Chapter 5: Regulation of palmitoylethanolamide and related lipid ethanolamides by mouse medullary interstitial cells

5.1 Introduction

It has been proposed that the kidney contains a potent vasodepressor system that originates from the renal medulla. The medullary interstitium can be split into three types of interstitial space, corresponding to the outer stripe, the inner stripe, and the inner medulla. An important non-tubular cell type of the inner medulla is the lipid-laden (Type I) interstitial cell (Lemley and Kriz, 1991). These cells have been proposed to play an important role in maintaining function and structural integrity of the kidney. Characteristics of this type of interstitial cell include its stellate-like cellular morphology with cytoplasmic projections and increased cell density toward the tip of the renal papilla. They are noticeable in stained sections of the renal medulla based on their long axes lying perpendicular to loop of Henle tubules and vasa recta cells, producing a characteristic ladder-like appearance. Although cytoplasmic projections from these cells do not make physical contact with loop of Henle or vasa recta, they have been suggested to play a role in signaling to these cell types in response to changing conditions (Lemley and Kriz, 1991). Another hallmark is the abundant presence of osmiophilic lipid granules which are rich in arachidonic acid, the precursor of eicosanoid metabolites such as prostaglandin E₂. The synthesis of prostaglandin E₂ by interstitial cells was stimulated by angiotensin II and other vasoactive peptides and certain physiologic conditions (Zusman and Keiser, 1977a). Changes in the number of these lipid droplets in experimental models of hypertension (Bohman and Jensen, 1976; Maric et al., 2002) suggested a role of these lipid droplets in the secretion of medullipin in response to elevated renal perfusion pressure (Muirhead, 1993; Folkow, 2007).

In the studies described earlier, intramedullary administration of PEA stimulated diuresis and natriuresis in C57BL/6J mice. In addition to these effects, renomedullary infusion of PEA also decreased mean arterial pressure in L-NAME-induced hypertension. These results suggest that PEA could serve as an antihypertensive regulator in the renal medulla, possibly regulated by the interstitial cell of the medulla. The putative role of interstitial cells in secreting a renomedullary antihypertensive substance led us to isolate these cells from the renal medulla of mice in order to study their responses to pharmacologic FAAH inhibition and to physiologic stimuli that mimic hypertensive states such as increased salt concentration and high pressure. The isolated cells were assessed for histological, immunohistochemical, and ultrastructural markers consistent with their identity as medullary interstitial cells, and also for the presence of biosynthetic and degradative enzymes of lipid ethanolamides. The effect of treating the cells with the pharmacologic and physiologic stimuli on the appearance of lipids in the medium of MMICs was also investigated.

5.2 Materials and Methods

Reagents

Trypsin-EDTA (10X, 0.5%), penicillin-streptomycin (100X), and glutamine (100X) were purchased from Gibco-Invitrogen (Gaithersburg, MD). Fetal bovine serum was from Serum Source International (Charlotte, NC). Dulbecco's modified Eagle's medium with high glucose (DMEM) was from Gibco/Life Technologies (Grand Island, NY). Polyclonal IgG antibodies to tenascin-C (H-300) and COX-2 (M19) from Santa Cruz Biotechnology (Dallas, TX); FAAH (C841F) from Cell Signaling (Danvers, MA) and NAPE-PLD from Cayman Chemical (Ann Arbor, MI). Sudan Black B was from Santa Cruz Biotechnology. Horseradish peroxidase (HRP)-conjugated anti-rabbit IgG antibodies were from Jackson ImmunoResearch Laboratories (West

Grove, PA). 3, 3'-Diaminobenzidine (ImmPACT DAB Peroxidase Substrate) was from Vector Laboratories (Burlingame, CA). PF-3845 was purchased from ApexBio (Houston, TX). PMSF, AEA, PEA, OEA and their deuterated internal standards (AEA-d₈, PEA-d₄, and OEA-d₄) were purchased from Cayman Chemical (Ann Arbor, MI). Ammonium acetate, formic acid, sodium chloride, chloroform, HPLC grade methanol, HPLC grade acetonitrile and HPLC grade water were purchased from Fisher Scientific (Hanover Park, IL). Medical grade nitrogen was purchased from Airgas (Richmond, VA)

Isolation and culture of mouse medullary interstitial cells

Mouse renomedullary interstitial cells were established in primary culture from transplants of isolated and fragmented mouse renal inner medulla using the approach of Muirhead (Muirhead et al., 1990) and subsequently applied and adapted by many others (Dunn et al., 1976; Zusman and Keiser, 1977b; Zou et al., 2001b; Moeckel et al., 2003) including our laboratories (Li et al., 2007; Wang et al., 2011). Briefly, C57BL/6J mice were anesthetized using thiobutabarbital (Inactin™, Sigma-Aldrich, St. Louis, MO) and ketamine (Ketathesia™, Henry Schein Animal Health, Dublin, OH) and sacrificed, and the kidneys removed aseptically. The kidneys were bisected and the inner medullary regions excised, minced, and suspended in DMEM. The suspended fragments were injected subcutaneously over the left rear flank of an isogenic recipient mouse using an 18-gauge syringe needle. After 7-10 days, the recipient mouse was anesthetized and sacrificed, and the yellowish nodules attached to the serosal surfaces over the injection sites excised. The nodules were minced, trypsinized with 0.05% trypsin-EDTA at 37°C for 15 min (GIBCO-Life Technologies, Grand Island, NY), and centrifuged at 500 x g for 5 min. The pellet was resuspended in DMEM containing 10% fetal calf serum and 100 U/mL penicillin G and 100 µg/mL

streptomycin and transferred to a single well of a 12 well tissue culture dish. For the first week after plating, the growth medium also contained amphotericin B (25 µg/mL). At 90% confluence, the cells were trypsinized and passaged successfully to larger dishes. At passage four, the cells were trypsinized, resuspended in frozen storage medium (80% DMEM, 10% fetal bovine serum, and 10% DMSO), and stored in frozen aliquots under liquid nitrogen. MMICs were maintained by regular feeding in complete growth medium, passaging every 7 days (1:3 split ratio). The experiments described in this work used MMICs between passages 4-15.

Immunohistochemistry of kidney tissue and cultured MMICs

MMICs were cultured on glass slides overnight and then fixed in 4% formaldehyde in 1X PBS for 15 min. Kidney tissue slides (5 µm sections) from fixed, paraffin-embedded tissue were subjected to deparaffination and antigen retrieval by placing slides in 95°C citrate buffer (10 mM citric acid, 0.05% Tween 20, pH 6) for 20 minutes. The slides were allowed to cool at room temperature and then washed with 3% H₂O₂ for 10 min. After washing in PBS-0.1% Tween (PBS-T), the samples were incubated with 3% blocking serum for 30 min at room temperature. Primary antibodies and their dilutions in PBS-T were: tenascin-C (1:50 dilution), COX-2 (1:50), NAPE-PLD (1:50) and FAAH (1:50). Secondary antibodies were diluted 1:200 in PBS-T. Incubations with primary antibodies were overnight at 4°C and with HRP-conjugated secondary antibodies for 30 min at room temperature with gentle rocking. HRP staining was detected using 3, 3'-diaminobenzidine as a substrate. After counterstaining nuclei with hematoxylin, stained tissues and cells were washed, mounted and observed by phase contrast microscopy.

Transmission electron microscopic analysis

For ultrastructural imaging, cells were trypsinized, pelleted, resuspended in phosphate-buffered saline, repelleted, and resuspended in 0.1M cacodylate buffer, pH 7, containing 2.5% glutaraldehyde at room temperature. Subsequently, the cells were fixed in osmium tetroxide, dehydrated, and embedded according to standard methods. Sections (600–700Å thick mounted on grids) were prepared using a Leica EM UC6i Ultramicrotome (Leica Microsystems, Buffalo Grove, IL) then stained with 5% uranyl acetate and Reynold's Lead Citrate. Imaging was performed with a JEOL JEM-1230 transmission electron microscope (Jeol U.S.A., Inc., Peabody MA, USA) with a Gatan Orius SC1000 digital camera (Gatan, Pleasanton, CA, USA).

Sudan Black B lipid staining

MMICs were stained for neutral lipids using Sudan Black B (Schneider et al., 2015). After washing and fixing as described above, the cells were washed with PBS, then with 70% ethanol followed by staining for 10 min at room temperature with Sudan Black B solution (0.7% in 70% ethanol, filtered immediately before use). Cells were washed with PBS and observed by phase contrast light microscopy.

Western blot analysis of cultured mouse medullary interstitial cells

MMICs were scraped in re-suspension buffer (0.1 M Tris -HCl pH 7.4, 1 mM EDTA and 20% glycerol) into a microcentrifuge tube. Cells were lysed by sonication for 30 seconds. The protein concentration was measured by BCA protein assay (Pierce Chemical Co.). Protein (30ug) was electrophoresed through a 12% SDS- polyacrylamide gel together with a protein size standard, followed by electroblotting onto a polyvinylidene difluoride membrane. The membranes were

blocked in 5% nonfat milk in Tris-buffered saline-0.1% Tween 20 (TBS-T). Membranes were probed for FAAH and NAPE-PLD proteins using antibodies from Cell Signaling Technology (FAAH, 38295) and Cayman Chemical (NAPE-PLD, 10305) at 1:1000 dilutions in TBS-T incubated overnight at 4°C. After washing, the membranes were incubated with 1:3000 horseradish peroxidase- conjugated anti-rabbit secondary antibody. Images were developed by using enhanced chemiluminescence detection solution and developed with Odyssey FC Imaging (LI-COR, Lincoln, NE). Housekeeping proteins were used to normalize for difference in protein loading. Image Studio 5.2 (LI-COR, Lincoln, NE) was used to quantify the intensities of the protein bands.

PF-3845, osmolarity, and high-pressure treatment of MMICs

MMICs (3×10^6 cells per T-175 sq cm flask) were plated and incubated with 10 μ M PF-3845 or in hypertonic culture medium (600 mOsm/L) for 24 hr in a humidified 37°C incubator with 5% CO₂. Hypertonic medium was prepared with equiosmolar amounts of sodium chloride and urea added to normal 300 mOsm/L DMEM. Cells also treated with high pressure were then placed in a sealable chamber which was pressurized to 20 torr with 5% CO₂ atmosphere for 2 hr. After treatment, the culture medium was collected and stored at -70°C for future analysis and the cells were either collected for protein analysis, or fixed for immunohistochemical or histochemical analysis. Image Pro Plus (Media Cybernetics, Rockville, MD) was used to quantify Sudan Black B lipid droplet staining.

Culture medium analysis of AEA, OEA, and PEA by ultra-high performance liquid chromatography-tandem mass spectrometry (UPLC-MS/MS)

Internal standard solution (10 μ L) containing 1 ng each of AEA-d₈, PEA-d₄, and was OEA-d₄ added to each culture medium (2 mL) or calibrator samples. 1 mM PMSF was added to all samples. Chloroform: methanol (3 mL of 2:1 (v/v)) and 0.73% sodium chloride (200 μ L) were added to all samples and calibrators. Samples and calibrators were mixed for 5 min then centrifuged at 3500 rpm for 5 min. The organic phases were collected and the aqueous phases were extracted twice more with chloroform (1 mL). The organic phases were combined and evaporated to dryness under nitrogen, reconstituted in 100 μ L 60:40 water: acetonitrile and placed in autosampler vials for UPLC-MS/MS analysis.

The UPLC-MS/MS analysis was performed on a Sciex 6500+ QTRAP system with an IonDrive Turbo V source for TurbolonSpray[®] (Ontario, Canada) attached to a Shimadzu Nexera X2 UPLC system (Kyoto, Japan) controlled by Analyst 1.6.3 software (Ontario, Canada). Chromatographic separation was performed on a Discovery[®] HS C18 Column 15cm x 2.1mm, 3 μ m (Supelco: Bellefonte, PA) kept at 40°C and 2 μ L of sample was injected. The mobile phase consisted of A: water with 1 g/L ammonium acetate and 0.1% formic acid and B: acetonitrile. The following gradient was used: 0.0 to 2.4 minutes at 40% B, 2.5 to 6.0 minutes at 60% B, hold for 2.1 minutes at 60% B, then 8.1 to 9 min 100% B, hold at 100% B for 3.1 min and return to 40% B at 12.1 min. The flow rate was 1.0 mL/min and total run time was 14 minutes. The acquisition mode used was Multiple Reaction Monitoring (MRM). The transition ions (m/z), deprotonation potentials (V), and corresponding collision energies (V) for all of the compounds can be found in Table 1. A calibration curve was constructed for the assay by linear regression using the peak area

ratios of the calibrators and internal standards. The standard curve ranged from 0.1-10 ng for AEA, PEA, and OEA. Calibration curves had a correlation (r^2) of 0.9982 or better.

Statistical Analyses

Data are presented as the mean \pm S.E.M. For multiple group comparisons, one- or two-way analysis of variance (ANOVA) was performed using a Tukey or Dunnett post-hoc test when significant differences were found. Data were considered statistically significant when $p \leq 0.05$.

5.3 Results

5.3.1 Characterization of cultured mouse medullary interstitial cells

The MMIC cell population established in the study stained positively for tenascin C (Fig. 20A), whereas cells exposed only to the HRP-conjugated secondary antibody were negative (Fig. 20B). To confirm the report of He et al. (2013) that tenascin C is a selective marker for medullary interstitial cells, sections of mouse kidney were also tested (He et al., 2013). Positive immunostaining by the tenascin C antibody was restricted to the inner medulla/papilla (Fig. 20C); the outer medullary (Fig. 20D) and cortical region (not shown) were negative. This immunostaining in the inner medulla was associated with the ladder-like structures of the medullary interstitial cells, which exhibited oblong nuclei on an axis perpendicular to the tubules of the inner medulla. The cultured MMICs also exhibited intense staining for COX-2 (Fig. 20E) and stained positively for the presence of FAAH (Fig. 20F). In addition, the cultured MMICs also exhibited abundant cytoplasmic granules visible by phase contrast light microscopy. Positive histochemical staining of cytoplasmic vesicles with Oil Red O and Sudan Black B (Fig. 20G and 20H) is consistent with the presence of neutral lipid-containing granules in the MMICs. The

apparent size and number of Sudan Black B stained vesicles varied over time, being most prominent after fresh medium changes.

Ultrastructural analysis of the MMICs by transmission electron microscopy revealed large prominent nuclei, abundant mitochondria, and dilated rough endoplasmic reticulum in their cytoplasm (Fig. 21). Stacks of Golgi apparatus could be found. The cytoplasm was rich in granular and vesicular elements, consistent with lipid droplets, vacuoles, lysosomes, and other structures. Multilamellar bodies with their characteristic whorled appearance were visible in some images of control MMICs (Fig. 21B, arrows). Microvilli were apparent on the plasma membrane. Similar analyses of PF-3845-treated MMICs revealed similar general characteristics as described above, with two notable exceptions. The PF-3845-treated MMICs exhibited pronounced nucleoplasmic invaginations (Figs. 21B and 21D), and the multilamellar bodies were larger and more numerous (Figs. 21B and 21D, arrows).

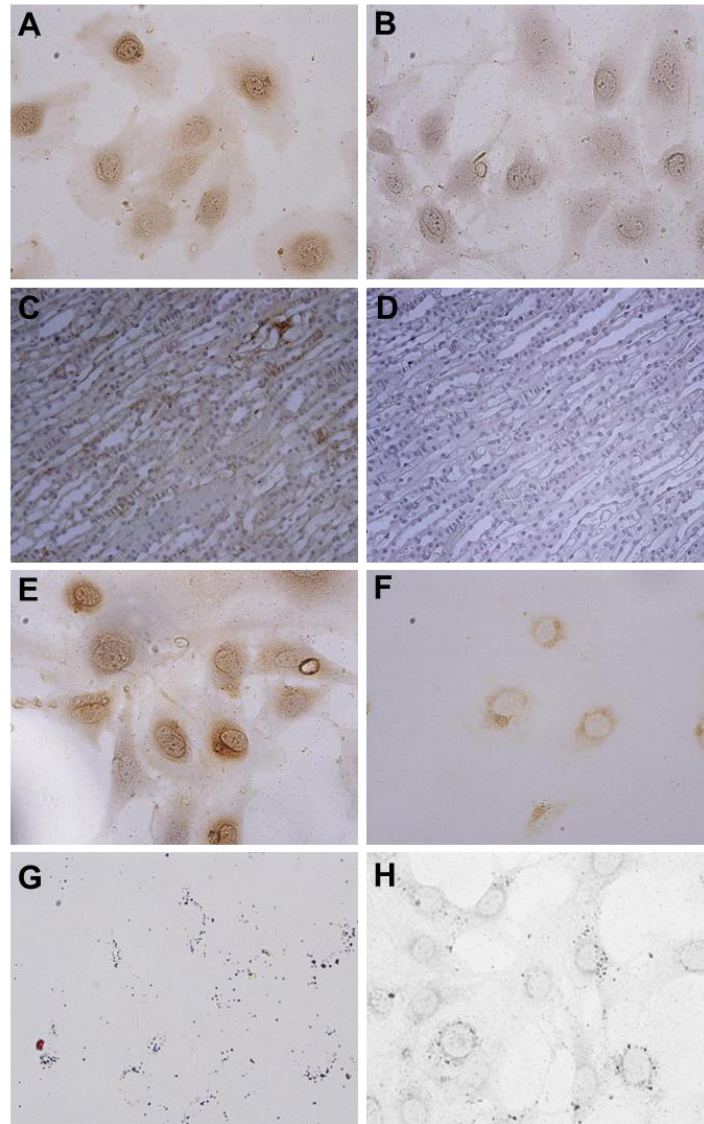


Figure 20. Immunohistochemical and histochemical analysis of cultured MMICs and kidney tissue sections. Cultured mouse medullary interstitial cells (MMICs) or kidney tissue sections were subjected to immunohistochemical or histochemical analyses as described. (A) MMICs stained with tenascin-C primary antibody. (B) Negative control MMICs stained only with horseradish peroxidase-conjugated secondary antibody. (C) Section of inner medullary region of mouse kidney stained for tenascin C antibody. (D) Section of outer medullary region stained for tenascin C. (E) COX-2-stained MMICs. (F) FAAH-stained MMICs. (G) Oil Red O-stained MMICs. (H) Sudan Black B-stained MMICs. Representative images of analyses performed in triplicate are shown (400x magnification).

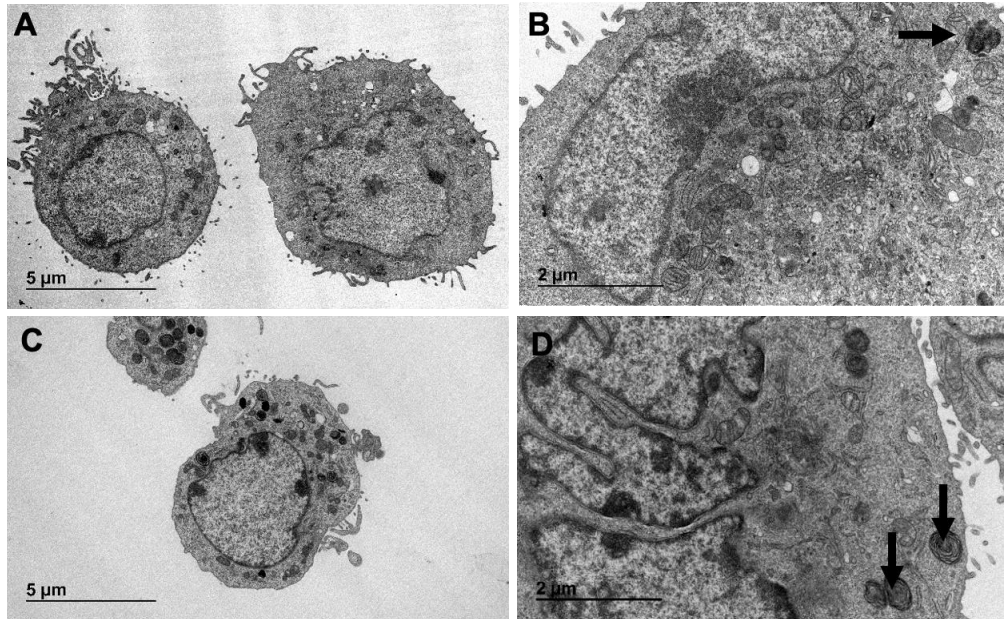


Figure 21. Transmission electron micrographs of vehicle- and PF-3845-treated MMICs. A and B, MMICs treated with vehicle (Veh, 0.1% ethanol) for 24 hr. C and D, MMICs treated with 10 μ M PF-3845 for 24 hr. Low (A, C) and high (B, D) magnification images are shown for each. Osmiophilic lipid granules are seen in the vehicle- and PF-3845-treated MMIC images, including multilamellar bodies (arrows). Cytoplasmic invaginations were also a frequent feature of the PF-3845-treated cells.

5.3.2 FAAH inhibition and high osmolarity increases Sudan Black B-stained lipid granules in cultured MMICs and lipid ethanolamide concentrations in MMIC culture medium

The isolated MMICs were treated with a variety of pharmacologic and physiologic stimuli to evaluate their production and regulation of palmitoylethanolamide and other lipid ethanolamides. Treatment with the FAAH inhibitor, PF-3845, increased the number and size of Sudan Black B-stained granules in cultured MMICs. The onset of the PF-3845 effect on the Sudan Black B staining pattern was evident within 2-4 hours after the start of treatment and was dose-dependent from 1-20 μ M PF-3845 (Fig. 22). These PF-3845-induced lipid granules typically showed greatest accumulation in the perinuclear region. Incubation of MMICs in hypertonic medium (600 mOsm/L) significantly increased the size and number of Sudan Black B stained granules compared to control MMICs ($p < 0.05$) (Figs. 23A and 23B). These granules typically

showed greatest accumulation around the nucleus but were apparent throughout the cytoplasm in some of the cells.

MMICs treated with PF-3845 or incubated in hypertonic medium were also exposed to high pressure (20 torr for 2 hr). In the case of PF-3845 plus high pressure, there was a trend toward an increase in lipid droplets from PF-3458 alone (Figs. 23D and 23E). However, MMICs exposed to high pressure in hypertonic medium decreased in lipid droplet number compared to hypertonic medium alone (Figs. 23A and 23C). Lipid droplet number did not appear to be affected by high pressure alone compared to control MMICs (Figs. 26C and 26F).

The culture medium from MMICs treated with PF-3845, PF-3845 plus high pressure, hypertonic medium, hypertonic medium plus high pressure, and high pressure alone was collected and analyzed by UPLC-MS/MS for PEA, AEA, and OEA (Fig. 24). PF-3845 treatment significantly increased the concentrations of PEA, AEA, and OEA in the medium, and the combination with high pressure did not significantly change this finding ($p < 0.05$). Incubation in hypertonic medium significantly increased PEA and OEA concentrations compared to control ($p < 0.05$) but did not affect AEA concentrations. The combination of hypertonic medium and high pressure slightly increased PEA and OEA from hypertonic alone, but this increase was not significant. High pressure alone did not change the concentrations of PEA, AEA, or OEA from the control group.

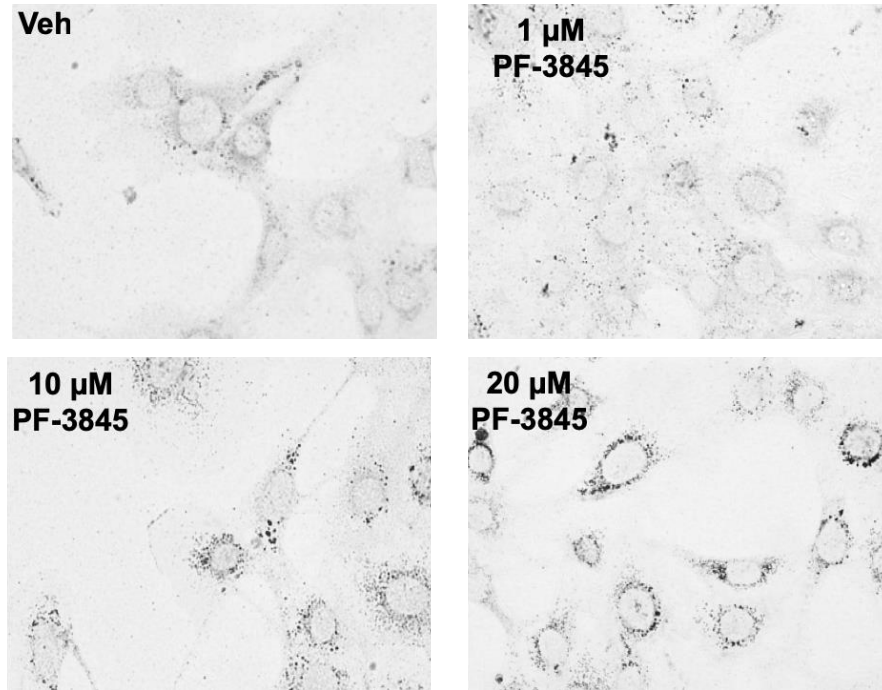


Figure 22. The effects of PF-3845 on lipid staining in cultured MMICs. MMICs cultured in the presence of vehicle (Veh, 0.1% ethanol) or PF-3845 (1, 10 or 20 μ M) for 24 hr were stained with Sudan Black B as described under Methods and Materials. Representative images of analyses performed in triplicate are shown (400x magnification).

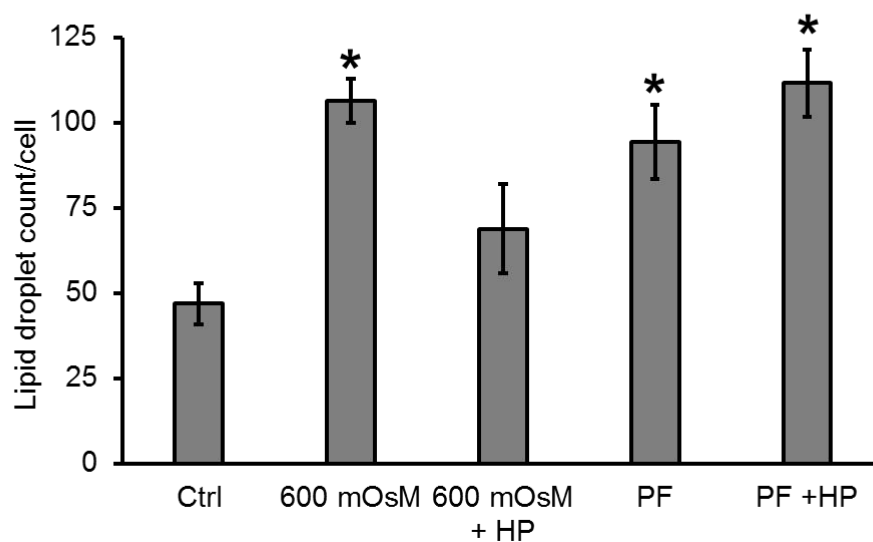
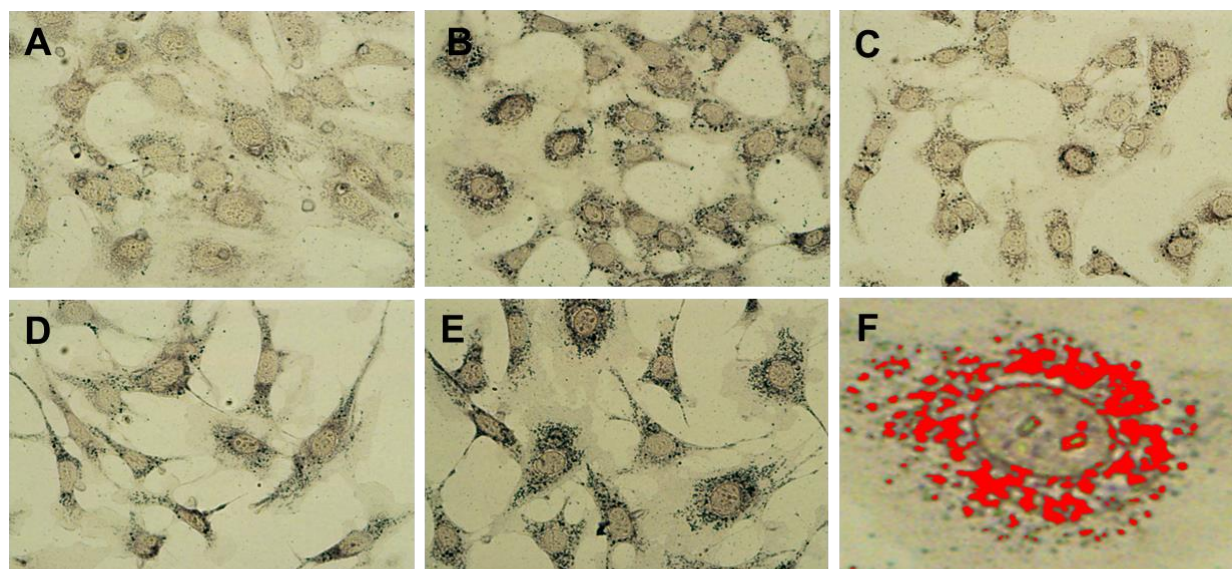


Figure 23. The effects of FAAH inhibition, increased osmolarity, and high-pressure treatment on lipid staining in cultured MMICs. MMICs cultured in normal medium (A), 600 mOsM medium (B), 600 mOsM medium and subjected to high pressure (C), with 10 μ M PF-3845 (D), and with 10 μ M PF-3845 and subjected to high pressure (E). Representative image of lipid droplet quantitation (F). Lipid droplet count per cell was determined using Image Pro Plus. Data represent the mean \pm the standard error of each group. Representative images of analyses performed in triplicate are shown (400x magnification). *Significant difference vs. the control group ($p < 0.05$; $n = 5$) HP, high pressure; PF, PF-3845.

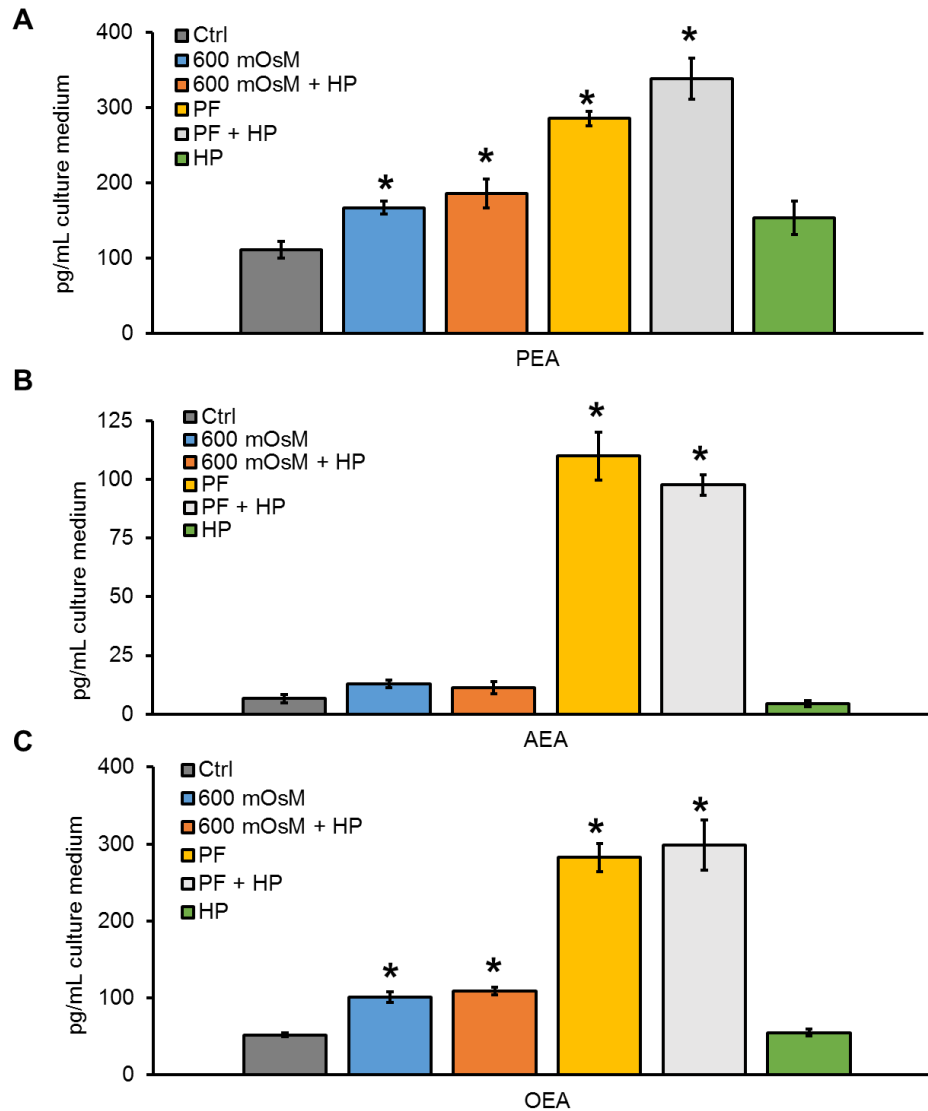


Figure 24. The effects of FAAH inhibition, increased osmolarity, and high pressure treatment on lipid ethanolamide concentrations in MMIC culture medium. (A) Palmitoylethanolamide (PEA), (B) Anandamide (AEA), and (C) oleoylethanolamide (OEA). Data represent the mean \pm the standard error of each group. *Significant difference vs. the control group ($p < 0.05$; $n = 5-7$ per group). The addition of high pressure treatment to either hypertonic medium or PF-3845 treatment did not affect the responses to the latter treatments alone. HP, high pressure; PF, PF-3845.

5.3.3 High osmolarity increases NAPE-PLD protein levels in cultured MMICs

MMICs treated with the different conditions described above were also analyzed by immunohistochemistry and western blot for the detection of NAPE-PLD and FAAH protein. MMICs incubated in hypertonic medium had more intense brown staining for NAPE-PLD compared to control cells (Fig. 25G). The combination of hypertonic medium and high pressure appeared to further intensify NAPE-PLD staining (Fig. 25I). PF-3845 or the combination of PF-3845 and high pressure did not appear to affect the staining pattern of NAPE-PLD (Figs. 26A and 26C). None of the treatments appeared to have an effect on the immunohistochemical staining pattern of FAAH (Figs. 25B, D, F, H, and J). Exposure to high pressure alone also did not appear to have an effect on NAPE-PLD or FAAH staining pattern in MMICs (Figs. 26A, B, D, and E).

The effects of different stimuli on NAPE-PLD and FAAH protein in MMICs by western blot analysis is shown in Figure 27. The relative level of NAPE-PLD was significantly increased by incubation in hypertonic medium ($p < 0.05$) (Fig. 27A). There was a slight increase with the combination of hypertonic medium and high pressure, but this was not significant. PF-3845 alone, the combination of PF-3845 and high pressure, and high pressure alone did not affect the level of NAPE-PLD. None of the treatments had a significant effect on the level of FAAH protein in MMICs (Fig. 27B). There was a trend toward a decrease from PF-3845 treatment, but this decrease was not significant.

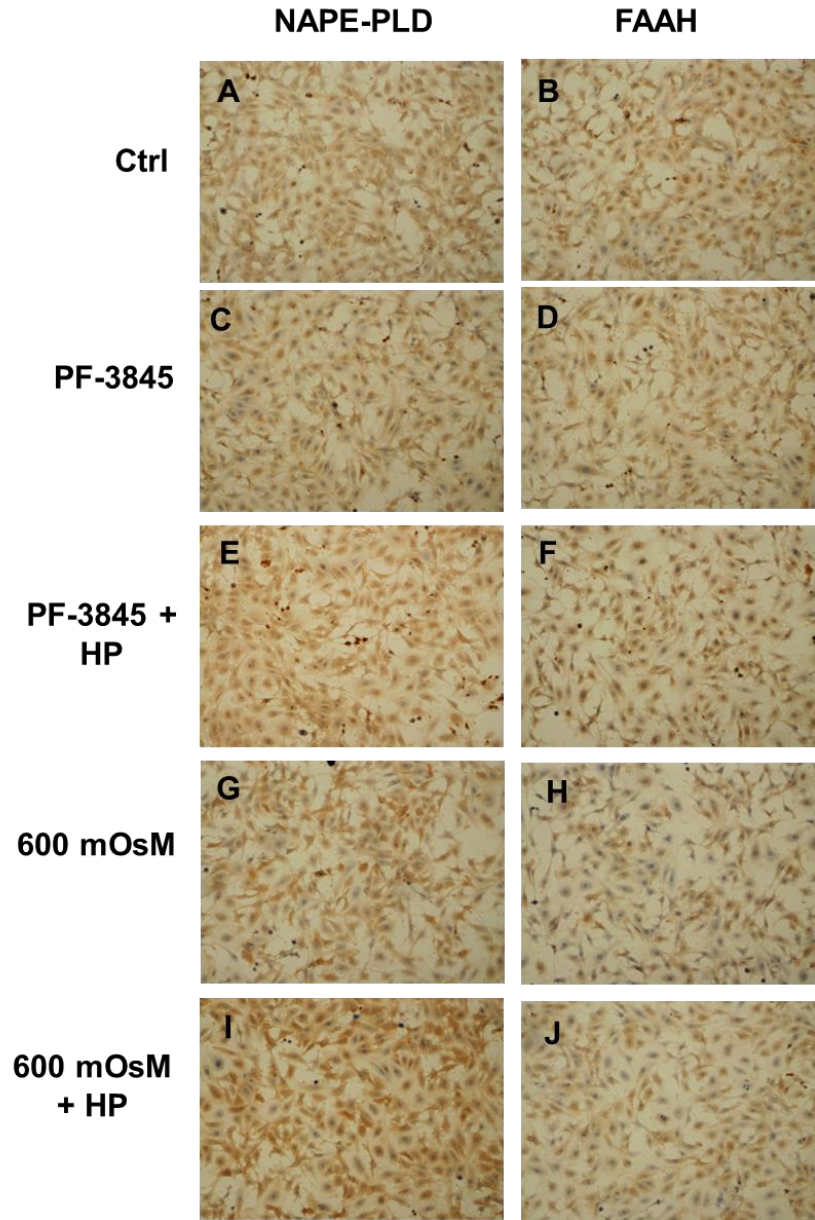


Figure 25. The effects of pharmacologic and physiologic stimuli on the immunohistochemical analysis of cultured MMICs treated. Cultured mouse medullary interstitial cells (MMICs) were subjected to immunohistochemical as described. Control MMICs stained with NAPE-PLD (A) and FAAH (B) primary antibody; PF-3845 treated MMICS stained with NAPE-PLD (C) and FAAH (D) primary antibody; PF-3845 treated MMICS subject to high pressure stained with NAPE-PLD (E) and FAAH (F) primary antibody; 600 mOsm treated MMICS stained with NAPE-PLD (G) and FAAH (H) primary antibody; 600 mOsm treated MMICS subject to high pressure stained with NAPE-PLD (I) and FAAH (J) primary antibody. Representative images of analyses performed in triplicate are shown (100x magnification). HP, high pressure; PF-3845; N-3-pyridinyl-4-[[3-[[5-(trifluoromethyl)-2-pyridinyl]oxy]phenyl]methyl]-1-piperidine carboxamide.

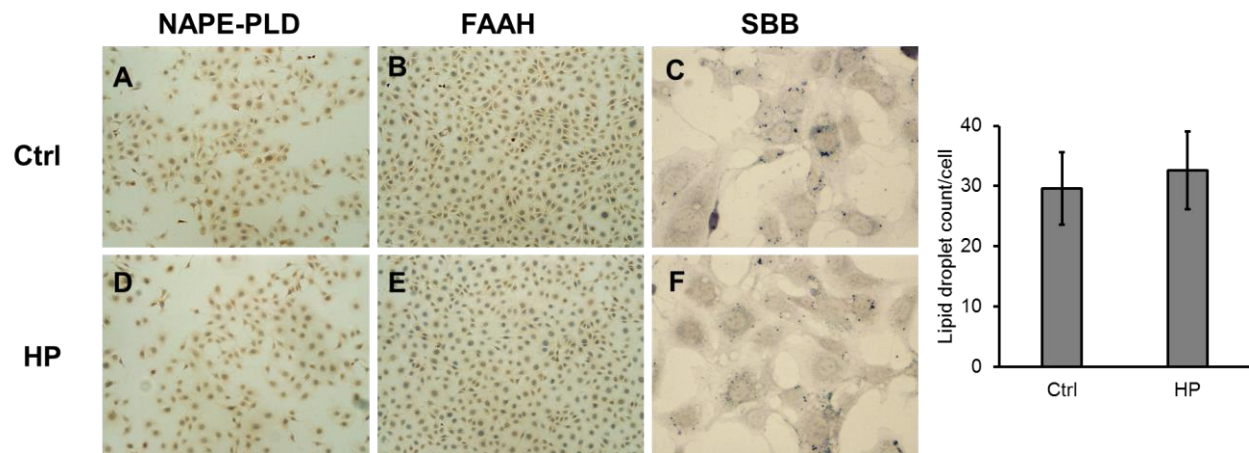


Figure 26. Immunohistochemical and histochemical analysis of cultured MMICs exposed to high pressure. Cultured mouse medullary interstitial cells (MMICs) were subjected to immunohistochemical as described. Control MMICs stained with NAPE-PLD (A) and FAAH (B) primary antibody and stained for lipids with Sudan Black B (C); High pressure treated MMICs stained with NAPE-PLD (D) and FAAH (E) primary antibody, and stained for lipids with Sudan Black B (F). Lipid droplet count per cell was determined using Image Pro Plus. Data represent the mean \pm the standard error of each group. Representative images of analyses performed in triplicate are shown (100x magnification A, B, D, E; 400x magnification C, F). HP, high pressure; SBB, Sudan Black B.

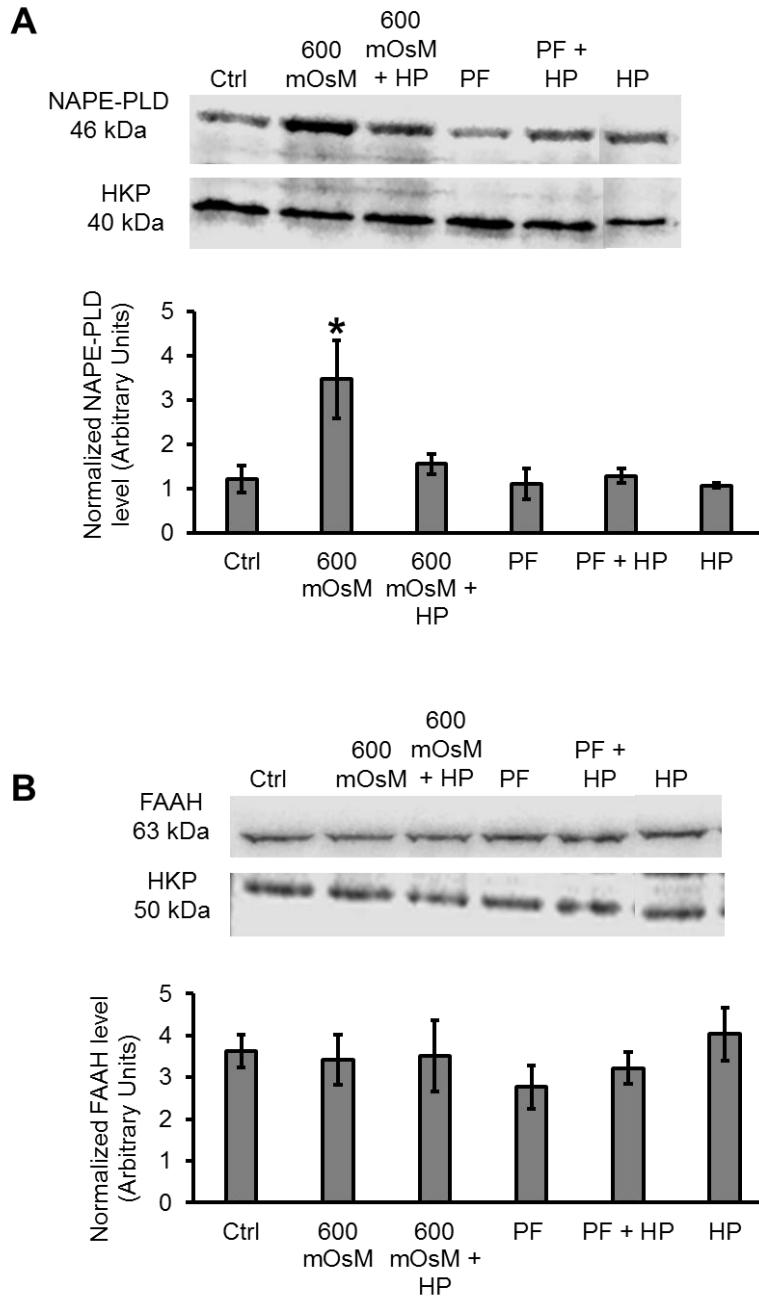


Figure 27. The effects of FAAH inhibition, increased osmolarity, and high-pressure treatment on NAPE-PLD (A) and FAAH (B) protein levels in cultured MMICs. Densitometric evaluations of protein levels were obtained from different experiments. Data represent the mean \pm the standard error of each group. *Significant difference vs. control group ($p < 0.05$; $n = 4-6$ per group). HKP, housekeeping protein; HP, high pressure; PF, PF-3845.

5.4 Discussion

This study characterized primary cultures of renal medullary interstitial cells isolated from the mouse kidney and determined the effect of various stimuli, both pharmacologic and physiologic, on the cells' production and regulation of palmitoylethanolamide and related lipids that may correspond to or be related to Muirhead's medullipin. The hypothesis that FAAH inhibition in the cells would lead to an increase in lipid ethanolamide concentrations was tested. The study also explored the hypothesis that physiologic stimuli that mimic aspects of hypertensive states, such as hypertonicity or exposure to high pressure, would affect lipid ethanolamide concentrations produced by the MMICs. These experiments revealed several novel observations. FAAH inhibition increased Sudan Black B stained lipid droplets in cultured MMICs, and increased lipid ethanolamide concentrations in the culture medium. In addition, the level of NAPE-PLD and PEA formation was induced by MMICs incubated in hypertonic medium.

In the studies described earlier, intramedullary administration of PEA stimulated diuresis-natriuresis and decreased mean arterial pressure in L-NAME-induced hypertension. These results suggest that PEA can act in the renal medulla as an antihypertensive regulator. The renal medulla, through its unique cellular anatomy, blood supply, hyperosmotic environment, and interactions of interstitial cells with renal tubules and vasa recta, has long been proposed to be critical as a long-term regulator of body fluid and sodium balance and blood pressure (Zhuo, 2000). The idea that interstitial cells secrete antihypertensive lipids appeared in the literature in the late 1960's with morphometric observations that the lipid granules of interstitial cells decrease in experimental models of hypertension (Muehrcke et al., 1969; Tobian and Ishii, 1969; Pitcock et al., 1981). The nature of these lipids has been a topic of intense research. Noted for their high content of arachidonic acid in lipid granules and the presence of high constitutive COX levels, interstitial

cells were demonstrated to synthesize and secrete prostaglandin E₂ in response to stimulation of receptors on their cell surface for vasopressor hormones such as angiotensin (Zusman and Keiser, 1977a). Prostaglandin E₂ is a vasodilator as well as diuretic and natriuretic (Hashimoto, 1980). To our knowledge, medullipin is the only other major antihypertensive lipid proposed to be produced and released by medullary interstitial cells (Brooks et al., 1994; Cowley, 1994).

Renal medullary interstitial cells were cultured from mouse kidney and their characteristics were found to be consistent with literature, including well developed and widened rough endoplasmic reticulum, abundant mitochondria, the presence of lipid droplets, and positive staining for COX-2 and tenascin-C (Lemley and Kriz, 1991; Moeckel et al., 2003; He et al., 2013). The cultured MMICs also stained positively for FAAH, which was unreported in literature. The finding that FAAH was expressed in MMICs provides evidence for the presence of the proposed target of PF-3845 in the studies described earlier. Another finding of interest for its possible relation to secretion of PEA and other lipid ethanolamides was the observed increase in lipid granules in MMICs exposed to PF-3845, as demonstrated using the neutral lipid dye, Sudan Black B. Ultrastructural analyses of control and PF-3845-treated MMICs suggested that the increased neutral lipid staining in the PF-3845-treated cells was associated at least in part with increased size and number of cytoplasmic multilamellar bodies. These organelles were found by us to be present in the vehicle-treated MMICs and by others in cultured medullary interstitial cells (Mathews et al., 1979) as well as in renomedullary interstitial cells *in situ* (Lewis and Prentice, 1979; Bohman, 1980). They are proposed to play roles in the storage and secretion of lipids (Schmitz and Muller, 1991). Further investigation is needed to determine if multilamellar bodies are involved in the PF-3845-induced mechanism of PEA release.

RMICs appear to play an important role in regulating salt absorption and renal medullary blood flow due to their interposition between the vasa recta, loops of Henle, and collecting ducts. Prostaglandin E₂ has been identified as an important component of this activity but does not fully explain the role of RMICs (Daniels et al., 1967). The cultured MMICs were also exposed to physiologic stimuli that mimic aspects of hypertensive states, such as increase in salt concentration and exposure to high pressure, to investigate how PEA and other lipid ethanolamides' production and release are regulated. It is well documented that a chronic high salt intake causes an increase in blood pressure and contributes to the development of hypertension (Ha, 2014). With the cultured MMICs, exposure to hypertonic medium produced an increase in NAPE-PLD protein levels, increased Sudan Black B stained lipid granules, and a significant increase in PEA and OEA production and release by analysis of the culture medium. AEA concentration was not changed by this treatment. Consistent with our findings, Nissen reported that a brief period of salt repletion in salt-depleted rats induced a significant increase in the number of lipid droplets in the renal medullary interstitial cells (Nissen, 1968). He concluded that the differences in number of lipid droplets are due to the droplets containing physiologically active substances that accumulate during salt repletion and release during depletion. The novel findings in this study support this hypothesis of physiologically important substances in the lipid droplets of RMICs and a role of RMICs in the regulation of PEA synthesis in the kidney. It is possible that in cases of high salt intake that could lead to a hypertensive state, the interstitial cells of the renal medulla would respond by stimulating the production of PEA in order to combat the increase in extracellular fluid volume. Previously described studies demonstrated that PEA can act in the renal medulla to increase fluid and salt excretion, and therefore decrease ECFV which would lead to a reduction in arterial pressure.

Pressure-natriuresis is associated with elevations in medullary blood flow and renal interstitial hydrostatic pressure (RIHP). The rise in RIHP is important in triggering pressure-natriuresis, since the removal of the renal capsule attenuates the natriuretic response after an increase in renal perfusion pressure (RPP) (Khraibi and Knox, 1989). It has been reported that in an increase in RPP from 100 to 150 mmHg, RIHP increased to 10 mmHg (Garcia-Estan and Roman, 1989; Williams et al., 2007). RMICs have been proposed to be sensors of an increase in RIHP, and therefore RPP (Carlsen et al., 2010). In this study cultured MMICs were also exposed to high pressure alone, and in combination with other stimuli to investigate the production of lipid ethanolamides. High pressure alone did not change lipid droplet number, NAPE-PLD or FAAH protein levels in MMICs, or concentrations of lipid ethanolamides in the culture medium. Interestingly, MMICs in hypertonic medium also exposed to high pressure resulted in a decrease in lipid droplets, a return to normal levels of NAPE-PLD, and no further increase in the release of PEA into the medium. In contrast, in PF-3845-treated MMICs also subjected to high pressure, lipid droplet number further increased, but there was not a change in NAPE-PLD or FAAH protein levels. Although not significant, there was a trend toward further increases in PEA and OEA concentrations with the addition of high pressure to hyperosmolarity, but AEA concentrations did not appear to be affected. It is clear that the mechanism by which increased pressure affects the production and release of PEA, AEA, and OEA from MMICs is complex and is possibly mediated by different mechanisms depending on the physiological state of the cells.

There is increasing evidence that supports the role of renal medullary interstitial cells as an important regulator of normal homeostasis. The current study investigated the cellular mechanisms in which the biologically active lipid ethanolamides PEA, AEA, and OEA are produced and released from cultured mouse medullary interstitial cells. In summary, inhibition of FAAH by PF-

3845 increased lipid droplets in MMICs and lipid ethanolamide concentrations in the culture medium. Furthermore, MMICs incubated in hypertonic medium resulted in an increase of NAPE-PLD levels, lipid droplets, and PEA concentrations in the culture medium. These data supports the hypothesis that MMICs produce and release PEA which may then serve as an important regulator of normal kidney function and in hypertensive states. Future studies are needed to evaluate *N*-acylethanolamines by analysis of the lipids contained in the lipid droplets of the MMICs.

Final discussion and conclusions

The role of the endocannabinoid system and related lipids in the kidney and control of blood pressure is not fully understood. The pursuit of the identification of neutral lipids that originate from the renal medulla and serve as antihypertensive regulators continues almost 70 years after Muirhead first described a feedback blood pressure control system operating from the interstitial cells of the renal medulla to down-regulate blood pressure. The purpose of the preceding studies was to investigate the mechanisms by which the renal medulla combats increased blood pressure by the proposed release of an antihypertensive substance. The studies included elevation of endogenous lipid ethanolamide concentrations via inhibition of the degradative enzyme FAAH, administration of exogenous PEA, and investigation of the cellular mechanisms by which PEA and other lipid ethanolamides are regulated by cultured MMICs.

We hypothesized that elevating endogenous AEA by chemical inhibition of FAAH by PF-3845 would elicit similar effects as exogenously administered AEA. This was confirmed with intramedullary and intravenously administered PF-3845 stimulating diuresis and natriuresis in a model of acute renal function. Furthermore, PF-3845 produced a decrease in mean arterial pressure, and these effects were accompanied by increased AEA, PEA, and OEA concentrations in kidney tissue. However, previous studies in our lab and others have demonstrated that exogenously administered AEA does not produce a decrease in blood pressure. This led us to hypothesize that the effects observed with PF-3845 may not be due to increased AEA in the kidney but may be mediated fully or partially by the endocannabinoid-like lipid PEA. The ability of PEA to modulate kidney function was then explored. Exogenously administered PEA stimulated urine and salt excretion in normotensive mice without changing MAP, and these effects were found to be independent of FAAH-mediated hydrolysis. Intramedullary PEA-induced diuresis was also

independent of CB₁, excluding the entourage effect as a possible mechanism. While the results of these studies do not confirm the hypothesis that the lowering of blood pressure by intramedullary PF-3845 infusion is mediated by increased PEA concentrations, since PEA did not affect MAP, this does not exclude PEA from being a contributor to the mechanism of PF-3845-induced diuresis and natriuresis. It is possible that the combination of increased AEA and PEA in the kidney is responsible for the decrease in mean arterial pressure observed with PF-3845. The effects of PEA administration in a chronic hypertension model was also evaluated. Intramedullary PEA was able to induce diuresis and natriuresis and also decrease mean arterial pressure in L-NAME-induced hypertensive mice, demonstrating PEA has the ability to serve as an antihypertensive agent in the renal medulla.

The last of the studies was designed to investigate the mechanisms of production and regulation of PEA and other lipid ethanolamides from cultured mouse medullary interstitial cells in response to pharmacologic and physiologic stimuli. We hypothesized that different stimuli would increase production of lipid ethanolamides and support the long-recognized idea that the interstitial cells of the renal medulla are the source of an antihypertensive substance. It was demonstrated that FAAH inhibition increased neutral lipid-containing granules in the MMICs and lipid ethanolamide concentrations in the culture medium. PF-3845 treated cells also exposed to elevated pressure to mimic the increase in RIHP in hypertensive states had further increased lipid granules in the perinuclear region and PEA concentrations in the medium. This suggests that under conditions with already increased PEA, a high pressure stimulus results in further synthesis and storage of PEA in the lipid granules of MMICs. It was also demonstrated that hypertonic medium increased NAPE-PLD protein levels in MMICs, an effect that was accompanied by increased lipid droplets and PEA concentrations in the culture medium. PEA concentrations remained elevated in

the medium of MMICs incubated in hypertonic medium also exposed to high pressure, but NAPE-PLD returned to control levels. These data indicate that the interstitial cells respond to an increase in salt concentration by inducing synthesis and release of PEA, furthering supporting the hypothesis that PEA has the ability to serve as an antihypertensive stimulus in the renal medulla.

The mechanisms by which the renal medulla responds to an increase in blood pressure remain unclear. However, this body of work supports the role of the endocannabinoid-related lipid PEA as a potential regulator of salt and water reabsorption and blood pressure originating from the interstitial cells. PEA was able to stimulate diuresis and natriuresis in normotensive mice, as well as decrease mean arterial pressure in a model of chronic hypertension. Furthermore, cultured renal medullary interstitial cells produce PEA in high abundance and respond to pharmacologic and physiologic stimuli by increasing synthesis and release of PEA. Data from the described experiments contributes to knowledge needed for the development of improved approaches for treatment or prevention of hypertension by enhancing the endogenous antihypertensive mechanisms of the kidney.

Funding

This work was supported by National Institute of Diabetes and Digestive and Kidney Disorders grant, DK102539, National Institute on Health (NIH) Center for Drug Abuse grant P30DA033934, and National Institute on Drug Abuse (NIDA) Training Grant T32DA007027-42.

References

- Ackermann A, Fernandez-Alfonso MS, Sanchez de Rojas R, Ortega T, Paul M and Gonzalez C (1998) Modulation of angiotensin-converting enzyme by nitric oxide. *Br J Pharmacol* **124**:291-298.
- Ahmad A, Daneva Z, Li G, Dempsey SK, Li N, Poklis JL, Lichtman A, Li PL and Ritter JK (2017) Stimulation of diuresis and natriuresis by renomedullary infusion of a dual inhibitor of fatty acid amide hydrolase and monoacylglycerol lipase. *Am J Physiol Renal Physiol* **313**:F1068-f1076.
- Ahmad A, Dempsey SK, Daneva Z, Li N, Poklis JL, Li PL and Ritter JK (2018) Modulation of mean arterial pressure and diuresis by renomedullary infusion of a selective inhibitor of fatty acid amide hydrolase. *Am J Physiol Renal Physiol* **315**:F967-F976.
- Ahn K, Johnson DS and Cravatt BF (2009a) Fatty acid amide hydrolase as a potential therapeutic target for the treatment of pain and CNS disorders. *Expert Opin Drug Discov* **4**:763-784.
- Ahn K, Johnson DS, Mileni M, Beidler D, Long JZ, McKinney MK, Weerapana E, Sadagopan N, Liimatta M, Smith SE, Lazerwith S, Stiff C, Kamtekar S, Bhattacharya K, Zhang Y, Swaney S, Van Becelaere K, Stevens RC and Cravatt BF (2009b) Discovery and characterization of a highly selective FAAH inhibitor that reduces inflammatory pain. *Chem Biol* **16**:411-420.
- Alexander SP and Kendall DA (2007) The complications of promiscuity: endocannabinoid action and metabolism. *Br J Pharmacol* **152**:602-623.
- Aloe L, Leon A and Levi-Montalcini R (1993) A proposed autacoid mechanism controlling mastocyte behaviour. *Agents Actions* **39 Spec No**:C145-147.
- Ambrosino P, Soldovieri MV, Russo C and Tagliabatella M (2013) Activation and desensitization of TRPV1 channels in sensory neurons by the PPARalpha agonist palmitoylethanolamide. *Br J Pharmacol* **168**:1430-1444.
- Arnal JF, el Amrani AI, Chatellier G, Menard J and Michel JB (1993) Cardiac weight in hypertension induced by nitric oxide synthase blockade. *Hypertension* **22**:380-387.
- Bachur NR, Masek K, Melmon KL and Udenfriend S (1965) Fatty acid amides of ethanolamine in mammalian tissues *J Biol Chem* **240**:1019-1024.
- Banks T and Oyekan A (2008) Peroxisome proliferator-activated receptor alpha activation attenuated angiotensin type 1-mediated but enhanced angiotensin type 2-mediated hemodynamic effects to angiotensin II in the rat. *J Hypertens* **26**:468-477.
- Baranowska-Kuczko M, Kozłowska H, Kloza M, Karpinska O, Toczek M, Harasim E, Kasacka I and Malinowska B (2016) Protective role of cannabinoid CB1 receptors and vascular effects of chronic administration of FAAH inhibitor URB597 in DOCA-salt hypertensive rats. *Life Sci* **151**:288-299.
- Barutta F, Piscitelli F, Pinach S, Bruno G, Gambino R, Rastaldi MP, Salvidio G, Di Marzo V, Cavallo Perin P and Gruden G (2011) Protective role of cannabinoid receptor type 2 in a mouse model of diabetic nephropathy. *Diabetes* **60**:2386-2396.
- Ben-Shabat S, Fride E, Sheskin T, Tamiri T, Rhee MH, Vogel Z, Bisogno T, De Petrocellis L, Di Marzo V and Mechoulam R (1998) An entourage effect: inactive endogenous fatty acid glycerol esters enhance 2-arachidonoyl-glycerol cannabinoid activity. *Eur J Pharmacol* **353**:23-31.

- Benvenuti F, Lattanzi F, De Gori A and Tarli P (1968) [Activity of some derivatives of palmitoylethanolamide on carragenine-induced edema in the rat paw]. *Boll Soc Ital Biol Sper* **44**:809-813.
- Biernacki M, Ambrozewicz E, Gegotek A, Toczek M, Bielawska K and Skrzydlewska E (2017) Redox system and phospholipid metabolism in the kidney of hypertensive rats after FAAH inhibitor URB597 administration. *Redox Biol* **15**:41-50.
- Biernacki M, Luczaj W, Gegotek A, Toczek M, Bielawska K and Skrzydlewska E (2016) Crosstalk between liver antioxidant and the endocannabinoid systems after chronic administration of the FAAH inhibitor, URB597, to hypertensive rats. *Toxicol Appl Pharmacol* **301**:31-41.
- Bing RF, Russell GI, Swales JD, Thurston H and Fletcher A (1981) Chemical renal medullectomy; effect upon reversal of two-kidney, one-clip hypertension in the rat. *Clin Sci (Lond)* **61 Suppl 7**:335s-338s.
- Bisogno T, Howell F, Williams G, Minassi A, Cascio MG, Ligresti A, Matias I, Schiano-Moriello A, Paul P, Williams EJ, Gangadharan U, Hobbs C, Di Marzo V and Doherty P (2003) Cloning of the first sn1-DAG lipases points to the spatial and temporal regulation of endocannabinoid signaling in the brain. *J Cell Biol* **163**:463-468.
- Bisogno T, Maurelli S, Melck D, De Petrocellis L and Di Marzo V (1997) Biosynthesis, uptake, and degradation of anandamide and palmitoylethanolamide in leukocytes. *J Biol Chem* **272**:3315-3323.
- Blankman JL, Simon GM and Cravatt BF (2007) A comprehensive profile of brain enzymes that hydrolyze the endocannabinoid 2-arachidonoylglycerol. *Chem Biol* **14**:1347-1356.
- Bohman SO (1980) The ultrastructure of the renal medulla and the interstitial cells, in *The renal papilla and hypertension* (Mandal AK and Bohman SO eds) pp 7-28, Plenum, New York.
- Bohman SO and Jensen PK (1976) Morphometric studies on the lipid droplets of the interstitial cells of the renal medulla in different states of diuresis. *J Ultrastruct Res* **55**:182-192.
- Braun-Menendez E, Fasciolo JC, Leloir LF and Munoz JM (1940) The substance causing renal hypertension. *J Physiol* **98**:283-298.
- Braun-Menendez E and Page IH (1958) Suggested Revision of Nomenclature--Angiotensin. *Science* **127**:242.
- Brooks B, Byers LW, Muirhead EE, Muirhead M, Pitcock JA, Maddipati KR and Maxey KM (1994) Purification of class I medullipins from the venous effluent of isolated normal kidneys perfused under high pressure with saline. *Blood Press* **3**:407-417.
- Buckley MM and Johns EJ (2011) Impact of L-NAME on the cardiopulmonary reflex in cardiac hypertrophy. *Am J Physiol Regul Integr Comp Physiol* **301**:R1549-1556.
- Bumpus FM, Schwarz H and Page IH (1957) Synthesis and pharmacology of the octapeptide angiotenin. *Science* **125**:886-887.
- Burnstock G, Evans LC and Bailey MA (2014) Purinergic signalling in the kidney in health and disease. *Purinergic Signal* **10**:71-101.
- Cadas H, di Tomaso E and Piomelli D (1997) Occurrence and biosynthesis of endogenous cannabinoid precursor, N-arachidonoyl phosphatidylethanolamine, in rat brain. *J Neurosci* **17**:1226-1242.
- Cahill PA, Redmond EM, Foster C and Sitzmann JV (1995) Nitric oxide regulates angiotensin II receptors in vascular smooth muscle cells. *Eur J Pharmacol* **288**:219-229.
- Calignano A, La Rana G, Giuffrida A and Piomelli D (1998) Control of pain initiation by endogenous cannabinoids. *Nature* **394**:277-281.

- Carlsen I, Donohue KE, Jensen AM, Selzer AL, Chen J, Poppas DP, Felsen D, Frøkiær J and Nørregaard R (2010) Increased cyclooxygenase-2 expression and prostaglandin E2 production in pressurized renal medullary interstitial cells. *American journal of physiology Regulatory, integrative and comparative physiology* **299**:R823-R831.
- Carmines PK, Bell PD, Roman RJ, Work J and Navar LG (1985) Prostaglandins in the sodium excretory response to altered renal arterial pressure in dogs. *Am J Physiol* **248**:F8-14.
- Cediel E, Vazquez-Cruz B, Navarro-Cid J, de las Heras N, Sanz-Rosa D, Cachofeiro V and Lahera V (2002) Role of endothelin-1 and thromboxane A2 in renal vasoconstriction induced by angiotensin II in diabetes and hypertension. *Kidney Int Suppl*:S2-7.
- Chen PY and Sanders PW (1991) L-arginine abrogates salt-sensitive hypertension in Dahl/Rapp rats. *J Clin Invest* **88**:1559-1567.
- Chopda GR, Vemuri VK, Sharma R, Thakur GA, Makriyannis A and Paronis CA (2013) Diuretic effects of cannabinoid agonists in mice. *Eur J Pharmacol* **721**:64-69.
- Conti S, Costa B, Colleoni M, Parolaro D and Giagnoni G (2002) Antiinflammatory action of endocannabinoid palmitoylethanolamide and the synthetic cannabinoid nabilone in a model of acute inflammation in the rat. *Br J Pharmacol* **135**:181-187.
- Costa B, Comelli F, Bettoni I, Colleoni M and Giagnoni G (2008) The endogenous fatty acid amide, palmitoylethanolamide, has anti-allodynic and anti-hyperalgesic effects in a murine model of neuropathic pain: involvement of CB(1), TRPV1 and PPARgamma receptors and neurotrophic factors. *Pain* **139**:541-550.
- Cowley AW, Jr. (1994) Franz Volhard Lecture. Evolution of the medullipin concept of blood pressure control: a tribute to Eric Muirhead. *J Hypertens Suppl* **12**:S25-34.
- Cowley AW, Jr., Mori T, Mattson D and Zou AP (2003) Role of renal NO production in the regulation of medullary blood flow, in *Am J Physiol Regul Integr Comp Physiol* pp R1355-1369, United States.
- Cravatt BF, Demarest K, Patricelli MP, Bracey MH, Giang DK, Martin BR and Lichtman AH (2001) Supersensitivity to anandamide and enhanced endogenous cannabinoid signaling in mice lacking fatty acid amide hydrolase. *Proc Natl Acad Sci U S A* **98**:9371-9376.
- Cravatt BF and Lichtman AH (2003) Fatty acid amide hydrolase: an emerging therapeutic target in the endocannabinoid system. *Curr Opin Chem Biol* **7**:469-475.
- Daniels EG, Hinman JW, Leach BE and Muirhead EE (1967) Identification of prostaglandin E2 as the principal vasodepressor lipid of rabbit renal medulla. *Nature* **215**:1298-1299.
- de Novellis V, Luongo L, Guida F, Cristino L, Palazzo E, Russo R, Marabese I, D'Agostino G, Calignano A, Rossi F, Di Marzo V and Maione S (2012) Effects of intra-ventrolateral periaqueductal grey palmitoylethanolamide on thermoceptive threshold and rostral ventromedial medulla cell activity. *European Journal of Pharmacology* **676**:41-50.
- De Petrocellis L and Di Marzo V (2009) An introduction to the endocannabinoid system: from the early to the latest concepts. *Best Pract Res Clin Endocrinol Metab* **23**:1-15.
- Deutsch DG and Chin SA (1993) Enzymatic synthesis and degradation of anandamide, a cannabinoid receptor agonist. *Biochem Pharmacol* **46**:791-796.
- Deutsch DG, Goligorsky MS, Schmid PC, Krebsbach RJ, Schmid HH, Das SK, Dey SK, Arreaza G, Thorup C, Stefano G and Moore LC (1997) Production and physiological actions of anandamide in the vasculature of the rat kidney. *J Clin Invest* **100**:1538-1546.
- Devane WA, Hanus L, Breuer A, Pertwee RG, Stevenson LA, Griffin G, Gibson D, Mandelbaum A, Etinger A and Mechoulam R (1992) Isolation and structure of a brain constituent that binds to the cannabinoid receptor. *Science* **258**:1946-1949.

- Di Marzo V, Bisogno T, Sugiura T, Melck D and De Petrocellis L (1998) The novel endogenous cannabinoid 2-arachidonoylglycerol is inactivated by neuronal- and basophil-like cells: connections with anandamide. *Biochem J* **331** (Pt 1):15-19.
- Di Marzo V, De Petrocellis L, Fezza F, Ligresti A and Bisogno T (2002) Anandamide receptors. *Prostaglandins, Leukotrienes and Essential Fatty Acids (PLEFA)* **66**:377-391.
- Di Marzo V, Melck D, Orlando P, Bisogno T, Zagoory O, Bifulco M, Vogel Z and De Petrocellis L (2001) Palmitoylethanolamide inhibits the expression of fatty acid amide hydrolase and enhances the anti-proliferative effect of anandamide in human breast cancer cells. *Biochem J* **358**:249-255.
- DiBona GF and Esler M (2010) Translational medicine: the antihypertensive effect of renal denervation. *Am J Physiol Regul Integr Comp Physiol* **298**:R245-253.
- DiBona GF and Kopp UC (1997) Neural control of renal function. *Physiol Rev* **77**:75-197.
- Dunn MJ, Staley RS and Harrison M (1976) Characterization of prostaglandin production in tissue culture of rat renal medullary cells. *Prostaglandins* **12**:37-49.
- Esposito E and Cuzzocrea S (2013) Palmitoylethanolamide is a new possible pharmacological treatment for the inflammation associated with trauma. *Mini Rev Med Chem* **13**:237-255.
- Esposito E, Paterniti I, Mazzon E, Genovese T, Di Paola R, Galuppo M and Cuzzocrea S (2011) Effects of palmitoylethanolamide on release of mast cell peptidases and neurotrophic factors after spinal cord injury. *Brain Behav Immun* **25**:1099-1112.
- Facci L, Dal Toso R, Romanello S, Buriani A, Skaper SD and Leon A (1995) Mast cells express a peripheral cannabinoid receptor with differential sensitivity to anandamide and palmitoylethanolamide. *Proc Natl Acad Sci U S A* **92**:3376-3380.
- Folkow B (2007) Incretory renal functions--Tigerstedt, renin and its neglected antagonist medullipin. *Acta Physiol (Oxf)* **190**:99-102.
- Fowler CJ (2013) Transport of endocannabinoids across the plasma membrane and within the cell. *Febs j* **280**:1895-1904.
- Garcia-Estan J and Roman RJ (1989) Role of renal interstitial hydrostatic pressure in the pressure diuresis response. *Am J Physiol* **256**:F63-70.
- García MeC, Adler-Graschinsky E and Celuch SM (2009) Enhancement of the hypotensive effects of intrathecally injected endocannabinoids by the entourage compound palmitoylethanolamide. *Eur J Pharmacol* **610**:75-80.
- Garvin JL, Herrera M and Ortiz PA (2011) Regulation of renal NaCl transport by nitric oxide, endothelin, and ATP: clinical implications. *Annu Rev Physiol* **73**:359-376.
- Gelosa P, Banfi C, Gianella A, Brioschi M, Pignieri A, Nobili E, Castiglioni L, Cimino M, Tremoli E and Sironi L (2010) Peroxisome proliferator-activated receptor {alpha} agonism prevents renal damage and the oxidative stress and inflammatory processes affecting the brains of stroke-prone rats. *J Pharmacol Exp Ther* **335**:324-331.
- Glaser ST, Kaczocha M and Deutsch DG (2005) Anandamide transport: a critical review. *Life Sci* **77**:1584-1604.
- Glodny B and Pauli GF (2006) The vasodepressor function of the kidney: further characterization of medullipin and a second hormone designated angiolysin. *Hypertens Res* **29**:533-544.
- Godlewski G, Alapafuja SO, Bátkai S, Nikas SP, Cinar R, Offertáler L, Osei-Hyiaman D, Liu J, Mukhopadhyay B, Harvey-White J, Tam J, Pacak K, Blankman JL, Cravatt BF, Makriyannis A and Kunos G (2010) Inhibitor of fatty acid amide hydrolase normalizes cardiovascular function in hypertension without adverse metabolic effects. *Chem Biol* **17**:1256-1266.

- Goldblatt H, Lynch J, Hanzal RF and Summerville WW (1934) Studies on experimental hypertension: I. The production of persistent elevation of systolic blood pressure by means of renal ischemia. *J Exp Med* **59**:347-379.
- Gomez-Ruiz M, Hernandez M, de Miguel R and Ramos JA (2007) An overview on the biochemistry of the cannabinoid system. *Mol Neurobiol* **36**:3-14.
- Gothberg G (1994) Physiology of the renomedullary depressor system. *J Hypertens Suppl* **12**:S57-64.
- Gothberg G, Lundin S and Folkow B (1982) Acute vasodepressor effect in normotensive rats following extracorporeal perfusion of the declipped kidney of two-kidney, one clip hypertensive rats. *Hypertension* **4**:101-105.
- Granger JP, Alexander BT and Llinas M (2002) Mechanisms of pressure natriuresis. *Curr Hypertens Rep* **4**:152-159.
- Granger JP and Scott JW (1988) Effects of renal artery pressure on interstitial pressure and Na excretion during renal vasodilation. *Am J Physiol* **255**:F828-833.
- Grollman A, Muirhead EE and Vanatta J (1949) Role of the kidney in pathogenesis of hypertension as determined by a study of the effects of bilateral nephrectomy and other experimental procedures on the blood pressure of the dog. *Am J Physiol* **157**:21-30.
- Guyton AC, Coleman TG, Cowley AW, Scheel KW, Manning RD and Norman RA (1972a) Arterial pressure regulation: Overriding dominance of the kidneys in long-term regulation and in hypertension. *The American Journal of Medicine* **52**:584-594.
- Guyton AC, Coleman TG and Granger HJ (1972b) Circulation: overall regulation. *Annu Rev Physiol* **34**:13-46.
- Ha SK (2014) Dietary salt intake and hypertension. *Electrolyte & blood pressure : E & BP* **12**:7-18.
- Haas JA, Granger JP and Knox FG (1988) Effect of intrarenal volume expansion on proximal sodium reabsorption. *Am J Physiol* **255**:F1178-1182.
- Hall JE (2003) Historical perspective of the renin-angiotensin system. *Mol Biotechnol* **24**:27-39.
- Hashimoto T (1980) Effects of prostaglandin E₂, I₂ and F₂ alpha on systemic and renal hemodynamics, renal function and renin secretion in anesthetized dogs. *Jpn J Pharmacol* **30**:173-186.
- He W, Xie Q, Wang Y, Chen J, Zhao M, Davis LS, Breyer MD, Gu G and Hao CM (2013) Generation of a tenascin-C-CreER2 knockin mouse line for conditional DNA recombination in renal medullary interstitial cells. *PLoS One* **8**:e79839.
- Hernández-Cervantes R, Méndez-Díaz M, Prospéro-García Ó and Morales-Montor J (2017) Immunoregulatory Role of Cannabinoids during Infectious Disease. *Neuroimmunomodulation* **24**:183-199.
- Ho WS, Barrett DA and Randall MD (2008) 'Entourage' effects of N-palmitoylethanolamide and N-oleoylethanolamide on vasorelaxation to anandamide occur through TRPV1 receptors. *Br J Pharmacol* **155**:837-846.
- Hou X, Shen YH, Li C, Wang F, Zhang C, Bu P and Zhang Y (2010) PPARalpha agonist fenofibrate protects the kidney from hypertensive injury in spontaneously hypertensive rats via inhibition of oxidative stress and MAPK activity. *Biochem Biophys Res Commun* **394**:653-659.
- Howlett AC and Abood ME (2017) CB1 and CB2 Receptor Pharmacology. *Adv Pharmacol* **80**:169-206.

- Hryciw DH and McAinch AJ (2016) Cannabinoid receptors in the kidney. *Curr Opin Nephrol Hypertens* **25**:459-464.
- Ichiki T, Usui M, Kato M, Funakoshi Y, Ito K, Egashira K and Takeshita A (1998) Downregulation of angiotensin II type 1 receptor gene transcription by nitric oxide. *Hypertension* **31**:342-348.
- Ivy JR and Bailey MA (2014) Pressure natriuresis and the renal control of arterial blood pressure. *J Physiol* **592**:3955-3967.
- Jaggari SI, Hasnie FS, Sellaturay S and Rice AS (1998) The anti-hyperalgesic actions of the cannabinoid anandamide and the putative CB2 receptor agonist palmitoylethanolamide in visceral and somatic inflammatory pain. *Pain* **76**:189-199.
- Jenkin KA, McAinch AJ, Grinfeld E and Hryciw DH (2010) Role for cannabinoid receptors in human proximal tubular hypertrophy. *Cell Physiol Biochem* **26**:879-886.
- Johns EJ, Kopp UC and DiBona GF (2011) Neural control of renal function. *Compr Physiol* **1**:731-767.
- Jonkers IJ, de Man FH, van der Laarse A, Frolich M, Gevers Leuven JA, Kamper AM, Blauw GJ and Smelt AH (2001) Bezafibrate reduces heart rate and blood pressure in patients with hypertriglyceridemia. *J Hypertens* **19**:749-755.
- Jonsson KO, Vandevorde S, Lambert DM, Tiger G and Fowler CJ (2001) Effects of homologues and analogues of palmitoylethanolamide upon the inactivation of the endocannabinoid anandamide. *Br J Pharmacol* **133**:1263-1275.
- Kanematsu Y, Yamaguchi K, Ohnishi H, Motobayashi Y, Ishizawa K, Izawa Y, Kawazoe K, Kondo S, Kagami S, Tomita S, Tsuchiya K and Tamaki T (2008) Dietary doses of nitrite restore circulating nitric oxide level and improve renal injury in L-NAME-induced hypertensive rats. *Am J Physiol Renal Physiol* **295**:F1457-1462.
- Karlstrom G and Gothberg G (1987) The humorally mediated antihypertensive system of the rat kidney: a physiological depressor mechanism? *J Hypertens Suppl* **5**:S91-94.
- Khraibi AA and Knox FG (1989) Effect of renal decapsulation on renal interstitial hydrostatic pressure and natriuresis. *Am J Physiol* **257**:R44-48.
- Koka S, Lang C, Niemoeller OM, Boini KM, Nicolay JP, Huber SM and Lang F (2008) Influence of NO synthase inhibitor L-NAME on parasitemia and survival of Plasmodium berghei infected mice. *Cell Physiol Biochem* **21**:481-488.
- Konrad RJ, Major CD and Wolf BA (1994) Diacylglycerol hydrolysis to arachidonic acid is necessary for insulin secretion from isolated pancreatic islets: sequential actions of diacylglycerol and monoacylglycerol lipases. *Biochemistry* **33**:13284-13294.
- Koura Y, Ichihara A, Tada Y, Kaneshiro Y, Okada H, Temm CJ, Hayashi M and Saruta T (2004) Anandamide decreases glomerular filtration rate through predominant vasodilation of efferent arterioles in rat kidneys. *J Am Soc Nephrol* **15**:1488-1494.
- Kuehl FA, Jacob TA, Ganley OH, Ormond RE and Meisinger MAP (1957) The identification of N-(2-hydroxyethyl)-palmitamide as a naturally occurring anti-inflammatory agent *Journal of the American Chemical Society* **79**:5577-5578.
- Kumar KV and Das UN (1997) Effect of cis-unsaturated fatty acids, prostaglandins, and free radicals on angiotensin-converting enzyme activity in vitro. *Proc Soc Exp Biol Med* **214**:374-379.
- Lackovic V, Borecky L and Kresakova J (1977) Effect of interferon treatment of interferon production and antiviral resistance of mice. *Arch Immunol Ther Exp (Warsz)* **25**:655-661.

- Lackovic V, Borecky L, Kresakova J and Doskocil J (1978) [N[2-hydroxyethyl] palmitamide repeated administration effect on interferon production in mouse organism after phage double-stranded ribonucleic acid [ds-RNA] application (author's transl)]. *Cesk Epidemiol Mikrobiol Imunol* **27**:38-45.
- Lake KD, Martin BR, Kunos G and Varga K (1997) Cardiovascular effects of anandamide in anesthetized and conscious normotensive and hypertensive rats. *Hypertension* **29**:1204-1210.
- Lambert DM and Di Marzo V (1999) The palmitoylethanolamide and oleamide enigmas : are these two fatty acid amides cannabimimetic? *Curr Med Chem* **6**:757-773.
- Lambert DM, DiPaolo FG, Sonveaux P, Kanyonyo M, Govaerts SJ, Hermans E, Bueb J, Delzenne NM and Tschirhart EJ (1999) Analogues and homologues of N-palmitoylethanolamide, a putative endogenous CB(2) cannabinoid, as potential ligands for the cannabinoid receptors. *Biochim Biophys Acta* **1440**:266-274.
- Larrinaga G, Varona A, Pérez I, Sanz B, Ugalde A, Cándenas ML, Pinto FM, Gil J and López JJ (2010) Expression of cannabinoid receptors in human kidney. *Histol Histopathol* **25**:1133-1138.
- Lemley KV and Kriz W (1991) Anatomy of the renal interstitium. *Kidney Int* **39**:370-381.
- Lentz KE, Skeggs LT, Jr., Woods KR, Kahn JR and Shumway NP (1956) The amino acid composition of hypertensin II and its biochemical relationship to hypertensin I. *J Exp Med* **104**:183-191.
- Lewis DJ and Prentice DE (1979) Ultrastructure of rhesus monkey renomedullary interstitial cells. *Lab Anim* **13**:75-79.
- Li J and Wang DH (2006) Differential mechanisms mediating depressor and diuretic effects of anandamide. *J Hypertens* **24**:2271-2276.
- Li N, Yi F, Sundry CM, Chen L, Hilliker ML, Donley DK, Muldoon DB and Li PL (2007) Expression and actions of HIF prolyl-4-hydroxylase in the rat kidneys. *Am J Physiol Renal Physiol* **292**:F207-216.
- Li N, Zhang G, Yi FX, Zou AP and Li PL (2005) Activation of NAD(P)H oxidase by outward movements of H⁺ ions in renal medullary thick ascending limb of Henle. *Am J Physiol Renal Physiol* **289**:F1048-1056.
- Liu J, Wang L, Harvey-White J, Osei-Hyiaman D, Razdan R, Gong Q, Chan AC, Zhou Z, Huang BX, Kim HY and Kunos G (2006) A biosynthetic pathway for anandamide. *Proc Natl Acad Sci U S A* **103**:13345-13350.
- Long JZ, LaCava M, Jin X and Cravatt BF (2011) An anatomical and temporal portrait of physiological substrates for fatty acid amide hydrolase. *J Lipid Res* **52**:337-344.
- LoVerme J, La Rana G, Russo R, Calignano A and Piomelli D (2005) The search for the palmitoylethanolamide receptor, in *Life Sci* pp 1685-1698, Netherlands.
- Lundberg JO, Weitzberg E and Gladwin MT (2008) The nitrate–nitrite–nitric oxide pathway in physiology and therapeutics. *Nature Reviews Drug Discovery* **7**:156.
- Maric C, Harris PJ and Alcorn D (2002) Changes in mean arterial pressure predict degranulation of renomedullary interstitial cells. *Clin Exp Pharmacol Physiol* **29**:1055-1059.
- Masek K, Perlik F, Klima J and Kahlich R (1974) Prophylactic efficacy of N-2-hydroxyethyl palmitamide (impulsin) in acute respiratory tract infections. *Eur J Clin Pharmacol* **7**:415-419.
- Mathews J, DuCharme DW and McCandlis M (1979) Morphology of cultured renomedullary interstitial cells. *Micron* **10**:185.

- Mattace Raso G, Pirozzi C, d'Emmanuele di Villa Bianca R, Simeoli R, Santoro A, Lama A, Di Guida F, Russo R, De Caro C, Sorrentino R, Calignano A and Meli R (2015) Palmitoylethanolamide treatment reduces blood pressure in spontaneously hypertensive rats: involvement of cytochrome p450-derived eicosanoids and renin angiotensin system. *PLoS One* **10**:e0123602.
- Mattace Raso G, Simeoli R, Russo R, Santoro A, Pirozzi C, d'Emmanuele di Villa Bianca R, Mitidieri E, Paciello O, Pagano TB, Orefice NS, Meli R and Calignano A (2013) N-Palmitoylethanolamide protects the kidney from hypertensive injury in spontaneously hypertensive rats via inhibition of oxidative stress. *Pharmacol Res* **76**:67-76.
- Mattson DL (2003) Importance of the renal medullary circulation in the control of sodium excretion and blood pressure. *Am J Physiol Regul Integr Comp Physiol* **284**:R13-27.
- Mattson DL, Lu S, Nakanishi K, Papanek PE and Cowley AW, Jr. (1994) Effect of chronic renal medullary nitric oxide inhibition on blood pressure. *Am J Physiol* **266**:H1918-1926.
- Mattson DL, Roman RJ and Cowley AW, Jr. (1992) Role of nitric oxide in renal papillary blood flow and sodium excretion. *Hypertension* **19**:766-769.
- McDonough AA (2010) Mechanisms of proximal tubule sodium transport regulation that link extracellular fluid volume and blood pressure. *Am J Physiol Regul Integr Comp Physiol* **298**:R851-861.
- Merai R, Siegel C, Rakotz M, Basch P, Wright J, Wong B and Thorpe P (2016) CDC Grand Rounds: A Public Health Approach to Detect and Control Hypertension. *MMWR Morb Mortal Wkly Rep* **65**:1261-1264.
- Milsom AB, Fernandez BO, Garcia-Saura MF, Rodriguez J and Feelisch M (2012) Contributions of nitric oxide synthases, dietary nitrite/nitrate, and other sources to the formation of NO signaling products. *Antioxidants & redox signaling* **17**:422-432.
- Moeckel GW, Zhang L, Fogo AB, Hao CM, Pozzi A and Breyer MD (2003) COX2 activity promotes organic osmolyte accumulation and adaptation of renal medullary interstitial cells to hypertonic stress. *J Biol Chem* **278**:19352-19357.
- Mombouli JV, Schaeffer G, Holzmann S, Kostner GM and Graier WF (1999) Anandamide-induced mobilization of cytosolic Ca²⁺ in endothelial cells. *Br J Pharmacol* **126**:1593-1600.
- Mozaffarian D, Benjamin EJ, Go AS, Arnett DK, Blaha MJ, Cushman M, de Ferranti S, Despres JP, Fullerton HJ, Howard VJ, Huffman MD, Judd SE, Kissela BM, Lackland DT, Lichtman JH, Lisabeth LD, Liu S, Mackey RH, Matchar DB, McGuire DK, Mohler ER, 3rd, Moy CS, Muntner P, Mussolino ME, Nasir K, Neumar RW, Nichol G, Palaniappan L, Pandey DK, Reeves MJ, Rodriguez CJ, Sorlie PD, Stein J, Towfighi A, Turan TN, Virani SS, Willey JZ, Woo D, Yeh RW and Turner MB (2015) Heart disease and stroke statistics--2015 update: a report from the American Heart Association. *Circulation* **131**:e29-322.
- Muehrcke RC, Mandal AK, Epstein M and Volini FI (1969) Cytoplasmic granularity of the renal medullary interstitial cells in experimental hypertension. *J Lab Clin Med* **73**:299-308.
- Muirhead EE (1980) Antihypertensive functions of the kidney: Arthur C. Corcoran memorial lecture. *Hypertension* **2**:444-464.
- Muirhead EE (1988) The renomedullary system of blood pressure control. *Am J Med Sci* **295**:231-233.
- Muirhead EE (1990a) Discovery of the renomedullary system of blood pressure control and its hormones. *Hypertension* **15**:114-116.
- Muirhead EE (1990b) Medullipin System of Blood Pressure Control. *Physiology* **5**:241-244.

- Muirhead EE (1991) The medullipin system of blood pressure control. *Am J Hypertens* **4**:556s-568s.
- Muirhead EE (1993) Renal vasodepressor mechanisms: the medullipin system. *J Hypertens Suppl* **11**:S53-58.
- Muirhead EE, Brooks B, Pitcock JA and Stephenson P (1972a) Renomedullary antihypertensive function in accelerated (malignant) hypertension. Observations on renomedullary interstitial cells. *The Journal of clinical investigation* **51**:181-190.
- Muirhead EE, Brooks B, Pitcock JA, Stephenson P and Brosius WL (1972b) Role of the renal medulla in the sodium-sensitive component of renoprival hypertension. *Lab Invest* **27**:192-198.
- Muirhead EE, Germain G, Leach BE, Pitcock JA, Stephenson P, Brooks B, Brosius WL, Daniels EG and Hinman JW (1972c) Production of renomedullary prostaglandins by renomedullary interstitial cells grown in tissue culture. *Circ Res* **31**:Suppl 2:161-172.
- Muirhead EE, Germain GS, Armstrong FB, Brooks B, Leach BE, Byers LW, Pitcock JA and Brown P (1974) Renomedullary endocrine system: its antihypertensive action. *Trans Assoc Am Physicians* **87**:288-297.
- Muirhead EE, Germain GS, Leach BE, Brooks B and Stephenson P (1973) Renomedullary interstitial cells (RIC), prostaglandins (PG) and the antihypertensive function of the kidney. *Prostaglandins* **3**:581-594.
- Muirhead EE, Pitcock JA, Nasjletti A, Brown P and Brooks B (1985) The antihypertensive function of the kidney. Its elucidation by captopril plus unclipping. *Hypertension* **7**:1127-135.
- Muirhead EE, Rightsel WA, Leach BE, Byers LW, Pitcock JA and Brooks B (1976) Anti-hypertensive lipid tissue from culture of renomedullary interstitial cells of the rat. *Clin Sci Mol Med Suppl* **3**:287s-290s.
- Muirhead EE, Rightsel WA, Leach BE, Byers LW, Pitcock JA and Brooks B (1977) Reversal of hypertension by transplants and lipid extracts of cultured renomedullary interstitial cells. *Lab Invest* **36**:162-172.
- Muirhead EE, Rightsel WA, Pitcock JA and Inagami T (1990) Isolation and culture of juxtaglomerular and renomedullary interstitial cells. *Methods Enzymol* **191**:152-167.
- Muirhead EE, Stirman JA and Jones F (1960) Renal autoexplantation and protection against renoprival hypertensive cardiovascular disease and hemolysis. *The Journal of clinical investigation* **39**:266-281.
- Munro S, Thomas KL and Abu-Shaar M (1993) Molecular characterization of a peripheral receptor for cannabinoids. *Nature* **365**:61-65.
- Nagano K, Ishida J, Unno M, Matsukura T and Fukamizu A (2013) Apelin elevates blood pressure in ICR mice with LNAME-induced endothelial dysfunction. *Mol Med Rep* **7**:1371-1375.
- Newaz M, Blanton A, Fidelis P and Oyekan A (2005) NAD(P)H oxidase/nitric oxide interactions in peroxisome proliferator activated receptor (PPAR)alpha-mediated cardiovascular effects. *Mutat Res* **579**:163-171.
- Nissen HM (1968) On lipid droplets in renal interstitial cells. II. A histological study on the number of droplets in salt depletion and acute salt repletion. *Z Zellforsch Mikrosk Anat* **85**:483-491.
- O'Connor PM and Cowley AW, Jr. (2010) Modulation of pressure-natriuresis by renal medullary reactive oxygen species and nitric oxide. *Curr Hypertens Rep* **12**:86-92.

- O'Hearn S, Diaz P, Wan BA, DeAngelis C, Lao N, Malek L, Chow E and Blake A (2017) Modulating the endocannabinoid pathway as treatment for peripheral neuropathic pain: a selected review of preclinical studies. *Ann Palliat Med* **6**:S209-S214.
- Oddi S, Fezza F, Pasquariello N, De Simone C, Rapino C, Dainese E, Finazzi-Agro A and Maccarrone M (2008) Evidence for the intracellular accumulation of anandamide in adiposomes. *Cell Mol Life Sci* **65**:840-850.
- Okamoto M, Tsuchiya K, Kanematsu Y, Izawa Y, Yoshizumi M, Kagawa S and Tamaki T (2005) Nitrite-derived nitric oxide formation following ischemia-reperfusion injury in kidney. *Am J Physiol Renal Physiol* **288**:F182-187.
- Ott CE, Navar LG and Guyton AC (1971) Pressures in static and dynamic states from capsules implanted in the kidney. *Am J Physiol* **221**:394-400.
- Overton HA, Babbs AJ, Doel SM, Fyfe MC, Gardner LS, Griffin G, Jackson HC, Procter MJ, Rasamison CM, Tang-Christensen M, Widdowson PS, Williams GM and Reynet C (2006) Deorphanization of a G protein-coupled receptor for oleoylethanolamide and its use in the discovery of small-molecule hypophagic agents, in *Cell Metab* pp 167-175, United States.
- Ozalp A and Barroso B (2009) Simultaneous quantitative analysis of N-acylethanolamides in clinical samples. *Anal Biochem* **395**:68-76.
- Pacher P, Batkai S and Kunos G (2006) The endocannabinoid system as an emerging target of pharmacotherapy. *Pharmacol Rev* **58**:389-462.
- Pacher P, Batkai S, Osei-Hyiaman D, Offertaler L, Liu J, Harvey-White J, Brassai A, Jarai Z, Cravatt BF and Kunos G (2005) Hemodynamic profile, responsiveness to anandamide, and baroreflex sensitivity of mice lacking fatty acid amide hydrolase. *Am J Physiol Heart Circ Physiol* **289**:H533-541.
- Page IH and Helmer OM (1940) A crystalline pressor substance (angiotonin) resulting from the reaction between renin and renin-activator. *J Exp Med* **71**:29-42.
- Pandey V, Garcia V, Gilani A, Mishra P, Zhang FF, Paudyal MP, Falck JR, Nasjletti A, Wang WH and Schwartzman ML (2017) The Blood Pressure-Lowering Effect of 20-HETE Blockade in Cyp4a14(-/-) Mice Is Associated with Natriuresis. *J Pharmacol Exp Ther* **363**:412-418.
- Paronis CA, Thakur GA, Bajaj S, Nikas SP, Vemuri VK, Makriyannis A and Bergman J (2013) Diuretic effects of cannabinoids. *J Pharmacol Exp Ther* **344**:8-14.
- Paterniti I, Impellizzeri D, Crupi R, Morabito R, Campolo M, Esposito E and Cuzzocrea S (2013) Molecular evidence for the involvement of PPAR-delta and PPAR-gamma in anti-inflammatory and neuroprotective activities of palmitoylethanolamide after spinal cord trauma. *J Neuroinflammation* **10**:20.
- Peart WS (1969) C. The renin-angiotensin system. A history and review of the renin-angiotensin system. *Proc R Soc Lond B Biol Sci* **173**:317-325.
- Perlik F, Krejci J, Elis J, Pekarek J and Svejcar J (1973) The effect of N-(2-hydroxyethyl)-palmitamide on delayed hypersensitivity in guinea-pig. *Experientia* **29**:67-68.
- Pertwee RG (2007) GPR55: a new member of the cannabinoid receptor clan? *Br J Pharmacol* **152**:984-986.
- Piomelli D and Sasso O (2014) Peripheral gating of pain signals by endogenous lipid mediators. *Nat Neurosci* **17**:164-174.
- Pitcock JA, Brown PS, Byers W, Brooks B and Muirhead EE (1981) Degranulation of renomedullary interstitial cells during reversal of hypertension. *Hypertension* **3**:li-75-80.

- Podjarny E, Hasdan G, Bernheim J, Rashid G, Green J and Korzets Z (2004) Effect of chronic tetrahydrobiopterin supplementation on blood pressure and proteinuria in 5/6 nephrectomized rats. *Nephrol Dial Transplant* **19**:2223-2227.
- Pollock DM, Polakowski JS, Divish BJ and Opgenorth TJ (1993) Angiotensin blockade reverses hypertension during long-term nitric oxide synthase inhibition. *Hypertension* **21**:660-666.
- Qiu C, Engels K and Baylis C (1994) Angiotensin II and alpha 1-adrenergic tone in chronic nitric oxide blockade-induced hypertension. *Am J Physiol* **266**:R1470-1476.
- Rajapakse NW and Mattson DL (2011) Role of L-arginine uptake mechanisms in renal blood flow responses to angiotensin II in rats. *Acta Physiol (Oxf)* **203**:391-400.
- Randall MD, Kendall DA and O'Sullivan S (2004) The complexities of the cardiovascular actions of cannabinoids. *Br J Pharmacol* **142**:20-26.
- Ritter JK, Li C, Xia M, Poklis JL, Lichtman AH, Abdullah RA, Dewey WL and Li PL (2012) Production and actions of the anandamide metabolite prostamide E2 in the renal medulla. *J Pharmacol Exp Ther* **342**:770-779.
- Roman RJ (1988) Pressure-diuresis in volume-expanded rats. Tubular reabsorption in superficial and deep nephrons. *Hypertension* **12**:177-183.
- Roman RJ, Cowley AW, Jr., Garcia-Estan J and Lombard JH (1988) Pressure-diuresis in volume-expanded rats. Cortical and medullary hemodynamics. *Hypertension* **12**:168-176.
- Romero TR and Duarte ID (2012) N-palmitoyl-ethanolamine (PEA) induces peripheral antinociceptive effect by ATP-sensitive K⁺-channel activation. *J Pharmacol Sci* **118**:156-160.
- Russell GI, Bing RF, Swales JD and Thurston H (1982a) Effect of Pharmacological Inhibition of Renin, Prostaglandin and Kallikrein Systems on Surgical Correction of Longstanding Two-Kidney, One-Clip Hypertension in the Rat. *Clinical Science* **63**:257s.
- Russell GI, Bing RF, Swales JD and Thurston H (1983) Hemodynamic changes induced by reversal of early and late renovascular hypertension. *Am J Physiol* **245**:H734-740.
- Russell GI, Bing RF, Thurston H and Swales JD (1982b) Surgical reversal of two-kidney one clip hypertension during inhibition of the renin-angiotensin system. *Hypertension* **4**:69-76.
- Russell GI, Godfrey NP, Forsling ML, Bing RF, Thurston H and Swales JD (1986) Selective renal medullary damage and hypertension in the rat: the role of vasopressin. *Clin Sci (Lond)* **71**:167-171.
- Ryberg E, Larsson N, Sjogren S, Hjorth S, Hermansson NO, Leonova J, Elebring T, Nilsson K, Drmota T and Greasley PJ (2007) The orphan receptor GPR55 is a novel cannabinoid receptor. *Br J Pharmacol* **152**:1092-1101.
- Sampaio LS, Taveira Da Silva R, Lima D, Sampaio CLC, Iannotti FA, Mazzarella E, Di Marzo V, Vieyra A, Reis RAM and Einicker-Lamas M (2015) The endocannabinoid system in renal cells: regulation of Na⁽⁺⁾ transport by CB1 receptors through distinct cell signalling pathways. *British journal of pharmacology* **172**:4615-4625.
- Schafer JA (1990) Transepithelial osmolality differences, hydraulic conductivities, and volume absorption in the proximal tubule. *Annu Rev Physiol* **52**:709-726.
- Schmid HH, Schmid PC and Natarajan V (1990) N-acylated glycerophospholipids and their derivatives. *Prog Lipid Res* **29**:1-43.
- Schmitz G and Muller G (1991) Structure and function of lamellar bodies, lipid-protein complexes involved in storage and secretion of cellular lipids. *J Lipid Res* **32**:1539-1570.

- Schneider JP, Pedersen L, Muhlfeld C and Ochs M (2015) Staining histological lung sections with Sudan Black B or Sudan III for automated identification of alveolar epithelial type II cells. *Acta Histochem* **117**:675-680.
- Shin SJ, Lim JH, Chung S, Youn DY, Chung HW, Kim HW, Lee JH, Chang YS and Park CW (2009) Peroxisome proliferator-activated receptor- α activator fenofibrate prevents high-fat diet-induced renal lipotoxicity in spontaneously hypertensive rats. *Hypertens Res* **32**:835-845.
- Shire D, Carillon C, Kaghad M, Calandra B, Rinaldi-Carmona M, Le Fur G, Caput D and Ferrara P (1995) An amino-terminal variant of the central cannabinoid receptor resulting from alternative splicing. *J Biol Chem* **270**:3726-3731.
- Showalter VM, Compton DR, Martin BR and Abood ME (1996) Evaluation of binding in a transfected cell line expressing a peripheral cannabinoid receptor (CB2): identification of cannabinoid receptor subtype selective ligands. *J Pharmacol Exp Ther* **278**:989-999.
- Silva GB, Atchison DK, Juncos LI and García NH (2013) Anandamide inhibits transport-related oxygen consumption in the loop of Henle by activating CB1 receptors. *Am J Physiol Renal Physiol* **304**:F376-381.
- Simon GM and Cravatt BF (2006) Endocannabinoid biosynthesis proceeding through glycerophospho-N-acyl ethanolamine and a role for alpha/beta-hydrolase 4 in this pathway. *J Biol Chem* **281**:26465-26472.
- Simon GM and Cravatt BF (2008) Anandamide biosynthesis catalyzed by the phosphodiesterase GDE1 and detection of glycerophospho-N-acyl ethanolamine precursors in mouse brain. *J Biol Chem* **283**:9341-9349.
- Skeggs LT, Jr., Marsh WH, Kahn JR and Shumway NP (1954a) The existence of two forms of hypertensin. *J Exp Med* **99**:275-282.
- Skeggs LT, Jr., Marsh WH, Kahn JR and Shumway NP (1954b) The purification of hypertensin I. *J Exp Med* **100**:363-370.
- Smart D, Jonsson KO, Vandevoorde S, Lambert DM and Fowler CJ (2002) 'Entourage' effects of N-acyl ethanolamines at human vanilloid receptors. Comparison of effects upon anandamide-induced vanilloid receptor activation and upon anandamide metabolism. *Br J Pharmacol* **136**:452-458.
- Sofia RD, Knobloch LC, Harakal JJ and Erikson DJ (1977) Comparative diuretic activity of delta9-tetrahydrocannabinol, cannabidiol, cannabinol and hydrochlorothiazide in the rat. *Arch Int Pharmacodyn Ther* **225**:77-87.
- Solorzano C, Zhu C, Battista N, Astarita G, Lodola A, Rivara S, Mor M, Russo R, Maccarrone M, Antonietti F, Duranti A, Tontini A, Cuzzocrea S, Tarzia G and Piomelli D (2009) Selective N-acyl ethanolamine-hydrolyzing acid amidase inhibition reveals a key role for endogenous palmitoylethanolamide in inflammation. *Proc Natl Acad Sci U S A* **106**:20966-20971.
- Stopponi S, Fotio Y, Domi A, Borruto AM, Natividad L, Roberto M, Ciccocioppo R and Cannella N (2018) Inhibition of fatty acid amide hydrolase in the central amygdala alleviates comorbid expression of innate anxiety and excessive alcohol intake. *Addict Biol* **23**:1223-1232.
- Sugiura T, Kishimoto S, Oka S and Gokoh M (2006) Biochemistry, pharmacology and physiology of 2-arachidonoylglycerol, an endogenous cannabinoid receptor ligand. *Prog Lipid Res* **45**:405-446.

- Sugiura T, Kondo S, Kishimoto S, Miyashita T, Nakane S, Kodaka T, Suhara Y, Takayama H and Waku K (2000) Evidence that 2-arachidonoylglycerol but not N-palmitoylethanolamine or anandamide is the physiological ligand for the cannabinoid CB2 receptor. Comparison of the agonistic activities of various cannabinoid receptor ligands in HL-60 cells. *J Biol Chem* **275**:605-612.
- Sun YX, Tsuboi K, Okamoto Y, Tonai T, Murakami M, Kudo I and Ueda N (2004) Biosynthesis of anandamide and N-palmitoylethanolamine by sequential actions of phospholipase A2 and lysophospholipase D. *Biochem J* **380**:749-756.
- Syed SK, Bui HH, Beavers LS, Farb TB, Ficorilli J, Chesterfield AK, Kuo MS, Bokvist K, Barrett DG and Efanov AM (2012) Regulation of GPR119 receptor activity with endocannabinoid-like lipids. *Am J Physiol Endocrinol Metab* **303**:E1469-1478.
- Takemoto M, Egashira K, Usui M, Numaguchi K, Tomita H, Tsutsui H, Shimokawa H, Sueishi K and Takeshita A (1997) Important role of tissue angiotensin-converting enzyme activity in the pathogenesis of coronary vascular and myocardial structural changes induced by long-term blockade of nitric oxide synthesis in rats. *J Clin Invest* **99**:278-287.
- Tam J (2016) The emerging role of the endocannabinoid system in the pathogenesis and treatment of kidney diseases. *J Basic Clin Physiol Pharmacol* **27**:267-276.
- Thomas CJ, Woods RL, Evans RG, Alcorn D, Christy IJ and Anderson WP (1996) Evidence for a renomedullary vasodepressor hormone. *Clinical and Experimental Pharmacology and Physiology* **23**:777-785.
- Thurston H, Bing RF and Swales JD (1980) Reversal of two-kidney one clip renovascular hypertension in the rat. *Hypertension* **2**:256-265.
- Tobian L and Ishii M (1969) Interstitial cell granules and solutes in renal papilla in post-Goldblatt hypertension. *Am J Physiol* **217**:1699-1702.
- Tobian L, Jr. and Azar S (1971) Antihypertensive and other functions of the renal papilla. *Trans Assoc Am Physicians* **84**:281-288.
- Tornel J, Madrid MI, Garcia-Salom M, Wirth KJ and Fenoy FJ (2000) Role of kinins in the control of renal papillary blood flow, pressure natriuresis, and arterial pressure. *Circ Res* **86**:589-595.
- Turcotte C, Chouinard F, Lefebvre JS and Flamand N (2015) Regulation of inflammation by cannabinoids, the endocannabinoids 2-arachidonoyl-glycerol and arachidonoyl-ethanolamide, and their metabolites. *J Leukoc Biol* **97**:1049-1070.
- Ueda N, Kurahashi Y, Yamamoto S and Tokunaga T (1995) Partial purification and characterization of the porcine brain enzyme hydrolyzing and synthesizing anandamide. *J Biol Chem* **270**:23823-23827.
- Varga K, Lake K, Martin BR and Kunos G (1995) Novel antagonist implicates the CB1 cannabinoid receptor in the hypotensive action of anandamide. *Eur J Pharmacol* **278**:279-283.
- Varga K, Lake KD, Huangfu D, Guyenet PG and Kunos G (1996) Mechanism of the hypotensive action of anandamide in anesthetized rats. *Hypertension* **28**:682-686.
- Vera T, Taylor M, Bohman Q, Flasch A, Roman RJ and Stec DE (2005) Fenofibrate prevents the development of angiotensin II-dependent hypertension in mice. *Hypertension* **45**:730-735.
- Wadei HM and Textor SC (2012) The role of the kidney in regulating arterial blood pressure. *Nature Reviews Nephrology* **8**:602.
- Wakui H, Uneda K, Tamura K, Ohsawa M, Azushima K, Kobayashi R, Ohki K, Dejima T, Kanaoka T, Tsurumi-Ikeya Y, Matsuda M, Haruhara K, Nishiyama A, Yabana M,

- Fujikawa T, Yamashita A and Umemura S (2015) Renal tubule angiotensin II type 1 receptor-associated protein promotes natriuresis and inhibits salt-sensitive blood pressure elevation. *J Am Heart Assoc* **4**:e001594.
- Waluk DP, Battistini MR, Dempsey DR, Farrell EK, Jeffries KA, Mitchell P, Hernandez LW, McBride JC, Merkler DJ and Hunt MC (2014) Chapter 9 - Mammalian Fatty Acid Amides of the Brain and CNS, in *Omega-3 Fatty Acids in Brain and Neurological Health* (Watson RR and De Meester F eds) pp 87-107, Academic Press, Boston.
- Wang J and Ueda N (2009) Biology of endocannabinoid synthesis system. *Prostaglandins Other Lipid Mediat* **89**:112-119.
- Wang Z, Tang L, Zhu Q, Yi F, Zhang F, Li PL and Li N (2011) Hypoxia-inducible factor-1alpha contributes to the profibrotic action of angiotensin II in renal medullary interstitial cells. *Kidney Int* **79**:300-310.
- Wasilewski A, Misicka A, Sacharczuk M and Fichna J (2017) Modulation of the endocannabinoid system by the fatty acid amide hydrolase, monoacylglycerol and diacylglycerol lipase inhibitors as an attractive target for secretory diarrhoea therapy. *J Physiol Pharmacol* **68**:591-596.
- Wilcox CS, Sterzel RB, Dunckel PT, Mohrmann M and Perfetto M (1984) Renal interstitial pressure and sodium excretion during hilar lymphatic ligation. *Am J Physiol* **247**:F344-351.
- Williams JM, Sarkis A, Lopez B, Ryan RP, Flasch AK and Roman RJ (2007) Elevations in renal interstitial hydrostatic pressure and 20-hydroxyeicosatetraenoic acid contribute to pressure natriuresis. *Hypertension* **49**:687-694.
- Yoon SS, Carroll MD and Fryar CD (2015) Hypertension Prevalence and Control Among Adults: United States, 2011-2014. *NCHS Data Brief*:1-8.
- Yousefipour Z and Newaz M (2014) PPAR α ligand clofibrate ameliorates blood pressure and vascular reactivity in spontaneously hypertensive rats. *Acta pharmacologica Sinica* **35**:476-482.
- Zanfolin M, Faro R, Araujo EG, Guaraldo AM, Antunes E and De Nucci G (2006) Protective effects of BAY 41-2272 (sGC stimulator) on hypertension, heart, and cardiomyocyte hypertrophy induced by chronic L-NAME treatment in rats. *J Cardiovasc Pharmacol* **47**:391-395.
- Zhang YB, Magyar CE, Holstein-Rathlou NH and McDonough AA (1998) The cytochrome P-450 inhibitor cobalt chloride prevents inhibition of renal Na,K-ATPase and redistribution of apical NHE-3 during acute hypertension. *J Am Soc Nephrol* **9**:531-537.
- Zhu C, Solorzano C, Sahar S, Realini N, Fung E, Sassone-Corsi P and Piomelli D (2011a) Proinflammatory stimuli control N-acylphosphatidylethanolamine-specific phospholipase D expression in macrophages. *Mol Pharmacol* **79**:786-792.
- Zhu Q, Xia M, Wang Z, Li PL and Li N (2011b) A novel lipid natriuretic factor in the renal medulla: sphingosine-1-phosphate. *Am J Physiol Renal Physiol* **301**:F35-41.
- Zhuo JL (2000) Renomedullary interstitial cells: a target for endocrine and paracrine actions of vasoactive peptides in the renal medulla. *Clin Exp Pharmacol Physiol* **27**:465-473.
- Zou AP, Li N and Cowley AW, Jr. (2001a) Production and actions of superoxide in the renal medulla. *Hypertension* **37**:547-553.
- Zou AP, Yang ZZ, Li PL and Cowley AJ (2001b) Oxygen-dependent expression of hypoxia-inducible factor-1alpha in renal medullary cells of rats. *Physiol Genomics* **6**:159-168.

Zusman RM and Keiser HR (1977a) Prostaglandin biosynthesis by rabbit renomedullary interstitial cells in tissue culture. Stimulation by angiotensin II, bradykinin, and arginine vasopressin. *J Clin Invest* **60**:215-223.

Zusman RM and Keiser HR (1977b) Prostaglandin E2 biosynthesis by rabbit renomedullary interstitial cells in tissue culture. Mechanism of stimulation by angiotensin II, bradykinin, and arginine vasopressin. *J Biol Chem* **252**:2069-2071.

Vita

Sara Kathleen Dempsey was born on December 14th, 1990 in Decatur, Georgia and graduated from Buford High School (Buford, GA) in 2009. She earned her Bachelors of Science in Forensic Chemistry from the University of Mississippi in 2013 and then earned her Masters of Science degree in Forensic Science from Virginia Commonwealth University in spring 2015. In the fall, she entered the Biomedical Sciences Doctoral Portal program at VCU, and spring 2016 joined the laboratory of Dr. Joseph Ritter. Upon acceptance of this dissertation, she will be awarded a Doctorate of Philosophy in Pharmacology and Toxicology.